A Value Based Approach to Leach Optimization at Rössing Uranium Limited

---

Nicole Jansen van Rensburg

Thesis submitted for the degree of:
Master of Science in Chemical Engineering

February 2014

Faculty of the Engineering and Built Environment
University of Cape Town

Declaration

I know the meaning of plagiarism and declare that all the work in the document, save for that which is properly acknowledged, is my own.

_____

Nicole Jansen van Rensburg

Acknowledgements

First and foremost, I would like to thank God for providing me with the ability, wisdom and perseverance to complete this thesis.

I would like to thank Rössing Uranium Limited who made it possible for me to study at the University of Cape Town by providing me with a bursary.

This work would not be possible without the support and guidance of a number of people, and I would like to take this opportunity to personally thank them.

- To my colleague and mentor Dr Jaidev Prasad - thank you for your continuous direction, support and encouragement throughout this project and the time that we worked together at Rössing.
- To my supervisors at the University of Cape Town, Dr Jochen Petersen and Dr Megan Becker – thank you for your guidance and for the review of this thesis.
- To my husband, family and friends – thank you for your encouragement, prayers and unconditional love.
- To the Processing Improvement team (both at Rössing and Rio Tinto Technology and Innovation) – I could not have hoped for a better team to support me in this valuable piece of improvement work. Thank you for the many hours spent conducting the laboratory test work at Rössing.

Synopsis

This thesis describes the development and execution of an experimental leach programme and the use of a techno-economic model to determine improved operating set-points for a uraninite/uranophane ore body, for plant-scale implementation, that consistently maximise value delivery. A mineralogical investigation of Rössing leach samples indicated that liberated uraninite remains in the leach residue, providing evidence of non-optimal leach conditions such as prevailing redox potential, incomplete leaching within the normal residence time or galvanic hindrance. Specific focus was, therefore, placed on the effect of oxidation reduction potential (ORP) on uranium extraction and reagent consumption and the determination of an improved ORP set-point as a function of ore type, residence time and the economic environment.

Agitated batch leach tests were conducted using two ores from the Rössing Uranium Limited (RUL) mine in Namibia. Both ores contained uraninite, uranophane and trace amounts of betafite. One ore contained a higher concentration of cordierite gneiss which has reductive properties and therefore, exerts a higher oxidant demand.

Results indicated that under standard operating conditions (pH 1.6, 35 °C and 7.8 hour residence time) uranium extraction increased with an increase in ORP for both ores.

Batch leach data was fitted to empirical models and combined with the exit age distribution equation for a continuous stirred tank reactor (CSTR) and Rössing operational information to determine economically improved set-points. Over the range tested (440 to 550 mV, Ag/AgCl 3M) an economic optimum ORP range (500 – 525 mV), at which net revenue is maximised, was found to exist for both ores.

The effect of total iron concentration was investigated and found to have a greater impact on uranium extraction in the lower ORP range (<475 mV), which compared well with an equivalent study in the literature conducted on a synthetic uraninite sample. Over the range tested (3 – 5 g/L) an economic optimum total iron concentration (4.5 g/L) was found to exist for the ore which contained the lower cordierite gneiss concentration.

Uranium extraction was also found to increase with a decrease in pulp density and an increase in temperature, indicating potential to determine the role that these variables could play in increasing financial value delivered by the Rössing leaching circuit.

This project is part of a broader leach optimization program at RUL that was initiated to maximise financial value delivered from the leaching plant by increasing uranium leach extraction and decreasing reagent consumption. Recommendations from this work will be trialled at plant scale and then implemented following a successful trial.

Table of Contents

List of Figures

List of Tables

List of Abbreviations and Symbols

[ ]	Concentration
%	Percentage
∝	Proportional
σ	Standard deviation
BSE	Backscattered electron analysis
˚C	Degree Celsius
CGS	Cordierite Gneiss
CSTR	Continuous stirred-tank reactor
d_{80}	80% passing
Eh	Voltage potential with respect to the standard hydrogen electrode
g/L	Grams per litre
ICP-MS	Inductively coupled plasma mass spectroscopy
K	Kelvin
kg	Kilogram
kg/t	Kilograms per tonne
kW	Kilowatt
lb	Pound
LCP	Leach Control Philosophy
µm	Micrometre
P80	Mill circuit product size, 80% passing
M	Molar
MLA	Mineral liberation analyser
mm	Millimetre
mol/min	Moles per minute
mSv	Milli-sievert
mV	Millivolt
ORP	Oxidation Reduction Potential
PID	Proportional-integral-derivative
ppm	Parts per million
PSD	Particle size distribution
QMA	Quantitative Mineralogical Analysis
ROM	Run of mine
rpm	Revolutions per minute
RTD	Residence time distribution
RUL	Rössing Uranium Limited

SD	Standard deviation
SEM	Scanning electron microscope
t	Tonne
t/h	Tonnes per hour
wt%	Weight percentage
UxC	Ux Consulting Company
XRD	X-ray diffraction

1 Introduction

1.1 Background

Rio Tinto Rössing Uranium Limited (RUL) operates a large, low-grade (average of 0.3 kg U_3O_8/t[1]), open cast uranium mine and processing plant in the Erongo region of Namibia. Ore is mined, crushed and milled and uranium is then extracted and recovered from the ore via sulphuric acid leaching, ion exchange, solvent extraction, precipitation of yellow cake and finally calcination to form a final uranium oxide product (Figure 1.1). Uranium oxide is transported to converters in Canada, China, France, United Kingdom and United States (Rössing, 2013a) where it is converted to uranium hexafluoride (UF_6). UF_6 is then further enriched and fabricated into uranium dioxide (UO_2) and used in power plants to generate electricity. Figure 1.2 illustrates the nuclear fuel cycle.

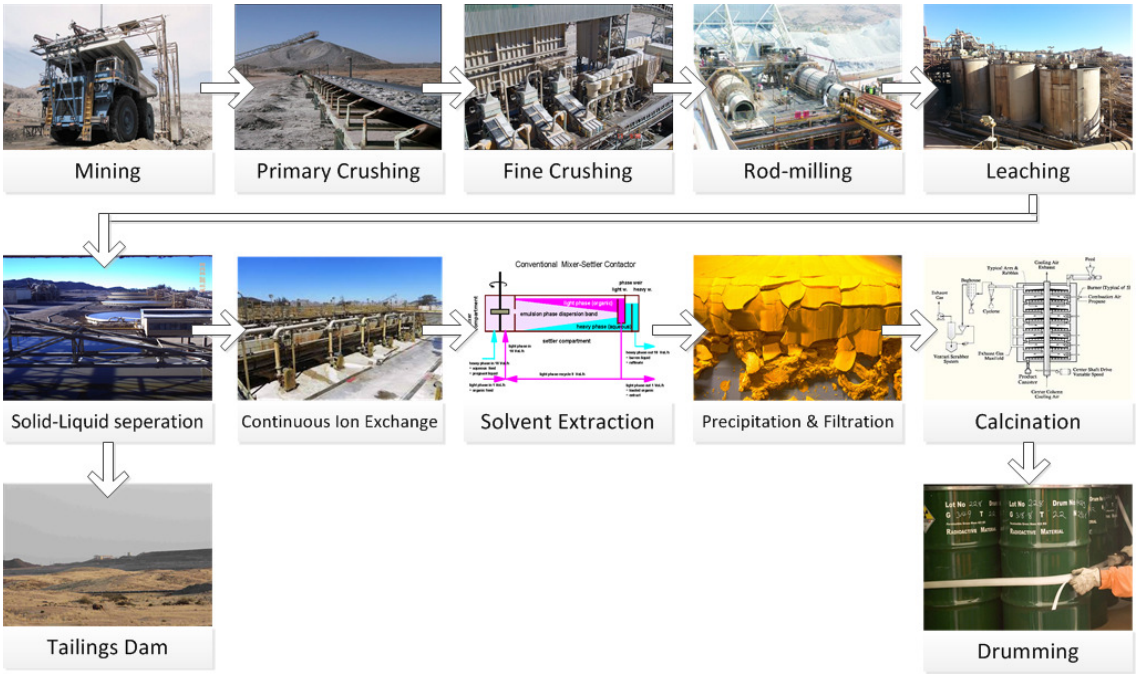

Figure 1.1: RUL U_3O_8 production process

[1] 1 kg U_3O_8/t is equivalent to 0.0848 wt% uranium.

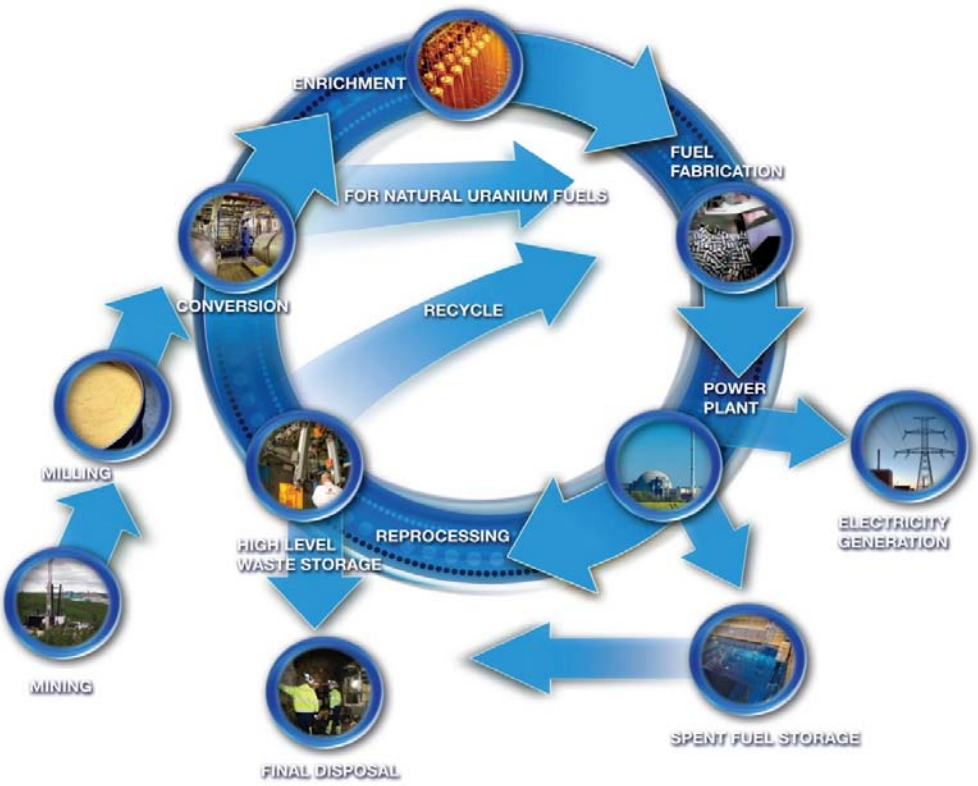

Figure 1.2: Nuclear fuel cycle (International Atomic Energy Agency, 2013)

For a low grade uranium oxide producer in the current economic uranium market (i.e. low uranium price[2]) it is essential that maximum value is delivered from every ton of ore processed, to remain competitive. This puts pressure on both the mining process and the metallurgical processing plant, as the key drivers in the value equation.

The leach circuit is essentially the heart of the metallurgical processing plant, i.e. the point at which uranium is actually extracted from the ore. Value delivered by the leaching circuit at RUL is highly dependent on the economic efficiency of the leach process, i.e. the ability to extract uranium from the ore and the variable cost at which it is extracted (including the cost of reagents added to the leach circuit, plant maintenance costs etc.).

[2] On 20 January 2014, U_3O_8 spot price = 35.75 US$/lb U_3O_8 (The Ux Consulting Company, 2014)

In 2012 Rössing embarked on a leach optimization program that focussed on maximising financial value delivered from the leaching circuit. Two key challenges with the historical operation and control of the plant were identified:

1. No standardized way of operating the leaching plant existed.
2. Control set-point targets were static, despite the plant working in a highly dynamic environment (varying ore type, equipment availability[3] and relative prices of product and reagents). There was a limited understanding of methods to determine improved leach conditions for varying environments.

These challenges resulted in high variability in leach extraction and reagent control and consequently in sub-optimal value delivered by the leaching circuit. The leach optimization program was, therefore, established to reduce variability and deliver higher sustained value from the leach circuit. The goals of the program were (i) to develop and implement standardised control responses to process deviations, (ii) to find improved leach set-points via laboratory test work, validate their benefit through plant trials and implement them in the leaching process and (iii) to develop and implement a flexible operating strategy which maximises value consistently from the leach circuit.

To close the gap, the following approach was set in motion:

1. Development of measurement techniques to measure the leaching circuit performance baseline (in terms of uranium extraction and reagent consumption) and quantify improvements.
2. Development of a leach control philosophy (LCP) for operation of the leach circuit, to achieve standardised responses and act as an enabler for implementation of improved set-points.
3. Development of a laboratory program and techno-economic leach optimisation model to determine the relative benefits of alternative and improved operating set-points.
4. Testing the LCP and implementing improved set-points.
5. Quantifying the benefits of the improvements implemented.

[3] Leach residence time is affected by plant equipment availability. The leach throughput rate is dependent on the number of rodmills online and the milling rate. The milling rate is in turn affected by any upstream mechanical problems in the fine crushing plant. Leach tank availability is dependent on the mechanical availability of the leach tanks (agitator and gearbox failures and general scheduled maintenance are factors which impact the mechanical availability of the leach tanks).

To date, steps one, two and part of step 3 have been completed. The leach control philosophy was developed and has been trialled and implemented in the Rössing leaching plant with great success, i.e. statistically proven improvements in both uranium extraction and reagent consumption have been seen (Prasad et al., 2012). A techno-economic model has been developed (Hamilton, 2010) but has not yet been used to determine the relative benefits of alternative and improved operating set-points.

The development of the laboratory test program and use of a techno-economic model is a key enabler for Rössing metallurgists to select economically improved set-points to increase value in the leach circuit, as a function of the external economic environment, ore type and plant operability (e.g. number of leach tanks online). This crucial step is, therefore, the focus of this project.

1.2 Geology and mineralogy of the Rössing deposit

The Rössing ore body comprises predominantly of alaskite, quartzite, marble, gneiss and schist (amphibolite and biotite) rock types. An aerial photograph of the RUL open pit (SJ area) is depicted in Figure 1.3. Figure 1.4 and Figure 1.5 contain geological maps showing (i) the setting of the Rössing uranium deposit and (ii) a closer look at the alaskite ore body. The country rock surrounding the alaskite deposit comprises deformed metasedimentary rocks of the Khan formation (located in the North) and Rössing formation (located in the South). These formations in turn, form part of the Nosib and Swakop groups, respectively (Roesener and Schreuder, 1992). The geology and exploration of the Rössing deposit has been described in greater detail by Berning et al. (1976).

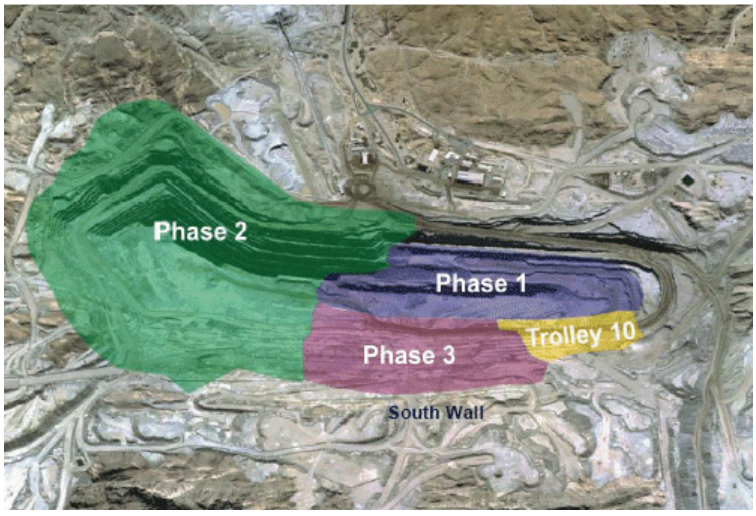

Figure 1.3: Aerial photograph of the RUL open pit (SJ area) (Infomine, 2013)

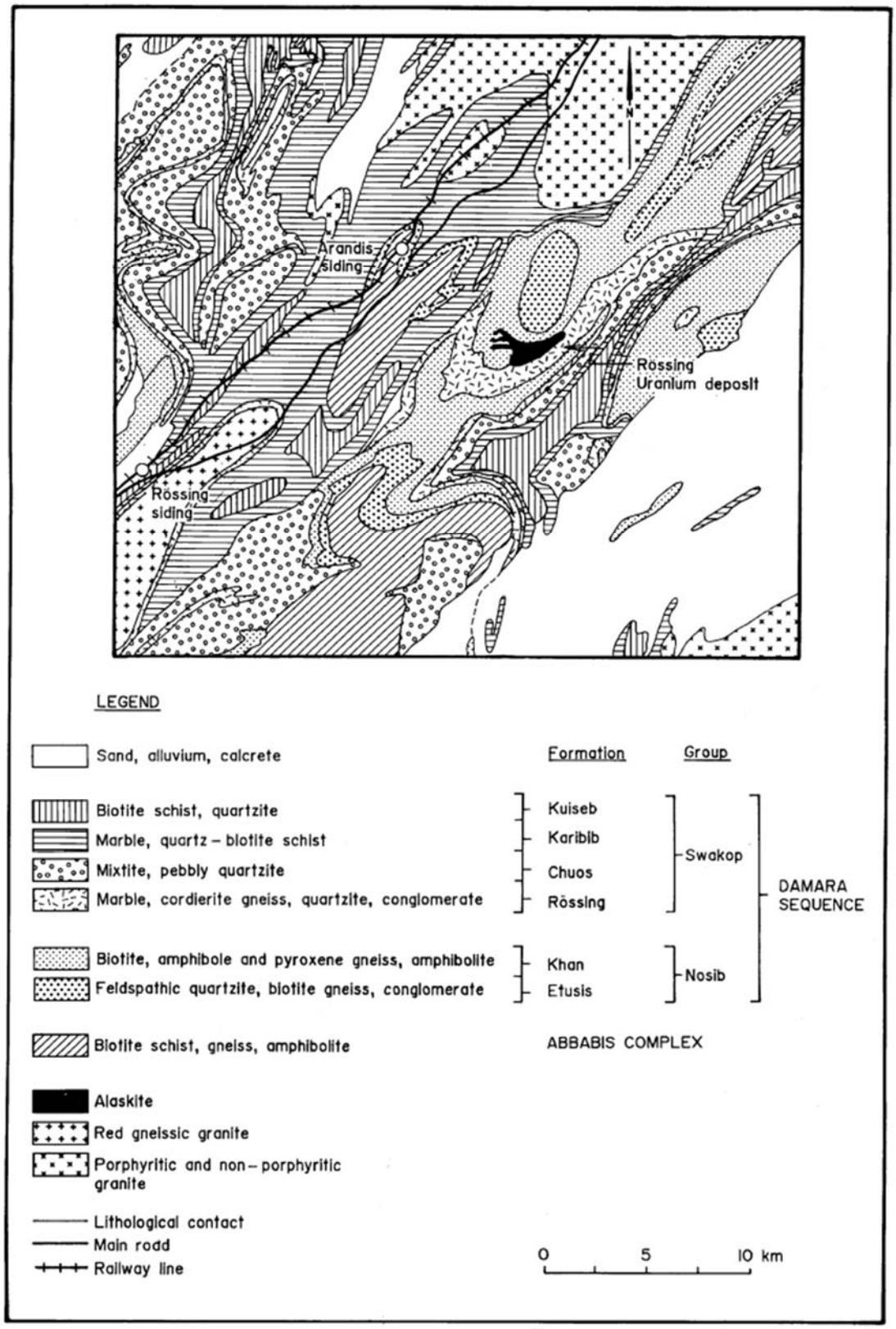

Figure 1.4: Geological map showing the setting of the RUL deposit (Berning, 1986)

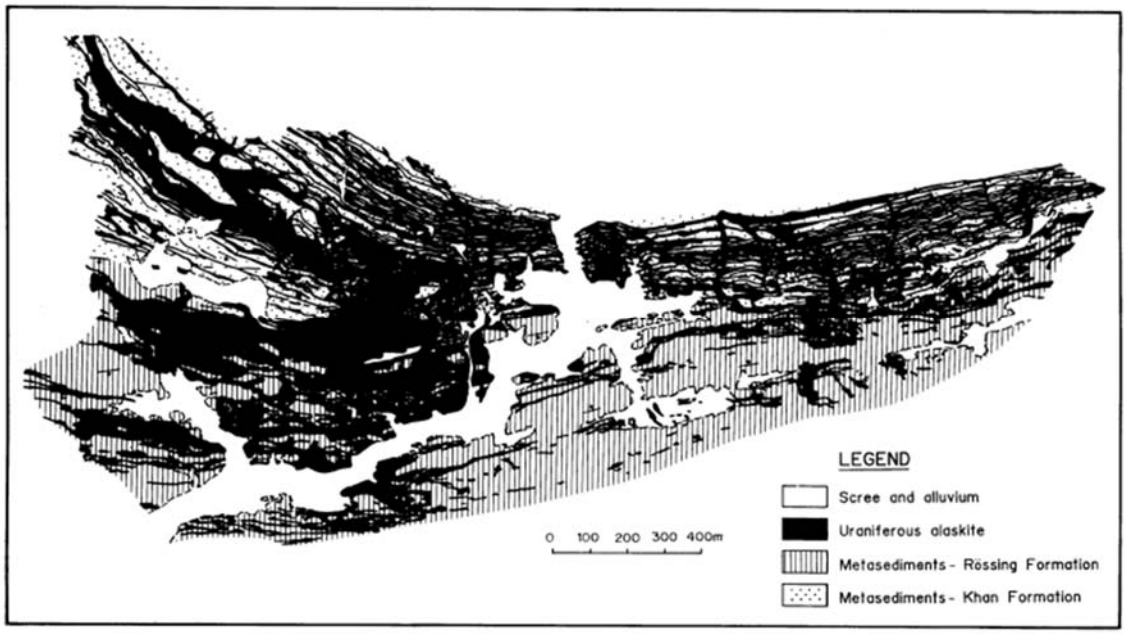

Figure 1.5: Generalised geological map of the RUL alaskite body (Berning, 1986)

In addition to the SJ pit (Figure 1.3), Rössing started mining a sub-anomaly (SK4) of an anomaly area (SK) located north east of the SJ pit in 2008 (Figure 1.6). The geology and mineralization of the SK area has been described in greater detail by Abraham (2009).

Figure 1.6: The location of the SJ and SK anomalies within the Rössing area (Rössing, 2007)

Uranium is hosted by a variety of different minerals in the RUL SJ deposit (Table 1.1): uraninite (65-80 % of total uranium), uranophane (20-30 %), betafite (2-4 %) and <0.2 % coffinite, brannertie and carnotite (Ryan, 2012a). The SK anticline contains 65 % betafite, 8 % uraninite and 27 % secondary uranium bearing minerals, whereas the SK4 syncline

contains 5 % betafite, 64 % uraninite and 31 % secondary uranium bearing minerals (similar to the SJ ore body with a slightly higher betafite concentration) (Abraham, 2009).

Uraninite ranges in grain size from a few micrometres to 2 mm and the bulk of it occurs in the 0.1 to 0.15 mm fraction (Vernon and Smit, 1985). Kesler and Fahrbach (1982) reported that the uraninite is mainly associated with grain boundaries and radial cracks in the rock forming minerals, exposing the uraninite grain faces. Leaching with sulphuric acid at a much coarser grind than expected was therefore, achievable at the time that their report was written. Uranophane occurs along cracks as thin films, as discrete crystals or in situ, i.e. replacing the original uraninite (Vernon and Smit, 1985).

Table 1.1: Uranium mineralogy (Ryan, 2013 and Barthelmy, 2012)

Mineral	% of total uranium in ore	Chemical Formula	Composition % U
uraninite	65 – 80	UO_2	88.2
uranophane	20 – 30	$Ca(UO_2)_2(HSiO_4)_2.5(H_2O)$	40.6
betafite	2 – 4	$(Ca,U)_2(Ti,Nb,Ta)_2O_6(OH)$	17.2
coffinite		$U(SiO4)_{1-x}(OH)_{4x}$	72.6
brannerite	<0.2	$(U,Ca,Ce)(Ti,Fe)_2O_6$	33.5
carnotite		$K_2(UO_2)_2V_2O_8.3(H_2O)$	52.8

Figure 1.7 depicts the gangue mineralogy of 6 typical rock types found in the Rössing deposit. The gangue mineralogy of the higher acid consuming ores (marble and amphibolite) comprise mainly of calcite (contained within the marble), Na- and K-feldspar orthoclase, quartz, hornblende (contained within amphibolite) and smaller portions of clay. The ore type fed into the RUL processing plant generally comprises a blend of the 6 rock types. This is illustrated by the first bar in Figure 1.7 showing the composition of a typical run of mine (ROM) ore sample that was taken from the leach feed in 2010.

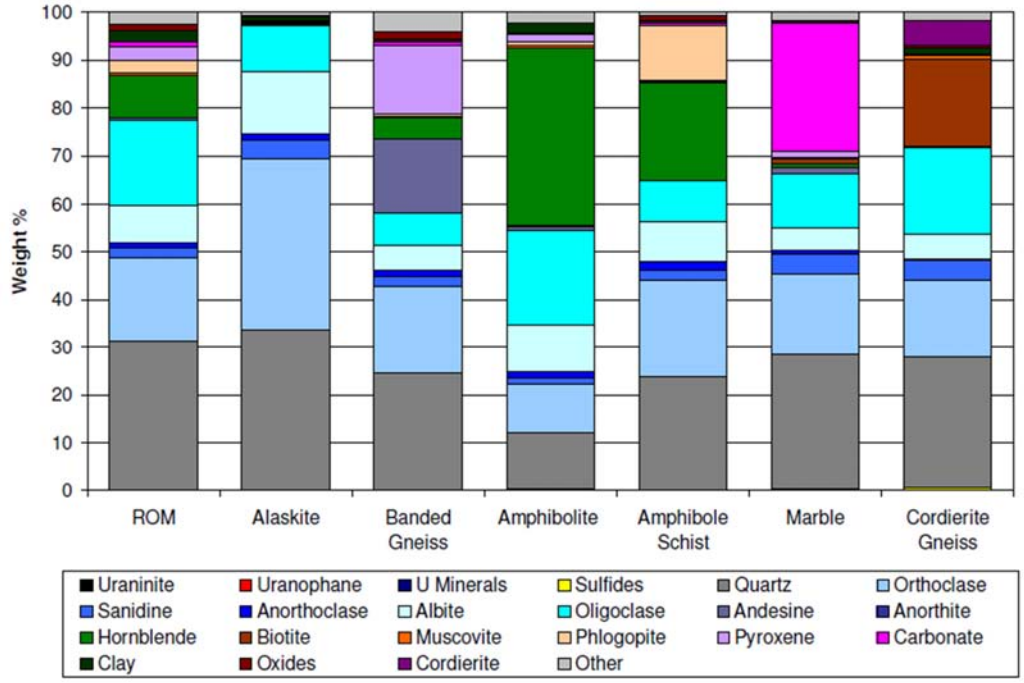

Figure 1.7: Gangue mineralogy of typical different rock types found in the Rössing deposit (Ryan, 2010)

1.3 The Rössing leaching process and chemistry

In the RUL leaching process, uranium is leached via (i) the oxidative acid dissolution of uraninite and (ii) the acid dissolution of uranophane. During the oxidative leaching of uraninite, insoluble U(IV) is oxidized by ferric (Fe^{3+}) to produce the soluble U(VI) species (equation 1):

$$UO_2(s) + 2Fe^{3+}_{(aq)} \rightarrow UO_2^{2+}_{(aq)} + 2Fe^{2+}_{(aq)} \quad [1]$$

The soluble U(VI) species then reacts with sulphuric acid to form uranyl sulphate complexes (equations 2 to 4) (Merritt, 1971):

$$UO_2^{2+}_{(aq)} + SO_4^{2-} \leftrightarrow UO_2SO_4 \quad [2]$$

$$UO_2^{2+}_{(aq)} + 2SO_4^{2-} \leftrightarrow [UO_2(SO_4)_2]^{2-} \quad [3]$$

$$UO_2^{2+}_{(aq)} + 3SO_4^{2-} \leftrightarrow [UO_2(SO_4)_3]^{4-} \quad [4]$$

Ferrous is regenerated to ferric via the reduction of MnO_2.

$$MnO_{2(s)} + 2Fe^{2+}_{(aq)} + 4H^{+} \rightarrow Mn^{2+}_{(aq)} + 2Fe^{3+} + 2H_2O \quad [5]$$

Uranophane exists as the U(VI) species and will therefore, readily dissolve in acidic solutions via equation 6 and also forms uranyl sulphate complexes via equations 2 to 4.

$$Ca(UO_2)_2(HSiO_4)_2.5(H_2O) + 6H^{+} \rightarrow Ca^{2+} + 2UO_2^{2+} + 2H_4SiO_4 + 5H_2O \quad [6]$$

The type of uranyl sulphate complex formed depends on acid and uranium concentration, temperature and other complex system variables. Table 1.2 provides the stability constants for these uranyl sulphate complexes at 25 ˚C and 1 bar pressure. A speciation diagram for an equimolar (UO_2^{2+}/SO_4^{2-}) solution is displayed in Figure 1.8. The dominant thermodynamic uranyl sulphate complex at a pH of 1.6 (average RUL leach pH) is UO_2SO_4 and $[UO_2(SO_4)_2]^{2-}$ is in the minority. Over the pH range 1 to 2 (RUL leaching system pH range), the ratio of UO_2SO_4 to $[UO_2(SO_4)_2]^{2-}$ increases as pH is decreased.

Table 1.2: Stability constants for the formation of uranyl sulphate complexes (Smith and Martell, 1976)

Reaction	**Log_{10} K_o (25 ˚C)**
$UO_2^{2+}_{(aq)} + SO_4^{2-} \leftrightarrow UO_2SO_4$	3.15
$UO_2^{2+}_{(aq)} + 2SO_4^{2-} \leftrightarrow [UO_2(SO_4)_2]^{2-}$	4.1
$UO_2^{2+}_{(aq)} + 3SO_4^{2-} \leftrightarrow [UO_2(SO_4)_3]^{4-}$	3.0

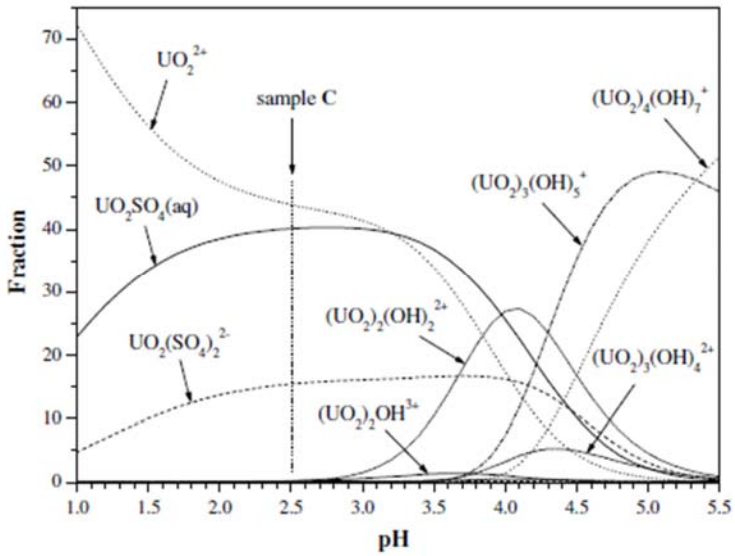

Figure 1.8: Speciation diagram for the uranyl sulphate system with increasing pH (0.05 M U(VI) and 0.05 M H_2SO_4) (Hennig et. al., 2007)

The RUL leaching process is depicted in Figure 1.9. The leaching plant consists of 2 trains of 6 leach reactors each (open to the atmosphere). Mill product (P_{80} = 1.1 mm) enters the leaching plant in a slurry form (73-75 % solids).

Conarc (an iron source) is added to the leach slurry in the first tank in each series (mixing tank). Conarc dust consists of haematite (Fe_2O_3, 64 %), magnetite (Fe_3O_4, 14 %), calcium oxide (CaO, 9 %), silica (SiO_2, 5 %), magnesium oxide (MgO, 4 %) and other metal oxides (<4 %). It is imported from an electric arc furnace/converter in South Africa. At RUL, conarc dust is slurried with water and then leached at 105 ˚C with sulphuric acid in a reaction vessel prior to adding it to the main uranium leach process (mixing tank). The temperature of the conarc leach is maintained by the exothermic reaction between sulphuric acid and water in the reaction vessel. Two key reactions take place within the conarc reactor (equations 7 and 8). The conarc slurry exiting the reactor contains iron in the ferric form, which is required in the oxidation of uraninite (equation 1). Iron (in the form of ferric and ferrous) is also present in the RUL ore. The leaching of this naturally occurring iron from the ore (within the RUL leach tanks) can result in iron concentrations of up to 2 – 3 g/L in solution. The total iron concentration is, therefore, measured in tank 2 (control tank) on an hourly basis. The flow of conarc from the reactor into the mixing tank is then adjusted manually, to achieve a total iron concentration between 4.2 and 5.0 g/L in the control tank.

$$Fe_2O_3 + 3H_2SO_4 \rightarrow Fe_2(SO_4)_3 + 3H_2O \qquad [7]$$

$Fe_3O_4 + 4H_2SO_4 \rightarrow Fe(SO_4)_3 + FeSO_4 + 4H_2O$ [8]

Concentrated sulphuric acid (H_2SO_4, 98 %) is added to the first (mixing) and second (control) leach tanks to achieve the required free acid concentration (or pH) in the control tank with the aim of maintaining a free acid concentration range in the terminal tank that is constrained by downstream processes (upper limit) and extraction value (lower limit). Sulphuric acid is consumed by several gangue minerals in the ore body, i.e. calcite and dolomite (accounting for ~50 % of acid consumption), amphibole (~26 %) and varying quantities of biotite, chlorite, apatite, pyrrhotite, goethite and titanomagnetite (Ryan, 2013). Uranium dissolution accounts for 1 to 2 % of the overall acid consumption.

A pyrolusite reagent (containing MnO_2) is slurried with water and added to the control tank to re-oxidise Fe^{2+} to Fe^{3+} via equation 5 and achieve the required oxidation reduction potential (ORP) set point in this tank. The pyrolusite reagent is sourced from Morocco as a milled concentrate (d_{80} = 40 µm) and contains ~86 % MnO_2, 2% Fe_2SO_3, 2% CaO, 1% MgO and ~10% other metal oxides. In this report "pyrolusite reagent" will thus refer to the reagent described in this paragraph.

The leach slurry then continues into the third, fourth, fifth and sixth leach tanks in series and exits the leach plant after tank six. No further reagents are added into tanks three to six.

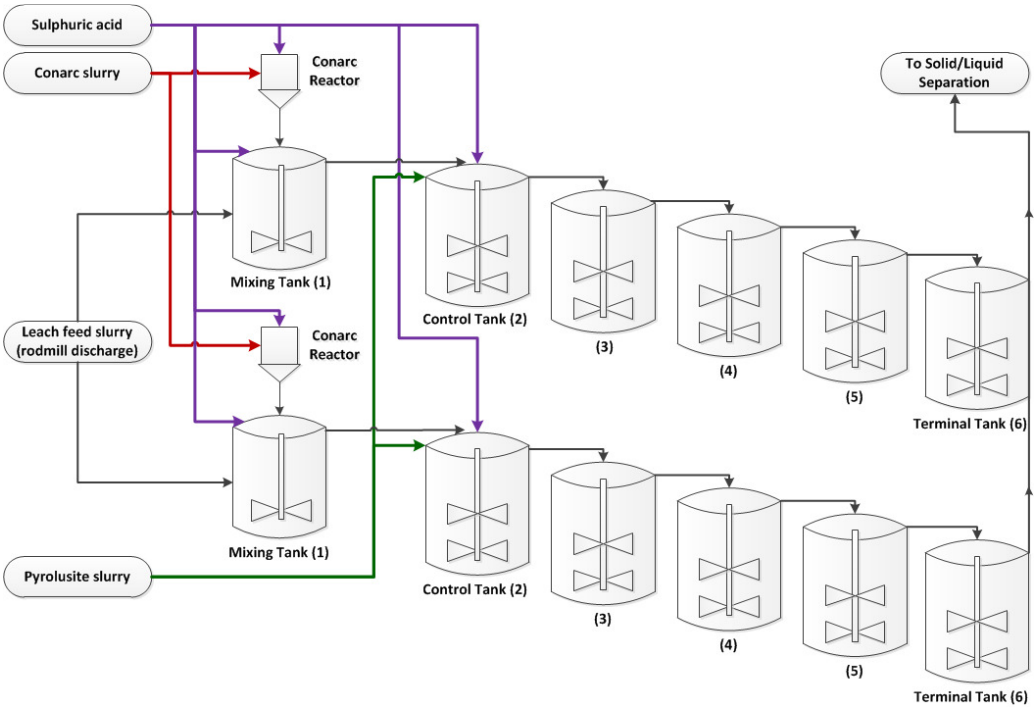

Figure 1.9: RUL leaching process

The following gangue minerals react with sulphuric acid in the leaching process:

Calcite: $CaCO_3 + H_2SO_4 + H_2O \rightarrow CaSO_4.2H_2O + CO_2$ [9]

Apatite: $Ca_5(PO_4)_3Cl + 5H_2SO_4 + 10H_2O \rightarrow 5CaSO_4.2H_2O + 3H_3PO_4 + HCl$ [10]

Sphene: $CaTiSiO_5 + H_2SO_4 + H_2O \rightarrow CaSO_4.2H_2O + TiO_2 + SiO_2$ [11]

Dolomite: $MgCa(CO_3)_2 + 2H_2SO_4 \rightarrow CaSO_4.2H_2O + MgSO_4 + 2CO_2$ [12]

Amphibole[4]*:* $Ca_2Mg_4FeSi_7AlO_{22}(OH)_2 + 2H_2SO_4 + 5H_2O \rightarrow 2CaSO_4.2H_2O + Mg_4FeSi_3AlO_9(OH)_8 + 4SiO_2$ [13]

Biotite: $2K(Mg,Fe^{2+})_3[AlSi]_3O_{10}(OH,F)_2 + H_2SO_4 \rightarrow K_2SO_4 + 2(Mg,Fe^{2+})_3[AlSi]_3O_{10}(OH,F)_2$ [14]

Chlorite: $(Mg,Fe)_5Al(Si_3Al)O_{10}(OH)_8 + 8H_2SO_4 \rightarrow 5(Mg,Fe)SO_4 + Al_2(SO_4)_3 + 3SiO_2 + 12H_2O$ [15]

Goethite: $2FeO(OH) + 3H_2SO_4 \rightarrow Fe_2(SO_4)_3 + 4H_2O$ [16]

Titanomagnetite: $2[Ti_{0.5}Fe^{2+}_{1.5}Fe^{3+}O_4] + 6H_2SO_4 \rightarrow 3FeSO_4 + Fe_2(SO_4)_3 + TiO_2 + 6H_2O$ [17]

Pyrrhotite: $Fe_{1-x}S + 2H^+ \rightarrow (1-x)Fe^{2+} + H_2S$ [18]

Pyrrhotite can also be dissolved through oxidative dissolution via equation 19.

$Fe_{1-x}S + (8 - 2x)Fe^{3+} + 4H_2O \rightarrow (9 - 3x)Fe^{2+} + SO4^{2-} + 8H+$ [19]

Evidence from field and laboratory studies (Steger, 1982; Jambor, 1986; Plysunin et al., 1990) suggests that reaction 19 does not, however, proceed to completion but instead produces elemental sulphur via equation 20.

$Fe_{1-x}S + (2 - 2x)Fe^{3+} \rightarrow (3 - 3x)Fe^{2+} + S^0$ [20]

[4] Rössing amphiboles are predominantly hornblende with a small amount of tschermakite (Ryan, 2012).

As a result of the dissolution of gangue minerals in the leaching process, the following half-cell reactions could potentially take place within the leaching circuit:

As a result of apatite dissolution:

$Cl_2 + 2e^- = 2Cl^-$ ($E^0 = 1.36$ V) [21]

From a thermodynamics perspective, it is unlikely that the presence of Cl^- will compete with Fe^{2+} in the reduction of MnO_2 to Mn^{2+} (E^0=1.33 V) as their E^0 values are very similar (1.36 and 1.33 V) and the driving force would, therefore, be very small.

As a result of pyrrhotite dissolution:

$S + 2H^+ + 2e^- = H_2S$ (E^0=0.17 V) [22]

In the Rössing leaching process, it is not certain which reaction mechanism is responsible for the dissolution of pyrrhotite (equations 18 or 20). In the case that pyrrhotite is leached by ferric (equation 20, $Fe_{1-x}S$ scavenges for Fe^{3+}); the effect of this would be an increase in the oxidant demand of the ore type to attain the target ORP of the leach. In the case where pyrrhotite is dissolved by sulphuric acid, H_2S is formed. H_2S could then react with MnO_2 (E^0 for H_2S = 0.17 V). In both cases the presence and dissolution of pyrrhotite could, therefore, have the effect of increasing the oxidant requirement for the ore to attain a certain ORP target in the leach.

As a result of biotite, pyrrhotite or amphibole dissolution:

$Fe^{3+} + e^- = Fe^{2+}$ (E^0=0.77 V) [23]

An increase in the concentration of Fe^{2+} in solution (from the dissolution of minerals such as biotite, pyrrhotite and amphibole) has the potential to lower the ORP in the leaching circuit. To achieve a certain ORP set point in the control tank, it is likely that a larger quantity of pyrolusite (oxidant) would be required at elevated concentrations of these mineral types.

No documented evidence could be found on test work conducted to establish whether the above redox reactions will take place within the Rössing leaching circuit. A thermodynamic analysis (using standard electrode potentials) of the reactions does, however, indicate that some of these redox reactions could indeed be plausible. Further test work would need to be conducted to establish the kinetics of these reactions (within the residence time of the Rössing leach circuit). The above list of potential redox reactions within the Rössing leaching circuit is also by no means exhaustive. It does, however, illustrate that several competing

reactions could take place within the circuit, depending on the concentrations of specific minerals in the ores treated by the plant. These competing reactions could hamper the regeneration of Fe^{2+} to Fe^{3+} and also the oxidation of UO_2 itself.

1.4 Historical RUL leach operation and control

1.4.1 Inherent control philosophy

In the past, the RUL leach control philosophy was based on operational experience. An experienced operator was required to make process control adjustments, i.e. start/stop the addition of conarc or pyrolusite to achieve the required total iron and ORP set points and adjust the control tank conductivity set-point to achieve a specific free acid concentration in the terminal tank. With a change in ore type, additional sulphuric acid also had to be added into the terminal tank if the control tank conductivity set point was not adjusted in time to cater for the different ore type, resulting in inefficient leaching in tanks three to five and the wastage of acid in the terminal tank. The inherent problem with this methodology was the lack of standardization, i.e. control responses to process deviations varied widely depending on the experience and opinion of the operator on shift. This contributed greatly towards variability in attaining plant set-points (i.e. reagents were frequently dosed in excess or deficit, leading to reduced average extraction and increased costs). This method of operation also hindered the development of an understanding of the influence of ore or process conditions on the leach circuit (Prasad et al., 2012).

To overcome the challenges associated with the control philosophy (section 1.4.1) a new leach control philosophy (LCP) that standardised operator responses to process deviations, was developed and implemented in 2012.

1.4.2 Control of reagent addition

The effective leaching of uraninite requires oxidizing conditions in the leach circuit. Historically, at RUL, oxidizing conditions have been achieved via the addition of conarc and pyrolusite. ORP during leaching is controlled by measuring ferric and ferrous concentrations in the control tank and adding pyrolusite to the control tank if the ratio of ferric to ferrous drops below a certain point (ORP can be related to the concentration of ferric and ferrous ions via the Nernst equation and is later defined in this work). Samples are taken from the upcomer every 20 minutes in the control leach tank via an automatic sampling system,

filtered and titrated for ferric and free acid concentrations (without manual intervention). Ferrous titrations are, however, conducted manually (the auto-titration system is limited to ferric and acid titrations only). Samples are also taken and analysed from the terminal tank every 60 minutes in the same manner. Data is transmitted to central process control (CPC) and the control operator is then required to take the necessary control action, e.g. start/stop the pyrolusite pump (if the ferric to ferrous ratio is not in range) or start/stop the addition of conarc (if total iron is not in range).

The inherent problems with this method of pyrolusite and conarc addition lie in the following:

- Control actions can only be taken every 20 minutes (limited by sampling methodology). The time taken to extract, filter and analyse a sample from a leach tank is close to 20 minutes, resulting in a 20 minute delay in measurement. The average residence time of a leach tank is ~100 minutes.
- Control actions are dependent on the operator.
- This has resulted in variable ORP control (±80 mV, 95 % confidence interval).

Acid concentration during leaching is controlled by measuring conductivity in-situ. A proportional-integral-derivative (PID) controller controls the conductivity in the control tank (opening/closing of acid control valves) to the required set-point. As with ferric concentration, free acid is also measured every 20 minutes via the auto-titration system. If free acid concentration is found to be out of range, the conductivity set-point has to be adjusted.

The inherent problem with this method of sulphuric acid addition lies in the following:

- Conductivity is a measure of an electrolyte solution's ability to conduct electricity, i.e. the ionic content of the solution (including H^+). Conductivity can be correlated to the concentration of H^+ ions in the leach slurry, but is influenced by interferences from other ions in solution (dissolution of cations in acid side reactions, section 1.3). The conductivity of the leach solution could, therefore, remain constant or even increase but the free acid concentration would decrease as a result of the consumption of acid by gangue minerals. This problem can be seen in the fact that the conductivity set point has to be changed from time to time (if the free acid concentration titration result is found to be out of range).

To overcome the problems with the current control of reagent addition to the plant (section 1.4.2) and to further improve on the new LCP, an online pH/ORP control system will be commissioned in the Rössing leaching plant in 2014. The system will involve the direct

measurement of pH (instead of conductivity) and ORP in the control tank, linked to a PID controller which controls the flow of sulphuric acid and pyrolusite reagent to the leaching circuit.

1.4.3 Selection of operating set points

Leach set-points (pH, ORP and total iron concentration) for the RUL leaching process are available, but the basis for selection is not well known. A method to reliably determine leach set-points, that maximize net revenue, is not available.

1.5 Research Objectives

This project aims to achieve the following objective:

To determine the impact of varying leach parameters on different ore types and in so doing develop improved (in terms on maximizing net revenue) set-points for plant-scale implementation.

In particular, this project will focus on the effect of ferric to ferrous ratio or oxidation-reduction potential (ORP), a controllable leach variable, on leaching efficiency. An economic trade-off study between uranium extraction and reagent consumption will be conducted to determine whether operating at an ORP higher than currently implemented at RUL will be economically viable.

1.6 Thesis scope and structure

This project is part of a broader leach optimization program at RUL that was initiated to maximise value delivered from the leaching plant. The focus is on the third phase of this program, i.e. the development of a laboratory test program use of a techno-economic model to determine the relative economic benefits of alternative and improved operating set-points. The study is limited to the investigation of uranium leaching factors that can be varied with minimal capital modifications to the RUL leaching process. The scope of this project includes the following key steps:

1. Literature review to help understand which controllable variables are likely to have the most impact on uranium leaching efficiency.

2. The development of a laboratory-scale, agitated batch leach test.

3. The use of a techno-economic model that fits batch leach data to empirical models and combines this with the exit age residence time distribution function and RUL operational data to determine the impact of set point changes on overall leach value.

4. The development of a method that can be used to select improved set points for the RUL leaching plant for a given ore type, equipment availability and economic environment.

Figure 1.10 illustrates the structure of the thesis. Chapter 1 provides the introduction and background to the study and outlines the research objectives and scope. Chapter 2 contains a literature review on the factors that impact uranium tank leaching, RUL uranium mineralogy and the use of techno-economic modelling. The experimental methods and development of the RUL leach circuit techno-economic model are presented in Chapter 3. The batch leach experimental results are firstly presented and discussed in Chapter 4. Chapter 5 applies the model to the experimental results from chapter 4 to determine the impact of varying the studied process parameters on the overall economic value of the RUL leach process. Chapter 6 summarizes the conclusions and recommendations from the study.

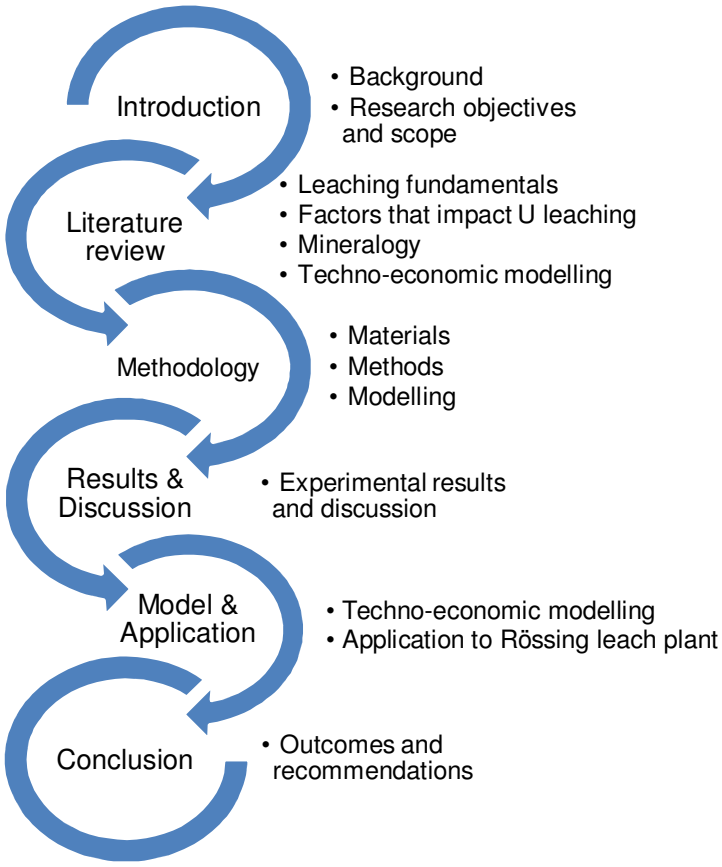

Figure 1.10: Schematic flow chart of the thesis structure

2 Literature review

2.1 Overview

A literature review was conducted to understand the fundamentals of leaching and the factors that impact uraninite and uranophane tank leaching. A summary of mineralogical studies conducted on Rössing leach slurries is provided as well as the opportunities identified through this work for improving leach extraction. The review then presents the concept of techno-economic modelling and its potential application to leach optimization.

2.2 Leaching fundamentals

Leaching is an extractive metallurgical process, used to extract a valuable soluble component (e.g. precious metal) from a solid through dissolution in a solvent. The industrial leaching method used to extract the component is dependent on several factors which impact the economic design of the process, i.e. the concentration of the component in the solid, the distribution thereof throughout the solid, the particle size of the component and the nature of the solid (Richardson et al., 2002). In uraninite leaching, the mineralogical characteristics, such as bulk composition, uranium mode of occurrence (grain size) and mineral composition of the ore greatly influence the extraction of uranium from the ore (Ram et al., 2013 and Lottering et al., 2008).

Figure 2.1 illustrates the three steps of leaching (Richardson et al., 2002). The required component dissolves (A) in the solvent and then diffuses (B) through the solvent in the pores of the solid to the outside of the particle. The dissolved component (solute) is then transferred (C) from the solid surface to the main bulk of the solution.

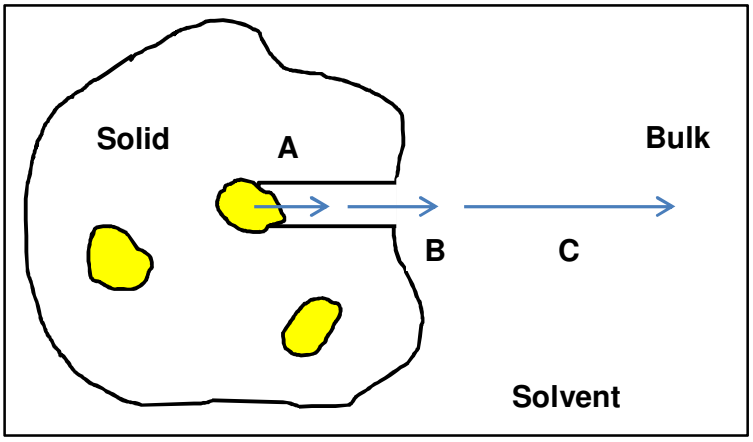

Figure 2.1: A schematic representation of the three steps of leaching

The rate at which any of these three steps takes place can impact the overall rate of extraction of the process. The step which governs the overall reaction rate is called the rate-determining (or limiting) step. The selection of the equipment to be used in the leaching method is dependent on which of these is the rate limiting step. The goal would be to enhance that particular step which limits the overall reaction and therefore, increase the overall rate of extraction. E.g. if step C were the rate limiting step in a tank leach scenario then enhancing agitation of the leach slurry could increase the transfer of the dissolved species from the solid surface to the bulk of the solution and consequently increase the overall rate of the dissolution reaction. Enhancing a particular step may, however, also have a negative economic impact on the process, e.g. in the case of acid leaching of uraninite bearing ores, where the leachable uranium is associated with other gangue minerals such as calcite. In this case, to increase the extraction rate of uranium by decreasing particle size, enhancing mixing in the tanks or increasing temperature, the rate of dissolution of calcite would also be enhanced, resulting in increased acid consumption. This would affect the overall economics of the process. When selecting the equipment and process set points for a leaching process, it is thus imperative that the economics are also considered.

At Rössing, a tank leaching method is applied to leach uranium (solute) from the ore (as described in the introduction). The factors that impact tank leaching efficiency have been reviewed and are discussed in the following section.

2.3 Factors that impact uraninite and uranophane leaching in tanks

In 1990, Johnson published an article which summarized the development of key operational principles employed by Rössing, to maximise uranium leaching efficiency and optimize the economics of the process over the first 14 years of operation. Early test work conducted by Mintek in the 1970's identified ferric concentration and temperature as two of the most important variables to consider in maximising uranium leach extraction. Heat used to be supplied to the Rössing leach process via heat exchangers at the rod mills, from steam off-take from the sulphuric acid plant on site. During the time that the acid plant was in operation, ferric was supplied to the leach process via the addition of calcine (a by-product of the sulphuric acid production plant at RUL which contained Fe_2O_3). The acid plant burned pyrite to produce sulphuric acid until 1997 and was later converted to burn sulphur. The conversion to sulphur meant that the ferric source had to be substituted. In 2000 the acid plant was decommissioned as the imported acid price fell below the onsite production cost. This meant the removal of heat to the leach process. Presently, no additional heat is added to the Rössing leach process and ferric is now added in the form of conarc, as described in the previous section.

In an attempt to identify the most important variables that affect the RUL leaching process, Kesler and Farbach (1982) reviewed the effect of ferric and temperature on leach extraction by conducting a statistical analysis of plant data during the first half of 1980. This analysis yielded the following regression equation:

$$\%\ \text{Leach extraction (over 10 hours)} = 91.25 + \frac{(7.7\text{F} + 0.4\text{T} - 49.5)}{\text{G}}\ 100 \qquad [24]$$

Where F = Ferric concentration in g/L,

T = Leach temperature in °C and

G = Head grade in ppm U_3O_8.

Over the range of parameters evaluated[5], this relationship also indicated that % uranium extraction was dependent on ferric concentration (an increase in ferric concentration from 1.0 to 1.5 g/L resulted in a 1.3 % increase in leach extraction) and to a lesser extent temperature (a 1.3 % increase in leach extraction required a 10 °C increase in leach

[5] It is unclear over which parameter ranges this equation is valid. The author of this work does, however, make reference to the standard plant conditions during the time that the plant data was referenced (50 °C and 0.8 – 1.5 g/L Fe^{3+}). It is, therefore, assumed that this equation is valid for these conditions.

temperature). Further statistical and laboratory studies indicated that an increase in leach temperature (within the 10 hour total residence time in the leaching plant) or an increase in residence time would result in significant increases in acid consumption for a small increase in leach extraction. This was an important observation as it indicated that after 10 hours of leaching, uranium extraction was close to its maximum and any variations in leaching parameters would only have small effects on uranium extraction at the expense of additional acid consumption. At this point in time, changing the ferric concentration was concluded to be the most effective way to increase leach extraction.

Other factors that are known to impact uranium leach extraction are particle size, leach mixing efficiency (agitation), the concentration of ions in the leach slurry (due to the dissolution of gangue), pH (free acid concentration), ORP (ferric/ferrous ratio), pulp density and uranium mineralogy (i.e. concentration of refractory minerals) (Merrit, 1971).

Several journal articles that investigate the effect of these variables on uranium leach extraction were reviewed. Section 2.3 summarizes the key findings from this review.

In this literature review, the percent uranium extraction or dissolution refers to the final % of uranium extracted (or the overall yield) over a certain period of time (i.e. the final point on the uranium extraction curve). The rate of uranium extraction or dissolution is defined as the rate at which uranium dissolves into solution over time (i.e. the slope of the uranium extraction curve).

2.3.1 Residence time

Residence time is defined as the amount of time that leach slurry is retained in a leaching circuit and exposed to leaching reagents. Residence time will impact the final % uranium extraction and reagent consumption in a leaching process. In some cases, a uranium extraction curve will plateau after a certain amount of time, whereas acid continues to be consumed by slower reacting gangue minerals. An economic optimal residence time is, therefore, generally selected, i.e. the optimal point may occur at the start of the extraction curve plateau or sometime before it, depending on the economic returns of the process.

At RUL, residence time is affected by several variables. The number of tanks online has the most significant impact on residence time (i.e. the mixing tank, tank 1 has an average residence time of 25 minutes and tanks 2 to 6 have an average residence time of 105

minutes each). If a leach tank (tank 2 to 6) is taken offline for maintenance, residence time is decreased by 105 minutes. Leach feed flow rate has a lesser effect on residence time. An increase in 40 t/h in the leach feed flow rate will result in a ~10 minute decrease in leaching residence time. Fillet[6] build-up in the RUL leach tanks is a regular occurrence in the larger tanks (tanks 2 to 6). The RUL leach tanks operate with an average fillet height of 1.9 m in tanks 2 to 6. An increase in fillet height of 0.5 m would, however, only result in a 3 minute decrease in residence time. Fillet height, therefore, has the lowest impact on residence time. The total leach residence time for each leach module at RUL is on average 445 minutes (at 1000 t/h per module and with 5 tanks online).

2.3.2 Particle size

A decrease in the particle size distribution of an ore can result in (i) an increase in mineral liberation[7] and therefore, an increase in the interfacial area of contact between the solvent and the solid and (ii) a reduction in the distance that a solvent needs to penetrate into the particles, to gain access to secluded pockets of solute (Richardson et al., 2002). The result of this is, therefore, an increase in the rate of extraction of the solute from the solid. Overgrinding may, however, result in the increase of fine particles and consequently an increase in slurry viscosity (Huynh et al., 2000, He et al., 2004 and 2006) which could negatively impact the rate of leach extraction (Merrit, 1971).

It is important to note that for a constant particle size, the degree of liberation may vary for different ore types, thus resulting in varying degrees of uranium dissolution for different ores (at a constant residence time).

Ram et al. (2013) studied the effect of particle size on uranium extraction from two natural uraninite samples sourced from the Palette and El Sharana mines, both located in the South Alligator Rivers region, Northern Territory, Australia. The results indicated that decreasing particle size, from 75 - 38 µm to <20 µm, increased the % uranium dissolution (over 90 min) for both samples. This was thought to be attributed to the liberation of trapped uraninite. No information on the effect of particle size reduction on gangue mineral dissolution was presented.

[6] The stagnant zone within the leach tank comprising of >90% settled solids.
[7] Liberation can be defined as the release of valuable minerals from their waste gangue minerals. A liberated particle consists only of the mineral of interest. Particles that do not consist of any mineral of interest are referred to as 'barren' (Wills, 1992).

Roshani and Mirjalili (2009) investigated the effect of particle size over the range 88 to 840 µm on leach extraction (6 hour batch leach tests) of an ore containing uranium in the form of coffinite and found a steady increase in uranium extraction up to 177 µm, which was found to be the optimal particle size for maximizing extraction, i.e. no further improvement in leach extraction was noted at a particle size less than 177 µm. They also commented on the downstream considerations that need to be taken into account when grinding to a finer particle size, i.e. difficulty in solid-liquid separation.

The particle size distribution of the Rössing leach feed (i.e. mill product) is relatively coarse, d_{80} = 1.1 ±0.1 mm (28 ± 3 % < 850 µm) (Ismet, 2013). The open circuit milling plant is comprised of rod mills which are designed to mill to a specific product. Plant trials have been conducted in the past to establish the effect of reducing the mill throughput on the mill grind. One particular trial (Johnson, 1990) involved reducing mill throughput from 500 t/h to 450 t/h for 11 days on one module and the effect on grind size established. This was repeated on the second module for 11 days. In both cases no change in grind size was noted for a decrease in mill rate from 500 to 450 t/h. The rod mills operate within a range of 1000 to 1200 kW (this is controlled by adding rods to the mills if the power draw drops below this range). In the 1980's a plant trial was conducted to establish the effect of power draw on rod mill grind. Within this power draw range tested, no measurable change in grind size was noted (Johnson, 1990).

Particle size distribution is not a parameter that can be significantly altered without making physical modifications to the plant, e.g. recycling of oversize material via the conversion of the current circuit into a closed circuit milling plant or the replacement of the rod mills with SAG mills. The leach optimization program is focused on parameters that can be altered quickly (< 2 month) and at a low cost. This study will therefore, not include test work on the effect of particle size distribution on uranium extraction and reagent consumption. Given the known effect of particle size on leach extraction, it will, however, be important to maintain a constant particle size distribution between samples used for leach test work. A rigorous sample preparation (i.e. blending and splitting) program will, therefore, need to be applied.

2.3.3 Temperature

The rate of extraction of a mineral can be influenced by temperature via the following: (i) the solubility of a mineral will generally increase with temperature and (ii) the diffusion coefficient will be expected to increase with an increase in temperature (Richardson et al., 2002). An increase in solubility or the rate of diffusion could, therefore, result in an increase in the rate

of leach extraction. Increasing the reaction rate will, therefore, decrease the reaction time required and subsequently increase the capacity of equipment. Increasing temperature also has the ability to improve extraction from refractory minerals (Merrit, 1971). An increase in temperature also results in increased reagent consumption due to the dissolution of other gangue minerals (Ring, 1980) and increased corrosion of equipment (Merrit, 1971).

Several studies on the effect of temperature on uranium extraction have been conducted. The study by Ram et al. (2013) of natural Australian uraninite ores, revealed a systematic increase in the rate of uranium dissolution with a consistent increase in temperature (35 – 95 °C at intervals of 15 °C, over a residence time of 90 min). Eligwe et al. (1982)[8] and Roshani and Mirjalili (2009)[9] reported an increase in the rate of and final % uranium extraction with an increase in temperature, but at the expense of increased acid consumption due to an increase in the dissolution of gangue minerals at higher temperatures. Ring (1980) noted a slight increase in the % uranium extraction with temperature (over a residence time of 24 hours), at the expense of a significant increase in acid consumption (a 50 °C leach required 25 kg/t more sulphuric acid than a 40 °C leach to maintain pH at 1.5). Lottering et al. (2008) did not find that a change in temperature from 40 to 60 °C produced a noticeable effect on % uranium extraction (over a 24 hour leaching period). A conclusion from the assessment of this literature is that an increase in temperature can be expected to increase the rate of uranium extraction. As the leaching time (residence time) is decreased, an increase in temperature would be expected to have more of an impact on the final % uranium extraction. For the Rössing leach circuit operated at a residence time of 445 min (7.4 hours), temperature is expected to have an effect on the % uranium extraction achievable within this time frame (Kesler and Farbach, 1982).

The Rössing mine is situated in the Namib Desert and the ambient temperature varies between an average maximum of 25 ˚C in winter and 30 ˚C in summer (an average minimum of 10 ˚C in winter and 14 ˚C in summer). The tank leaching process at Rössing is open to the atmosphere. The leach slurry temperature is on average 35 °C and is susceptible to natural temperature fluctuations (i.e. day versus night and summer versus winter). The leach slurry temperature can vary between 30 and 40 °C. Apart from the effect of the ambient climate on the leach temperature, another constant source of heat to the leach process is the heated conarc slurry (~105˚C) which is added to the leaching process in the mixing tank. The only other constant source of heat comes from the heat of reaction

[8] % uranium extraction (yield) was determined after 4 hours of leaching.
[9] % uranium extraction (yield) was determined after 6 hours of leaching

between sulphuric acid and water (exothermic reaction) when it is added to the leaching process in tanks 1 and 2 (this is, however, minimal). The temperature of the Rössing leach is, therefore, not considered to be a controllable variable at this point in time. Although temperature cannot be controlled in the leach circuit, it needs to be taken into consideration when determining optimal operating conditions. If optimal operating conditions are selected based on value delivered (i.e. uranium extracted at the cost of reagents consumed), the set of optimal operating conditions required for summer may be different to that required for winter. An increase in leach slurry temperature in the summer could result in increased uranium extraction at a certain set of conditions for a given residence time, but at the cost of increased acid consumption due to increased gangue mineral dissolution. A less aggressive pH set point may, therefore, be selected for summer, to counteract the effect of increased gangue mineral dissolution, but still maintaining the required uranium extraction (due to the higher leach slurry temperature). Although this is an interesting concept to test, the value in doing so needs to be taken into account. The question that needs to be answered prior to conducting this test work is, will a notable change in uranium extraction and acid consumption be seen when the leach temperature is increased by 10 ℃ (within the limits of the current Rössing leach residence time)?

2.3.4 The effect of acid concentration and pH

Uranium ores generally comprise several acid consuming gangue minerals such as calcite ($CaCO_3$), chlorite in the form of chamosite ($(Fe_5Al)(AlSi_3)O_{10}(OH)_8$) or chlinocore ($(Mg_5Al)(AlSi_3)O_{10}(OH)_8$), pyrrhotite ($Fe_{(1-x)}S_{(x=0-0.17)}$) and apatite ($Ca_5(PO_4)_3Cl$). Maintaining a free acid concentration that is sufficient to dissolve the uranium minerals without dissolving excessive amounts of gangue minerals is an important objective of the leaching process. Maintaining the correct free acid concentration is also important to ensure that re-precipitation of the uranium does not occur (Merrit, 1971).

The rate of uranium extraction can be expected to increase with a decrease in pH and increase in free acid concentration (according to equations 2 – 4). Eligwa et al. (1982) found that % uranium extraction increased with a decrease in pH from 4 to 8 (over a 4 hour leach). Lottering et al. (2008) also found that acid dosage (9.9 to 16.3 kg/t) had the greater effect on uranium extraction (over 24 hours), when compared with the effect of temperature on uranium dissolution, 40 to 60 ˚C (ore sample contained brannerite, U-phosphate, uraninite and coffinite). This suggests that reaction rate was mass-transfer controlled over this range (40 to 60 ˚C) (either internal or external).

At a sufficiently high (non-limiting) free acid concentration, however, the rate of uranium extraction could be determined by the rate of competing reactions such as equations 9 to 18 and 20 (depending on the type of uranium mineralization). Ram et al. (2013) found that the rate and % of uranium dissolution was independent of H_2SO_4 concentration over a range of 0.015 M to 0.7 M, which most likely indicates that acid concentration was not rate limiting over this range.

During a cost reduction exercise at Rössing in 1988, the effect of reducing the terminal acid concentration in the leach train, on uranium extraction and reagent consumption was evaluated in a plant trial. Prior to the plant trial, a belief existed that uranium would precipitate as uranyl phosphate at a terminal acid concentration below 2.5 g/L. Laboratory test work found that no uranium precipitate formed within a pH range of 1.76 and 3.35 (approximately equal to a free acid concentration range of 3.1 to 0.1 g/L). A loss in ferric was, however, noted and it was concluded that ferric had precipitated as ferric phosphate. Further laboratory test work confirmed that at a terminal acid concentration of 1.2 g/L, uranium extraction decreased by 1.1 %. Above an acid concentration of 1.5 g/L, the decrease in uranium extraction was found to be negligible. During the plant trial in 1988, where the terminal acid concentration was reduced from 3.2 to 2 g/L, a reduction in % uranium extraction of 0.26 % and a reduction in acid addition of 1.3 kg/t was noted (Johnson, 1990). At that point in time, the strategy was implemented due to the fact that, at that stage, the reduction in reagent addition was worth more than the loss in uranium extraction.

Another important aspect to consider in terms of the effect of pH on uranium leaching is the effect that it has on the solubility of ferric ions. To prevent ferric precipitating as ferric hydroxide (Bhappu et al., 1969), a pH of less than 2.5 is required. At a pH below 2.0, the formation of the most effective ferric complex, $FeSO_4^+$, is favoured (Nicol et al., 1975 and Ring, 1980).

2.3.5 ORP (Indicated by the ratio of $[Fe^{3+}]$ to $[Fe^{2+}]$)

The oxidative dissolution of UO_2 via ferric can be written as two half reactions (equations 25 and 26), the sum of which equates to equation 1. The oxidation of UO_2 is mediated by the ferric/ferrous couple which serves as an electron transfer catalyst between MnO_2 and UO_2 (equation 5). Figure 2.2 illustrates the specific Eh-pH window in which the UO_2 dissolution reaction occurs in a sulphate system.

Anodic reaction: $UO_{2(s)} \rightarrow UO_2^{2+}{}_{(aq)} + 2e^-$ [25]

Cathodic reaction: $2Fe^{3+}{}_{(aq)} + 2e^- \rightarrow 2Fe^{2+}{}_{(aq)}$ [26]

$MnO_{2(s)} + 2Fe^{2+}{}_{(aq)} + 4H^+ \rightarrow Mn^{2+}{}_{(aq)} + 2Fe^{3+} + 2H_2O$ [5]

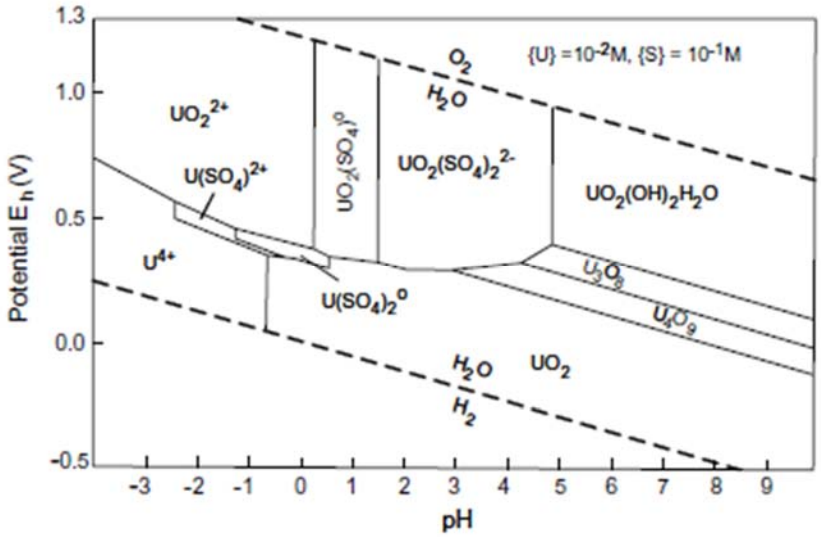

Figure 2.2: Eh/pH diagram of a U–S–H_2O system @ 25 _C (Hayes, 2003).

It is generally accepted that the electrochemical model of the leaching process can be used to quantitatively and qualitatively describe the leaching behaviour of UO_2 (Nicol, 1980). Three models which describe the leaching of UO_2 with Fe^{3+} over different Fe^{2+} concentration ranges were presented in the work by Nicol et al. (1975). At low Fe^{2+} concentrations, the rate of UO_2 leaching was found to be independent of Fe^{2+} concentration (i.e. Rate $\propto [Fe^{3+}]^{0.73}$). For the case where Fe^{2+} concentration is significant, the rate is proportional to the square root of the Fe^{3+}, Fe^{2+} ratio (i.e. Rate $\propto ([Fe^{3+}]/[Fe^{2+}])^{1/2}$. For the case where Fe^{2+} concentration is much greater than the Fe^{3+} concentration, the rate is proportional to the ratio of Fe^{3+} to Fe^{2+} (i.e. Rate $\propto [Fe^{3+}]/[Fe^{2+}]$).

The Oxidation Reduction Potential (ORP) can be defined as the potential (mV) of an inert metallic electrode measured in a system of oxidants and reductants. It is a measure of the tendency of the solution to gain or lose electrons when a new species is introduced. A silver/silver chloride electrode (a partially anodized silver wire immersed in a solution of potassium chloride) is commonly used to measure the ORP of a solution.

In uranium sulphuric acid leaching processes, changes of oxidation state occur in some elements taking part in the reactions, resulting in changes in the solution ORP. The Nernst equation relates the equilibrium ORP of a half-cell in an electrochemical cell to the activity of the half-cell reaction. In dilute solutions, concentrations can be used instead of activities. For the Fe^{3+}/Fe^{2+} half-cell reaction, the Nernst equation relates the ratio of Fe^{3+} and Fe^{2+} concentrations to the solution potential as follows (Sommer, et al., 1973):

$$E_c = 397 + 0.1984.T \log_{10} \frac{[Fe^{3+}]}{[Fe^{2+}]} \quad [27]$$

Where E_c = solution potential relative to saturated calomel electrode at 35 ℃

T = temperature (K)

[ ] = molar concentration

At 35 ˚C, equation 27 simplifies to:

$$E_c = 397 + 61.11 \log_{10} \frac{[Fe^{3+}]}{[Fe^{2+}]} \quad [28]$$

For Rössing process solutions, the following relationship was found to exist between ORP and ferric/ferrous ratio, relative to a saturated calomel electrode at 35 ℃ (Morkel, 2013):

$$ORP = 404 + 28 \ln \frac{[Fe^{3+}]}{[Fe^{2+}]} \quad [29]$$

The parameters in the equation fitted to data obtained from measuring Rössing process solutions (29) are very similar to those in the Nernst equation (28). Both equations clearly demonstrate the effect of Fe^{3+}/Fe^{2+} ratio on the solution ORP, i.e. the higher the Fe^{3+} concentration and the lower the Fe^{2+} concentration, the higher the ORP and vice versa.

The effect of ORP, Fe^{3+}, Fe^{2+} and total Fe concentration on uraninite extraction has been studied by several authors. Ring (1980), studied the effect of (i) adding ferric sulphate to the leach liquor and (ii) controlling redox potential via the addition of pyrolusite on the rate of uranium extraction. Leaching with ferric sulphate solution was found to lower acid consumption. The initial rate of uranium extraction was increased (final uranium extraction, after 24 hours, was not affected). The ore tested contained both uraninite and brannerite.

Roshani and Mirjalili (2009) tested the effect of ferric chloride concentration on uranium dissolution and found that the % uranium dissolution (after 6 hours) increased with an increase in ferric chloride concentration. A uranium dissolution optimum was found to exist at 3 M ferric chloride. The effect of ORP was also explicitly tested by varying the addition rate of MnO_2 (0 to 20 kg/t) resulting in an ORP range of 350 to 580 mV. % uranium dissolution was again found to increase with an increase in MnO_2 addition rate and a uranium dissolution optimum was found at 5 kg/t (corresponding to an ORP of 480 mV, the electrode type was not specified).

Ram et al (2011) found that over the range 460 to 565 mV (Ag/AgCl), a small change in total Fe was found to significantly increase the rate of uranium dissolution for a synthetic uraninite sample (Figure 2.3). At lower ORP values (420 and 380 mV) a significantly lower dependency was found. The dependence of the rate of uranium dissolution on total Fe was found to be at a maximum for a solution with an ORP >420 and ≤460 mV. The rate of uranium dissolution was found to increase linearly with an increase in Fe^{3+} concentration. In 2013, further test work was conducted on natural uraninite ore samples (Ram et al., 2013) where the rate and % uranium dissolution (over 90 min) was determined to increase with an increase in ORP (range: 380 – 565 mV, Ag/AgCl) and with an increase in total Fe concentration.

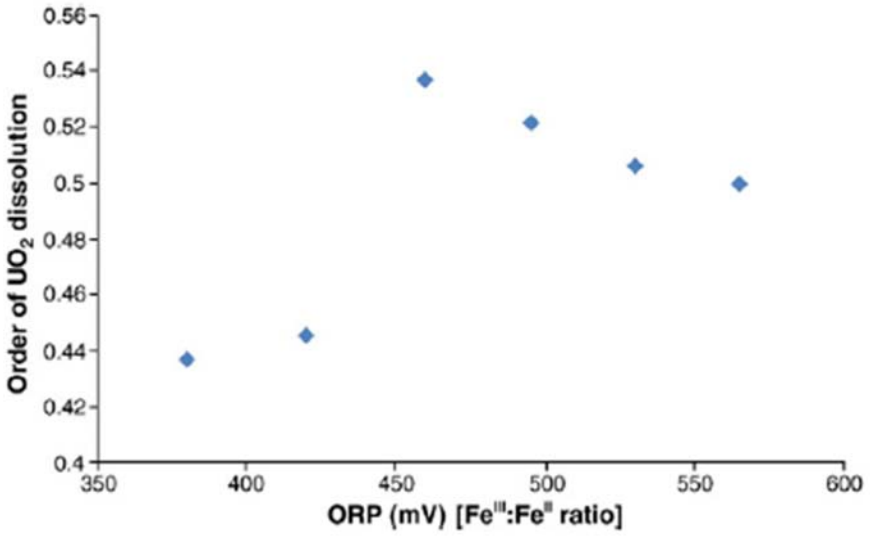

Figure 2.3: Order of UO_2 dissolution with respect to Fe at different ORP's. (Ram et al., 2011)

During a cost reduction exercise at Rössing in 1987 (U_3O_8 spot price ~17 US$/lb), the effect of reducing ferric concentration from 3.5 to 3 g/L on uranium extraction and reagent consumption was evaluated in a plant trial. A reduction in % uranium extraction of 0.33 % and a reduction in acid and pyrolusite consumptions of 0.61 and 0.37 kg/t, respectively were noted (Johnson, 1990). At that stage, the proposed reduction in ferric concentration was implemented due to the fact that the reduction in reagent consumption was worth more than the loss in uranium extraction.

When the uranium market picked up in 2005 (U_3O_8 spot price >20 US$/lb), changes were again made to the total iron operating set-point as the relative value of uranium extraction to reagent cost improved. The RUL leach plant now operates within a total iron range of 4.2 – 5 g/L.

The Rössing ore body (refer to Figure 1.5) can essentially be divided into two key zones, i.e. the Nosib series (North of the amphibole schist horizon), where the uranium mineralization is predominantly in the hexavalent state, and the Hakos/Swakop series (South of the amphibole schist horizon), where mineralization is predominantly uraninite (Vernon and Smit, 1985). Early test work, demonstrating the importance of ferric concentration on leach extraction, showed that an increase in ferric concentration had a greater effect on uranium extraction for the "South" material (Hakos) compared to the Nosib ore (e.g. an increase in ferric concentration from 1 to 2 g/l increased the Hakos ore extraction by ~26% and the Nosib ore extraction by 9%). This work also established that above a ferric concentration of 3 g/L, leach extraction was less sensitive to mineralogical variations (Kesler and Farbach, 1982).

2.3.6 The use of MnO_2 as an oxidant

As mentioned, MnO_2 is used to re-oxidize Fe^{2+} to Fe^{3+} in the Rössing leach plant to ensure a constant supply of Fe^{3+} ions for the UO_2 dissolution reaction. The overall reaction (6) comprises of the following two half-cell reactions. These reactions occur on the surface of the MnO_2 particles.

$$MnO_{2(s)} + 4H^+ + 2e^- \rightarrow Mn^{2+}_{(aq)} + 2H_2O \quad [30]$$

$$2Fe^{2+}_{(aq)} \rightarrow 2Fe^{3+}_{(aq)} + 2e^- \quad [31]$$

The rate of MnO_2 dissolution was suggested to follow a shrinking particle model (Nicol, 2011). The rate of dissolution was tested for different particle sizes (-250 to -53 µm) in a

solution containing 0.2M Fe^{2+} and 0.05M acid at 50 °C. The rate of reduction of MnO_2 was found to increase with a decrease in particle size. The kinetics of this reaction are very rapid, i.e. half-life of approximately 2 minutes under the tested conditions. Nicol (2011) stated that the fact that this reaction rate is so rapid is beneficial to the UO_2 oxidation reaction, in that it enables the ORP of the solution to be maintained at the required ORP by ensuring a high ratio of Fe^{3+} to Fe^{2+} ions in solution. It is, therefore, very important that the pyrolusite reagent (refer to section 1.3 for a description and composition of this reagent) used in the RUL leach (containing ~ 70 % MnO_2) is milled to a small enough particle size, due to the fact that the rate of reaction follows the shrinking particle model. This would be especially important for a leach plant operated at a higher ORP set-point. It could be expected that the rate of MnO_2 dissolution might decrease at a higher ORP set-point (according to standard electrochemical theory). At a higher ORP set-point, the grind size of the pyrolusite reagent would need to be tightly controlled and/or possibly reduced to counter the possible effect of a change in ORP on the MnO_2 dissolution reaction rate.

In the Rössing leaching plant, the pyrolusite reagent is added into the up-comer between the first (mixing) and second (control) tanks in series. This allows the initial reaction between uraninite and ferric to take place in the first tank (residence time ~25 min), which lowers the ORP. The pyrolusite reagent meets a slurry with a lower ORP in the second tank (and MnO_2 dissolution is enhanced at lower ORP values). MnO_2 then reacts with Fe^{2+} ions to oxidize them back to Fe^{3+} ions which in turn, increases the ORP in the control tank (second tank)[10].

2.3.7 Pulp density

For economic purposes, pulp density is generally maximized as far as possible in a slurry leaching process, i.e. (i) less acid and oxidant are required to obtain required set point concentrations, (ii) equipment sizing is affected by ore flow rate and (iii) degree of agitation required to maintain coarse particles in suspension is affected at lower pulp densities.

The maximum plausible pulp density is dependent on maintaining sufficient fluidity in the leach slurry to ensure sufficient contact between particle surfaces and the solvent. The concentration of the solid phase in a mineral slurry is known to affect the rheological behaviour of the slurry. At low solids concentrations, slurries generally behave like Newtonian fluids. As the solids concentration is increased, particle-particle interactions

[10] In the RUL leach circuit, ORP is increased by ~200 mV from tank 1 to tank 2 via the addition of pyrolusite. By the time that the slurry exits tank 6, ORP has decreased by 60 - 160 mV (variability depends on how well ORP is controlled in tank 2 and the oxidant demand of the ore).

become more important and the slurry changes into a non-Newtonian fluid (Kawatra et al., 1996). In a rheological study of limestone slurries conducted by He et al. (2004), it was found that the rheological behaviour of a limestone slurry was transformed from a weakly dilatant fluid to a pseudoplastic fluid with a yield stress as the solids concentration was increased from 60 wt.% to 78.5 wt.%. At a given shear rate, the apparent viscosity and relative viscosity were found to increase exponentially with solids concentration. In the rheological test work conducted by Vagias et al. (2010) on Rössing leach slurry, apparent viscosity and yield stress were found to increase with solids concentration. A high viscosity slurry could result in the leaching rate becoming diffusion-limited instead of being kinetically-limited which would result in a slower rate of leaching (Merrit, 1971). At high densities, constituents dissolved from gangue minerals in the ore may decrease the rate of uranium extraction or cause re-precipitation of uranium to occur.

Demopolous (1985) studied the effect of pulp density (among other variables), 40 – 60 % solid concentration, on % uranium extraction for acid pressure leaching of a sulphidic uranium ore. Tests were conducted in an autoclave where agitation was provided by two 6-bladed axial turbine impellers. Final uranium extraction (after 6 hours) was found to drop by 1.5 % for tests conducted at pulp densities lower than 60 % solids. In the work conducted by Roshani and Mirjalili (2009) it was, however, found that % uranium extraction increased with a decrease in % solids concentration (63 – 33 % solid concentration). The optimum % solid concentration was found to be at 45 % solid concentration, at which % uranium extraction was maximized. The difference in trends noted could be due to a difference in the controlling step for the rate of uranium extraction, i.e. although similar pulp density ranges were tested, tests were conducted under different temperature ranges and pressures. The uranium mineralogy between the two pieces of work was also quite different. Variations in mineral composition are expected to impact the rheology of mineral slurries. Ndlovu et al. (2014), for example, conducted a study on the impact of different phyllosilicate minerals on slurry rheology and observed variations in the rheological behaviour of talc, kaolinite and illite. The comparison of the two studies on the effect of pulp density on uranium extraction (Demopolous (1985) and Roshani and Mirjalili (2009)) illustrates the complex nature of uranium leaching and how different variables interact with each other to result in different rates of uranium extraction, dependent also on the type of uranium mineral being leached (Lottering et al., 2008).

2.3.8 Refractory uranium

Some uranium ores contain multiple oxide type uranium minerals and are generally difficult to leach. Minerals such as brannerite and betafite require leach processes with high temperatures (up to 80 ℃) and high reagent concentrations (up to 100 g/L H_2SO_4) for effective uranium leaching to take place (Merrit, 1971). In the study conducted by Lottering et al. (2008), ores containing 32.3 – 49.6 % brannerite and 42.1 – 52.8 % uraninite[11] were leached under normal acid leaching conditions (9.9 – 16.3 kg/t sulphuric acid dosage, 40 – 60 ˚C and 2 – 4 kg/t MnO_2 dosage). Under these test conditions, uranium recovery never exceeded 90 % and it was concluded that the intrinsic inertness of brannerite contributed towards this. The presence of refractory uranium minerals in run-of-mine ore to the RUL leach plant can, therefore, impact the extent of uranium extraction if the leach is run at ambient conditions. As outlined in section 1.2, the Rössing ore body contains some of these refractory minerals, i.e. betafite (2-4 % of total uranium in ore) and smaller quantities of brannerite (Table 1.1).

A longer leach residence time can in some cases increase the extent to which the refractory minerals can leach. For Rössing ores, where 2-4 % of the total uranium is contained in betafite, this would mean at least doubling (McMaster et al., 2012) the RUL leach residence time which is not economically feasible, due to the increased reagent consumption and either decrease in throughput (to increase residence time) or capital requirement (to do so without sacrificing throughput). McMaster et al. (2012) studied the effect of varying total iron concentration, sulphuric acid concentration and temperature for a natural ore sample containing 100 ppm uranium as betafite. Uranium extraction was found to increase with an increase in total iron concentration, sulphuric acid concentration and temperature over 24 hours. The highest % uranium extraction (43 %) was achieved at 74 ℃ after 24 hours of leaching. For a test conducted at 34 ˚C, 510 mV vs. Ag/AgCl, 6 g/L total Fe and 5 g/L H_2SO_4 concentration (conditions similar to the RUL plant conditions), uranium extraction increased by ~5 % when residence time was increased from 400 minutes to 1400 minutes.

2.3.9 Other aspects that impact uraninite and uranophane leaching in tanks

Agitation/Mixing

The diffusion of a solvent from the bulk solution to the solute in the ore particles and the diffusion and transfer of the solute from the solid surface of the ore to the main bulk of the

[11] The remainder of the ore contained 2.5 – 5.7 % U-Phosphate and 5.8 – 9.2 % coffinite.

solution is affected by the degree of agitation of the leach slurry. Eddy diffusion is increased with an increase in agitation. Sufficient agitation of particles in mineral slurries is also required to prevent sedimentation (Richardson et al., 2002). When the degree of mixing is optimized, dissolution is controlled by the rate of chemical reaction occurring at the mineral surface (chemical reaction is maximized when reagents and dissolved products are continuously replaced) (Merrit, 1971).

The concentrations of foreign ions in the leach slurry

It has been shown that the dissolution of gangue minerals can have a significant effect on uranium dissolution and reagent consumption (Laxen, 1973). Gangue mineral dissolution can influence the dissolution of UO_2 by (i) reducing the acid concentration of slurry (via equations 9 to 18) and (ii) releasing foreign ions into solution (Ram, 2013).

The dissolution of metal ions such as Mn, Cu, Ni, Co and V from gangue minerals has been found to increase uranium extraction and lower the acid concentration at which dissolution occurs (Nesmeyanova and Alkhazashvili, 1962).

In a study conducted by Ram et al. (2011) on the effect of different Fe^{3+} salts on uranium extraction, it was found that the rate of uranium dissolution was at its highest when ($FePO_4$) and ($Fe(NO_3)_3$) salts were used (1.17 x 10^{-7} and 1.20 x 10^{-7} mol/min, respectively). The second highest rate of uranium dissolution was found when ($FeCl_3$), ($Fe_2(SO_4)_3$), (Fe_2O_3) and ($FeBr_3$) salts were used (6.5 x 10^{-6}, 6.94 x 10^{-6}, 6.80 x 10^{-6} and 6.96 x 10^{-6} mol/min, respectively). The uranium dissolution rate was at its slowest when FeF_3 was used (4.92 x 10^{-6} mol/min). In this case, the salts were artificially added to the solution. Further test work was conducted on the effect of the anions of these salts, by increasing the concentration of F^-, Cl^-, Br^-, SO_4^{2-}, NO^{3-} and PO_4^{3-} at constant Fe concentrations. An increase in F^- concentration was found to have the largest effect on uranium dissolution (increase in rate of dissolution). This effect was suggested to be due to the reactivity of different Fe(III)-F^- complexes formed at the different F^- concentrations and/or the influence of F^- on the equilibrium position of reactions 1 to 4 (Ram, 2013). Uranium dissolution was found to decrease with an increase in SO_4^{2-}, which was suggested to be due to the prevention or slowing down of the formation of effective Fe(III) complexes, resulting in a decrease in ORP. Uranium dissolution increased with NO_3^- (NO_3^- will oxidize ferrous to ferric). At PO_4^{3-} concentrations above 5.26 x 10^{-2}M, uranium dissolution stopped. This was suggested to be due to the precipitation of colloidal $FePO_4$.

There is potential for F^-, Cl^-, SO_4^{2-} and PO_4^{3-} anions to be present in RUL leach solutions as a result of gangue mineral dissolution such as apatite and biotite (equations 9 to 18). Effects similar to those reported in this work would thus be expected. The extent thereof would, however, be dependent on the extent of these dissolution reactions and the resulting concentration of anions in solution.

2.4 Mineralogical investigation of Rössing leach slurries

A mineralogical investigation of Rössing leach slurries was conducted, to establish the key mineralogical drivers that control acid consumption and influence uranium extraction. Monthly composite samples of Rössing leach feed and tailings samples were collected throughout 2011 and 2012 and analysed via the use of Quantitative Mineralogical Analytical (QMA) techniques. This section summarizes the major findings from this work (Ryan, 2013).

2.4.1 Acid Consumption

Around 50 % of acid consumption was found to be due to the dissolution of calcite and dolomite and around 26 % due to the dissolution of amphibole. Varying quantities of biotite, chlorite, apatite, pyrrhotite, goethite and titanomagnetite were also determined to have contributed towards acid consumption (~24 %). The data indicated that the grain size of calcite and amphibole controlled the degree of acid consumption. Figure 2.4 and Figure 2.5 illustrate the results from a size-by-size mineralogical analysis of a leach feed sample and leach residue sample. The mean calcite grain size (50 % passing) of the feed sample was ~200 µm. In the leach feed sample, calcite concentration increased with a decrease in particle size. Although calcite concentration was seen to decrease significantly across all particle sizes (comparing the feed with the residue sample), the extent of calcite dissolution was higher in the finer particle size fractions due to the increase in mineral liberation, i.e. increase in reactive mineral surface area at a finer particle size. By reducing the concentration of fine material in the leach feed, the consumption of acid could be reduced. The dissolution of goethite and titano-magnetite were found to release ferric ions into solution (Ryan, 2013).

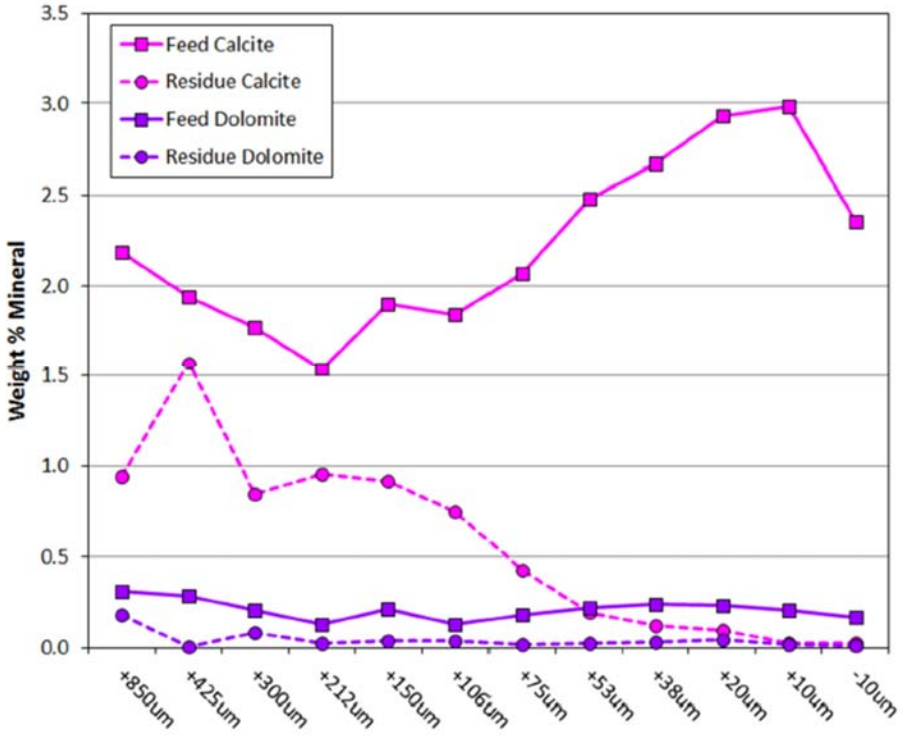

Figure 2.4: Calcite and dolomite abundance by size for the April-12 feed and residue samples (Ryan, 2013)

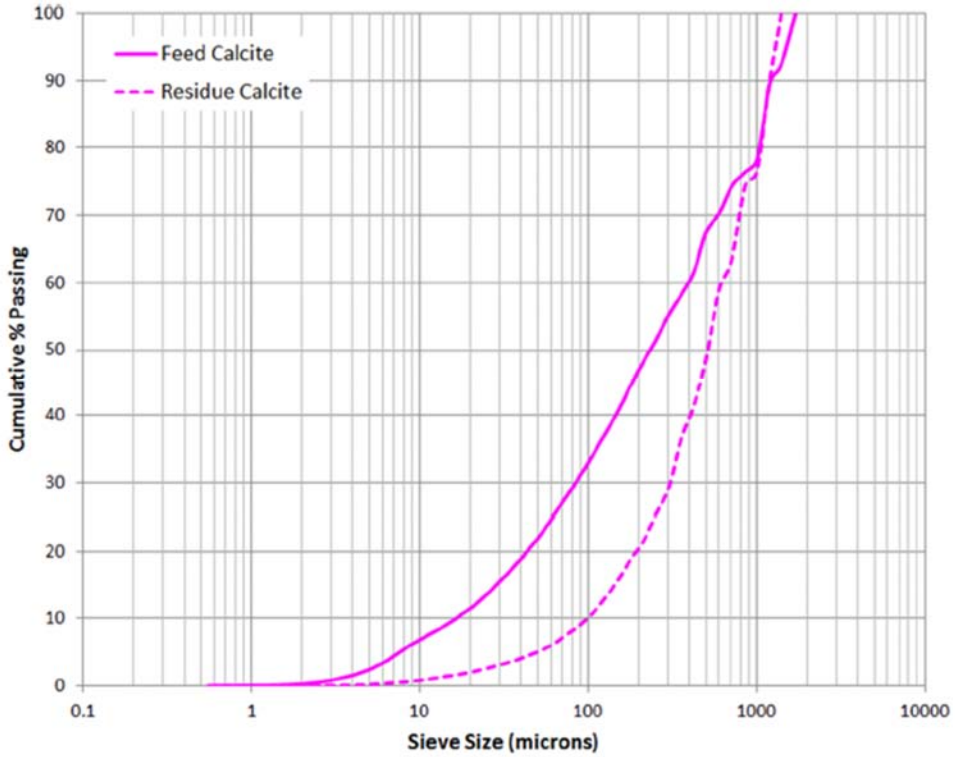

Figure 2.5: Calcite grain size distribution in the April-12 feed and residue samples (Ryan, 2013)

2.4.2 Uranium extraction

Figure 2.6 and Figure 2.7 illustrate the uranium extraction and distribution by size for matched leach feed and residue samples taken in 2012. Figure 2.8 indicates the blend of ore sources sent to the leach plant over the same period of time. The concentration of uranium in the feed samples increased with a decrease in size fraction. This correlates with the expected increase in mineral liberation with finer particle sizes (Figure 2.6). Uranium was found to concentrate significantly in the -10 µm fraction.

It was also found that up to 30 % of total residual uranium (both uranophane and uraninite) was deported as locked grains in the +850 µm size fraction (uranophane was less liberated than uraninite). Additional liberation of this size fraction could, therefore, have resulted in improved leach extraction. Uranium extraction was found to reach an optimal value of ~90 % in the +150 µm size fraction. A recommendation from this work was to tighten the particle size distribution, to liberate more uranium from the +850 µm size fraction but at the same time prevent an increase in fines, which could result in increased acid consumption. This may be done by close-circuiting the milling circuit at Rössing.

For the matched residue samples, 50 to 70 ppm uranium was typically found to remain in the -10 µm fraction in the leach residue. Half of this was concluded to be contained within refractory betafite (estimated from the Niobium assay) and the other half should have been leachable (i.e. fully liberated uraninite and coffinite).

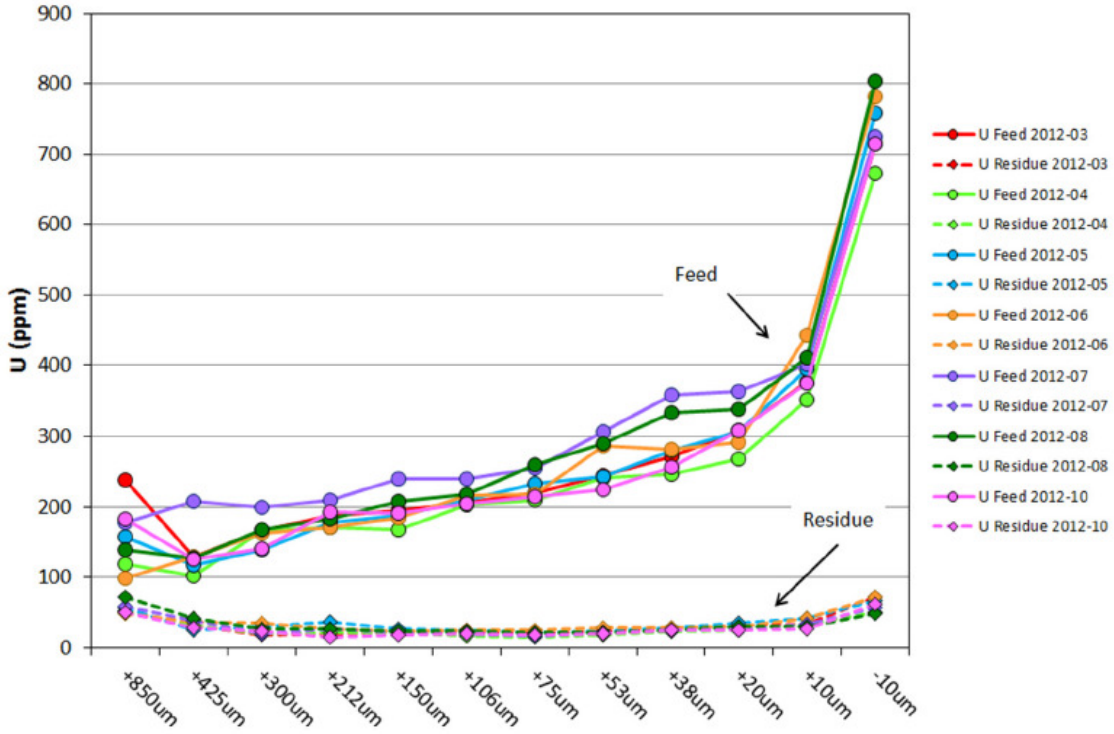

Figure 2.6: Uranium distribution by size for feed and residue across seven months (Ryan, 2013)

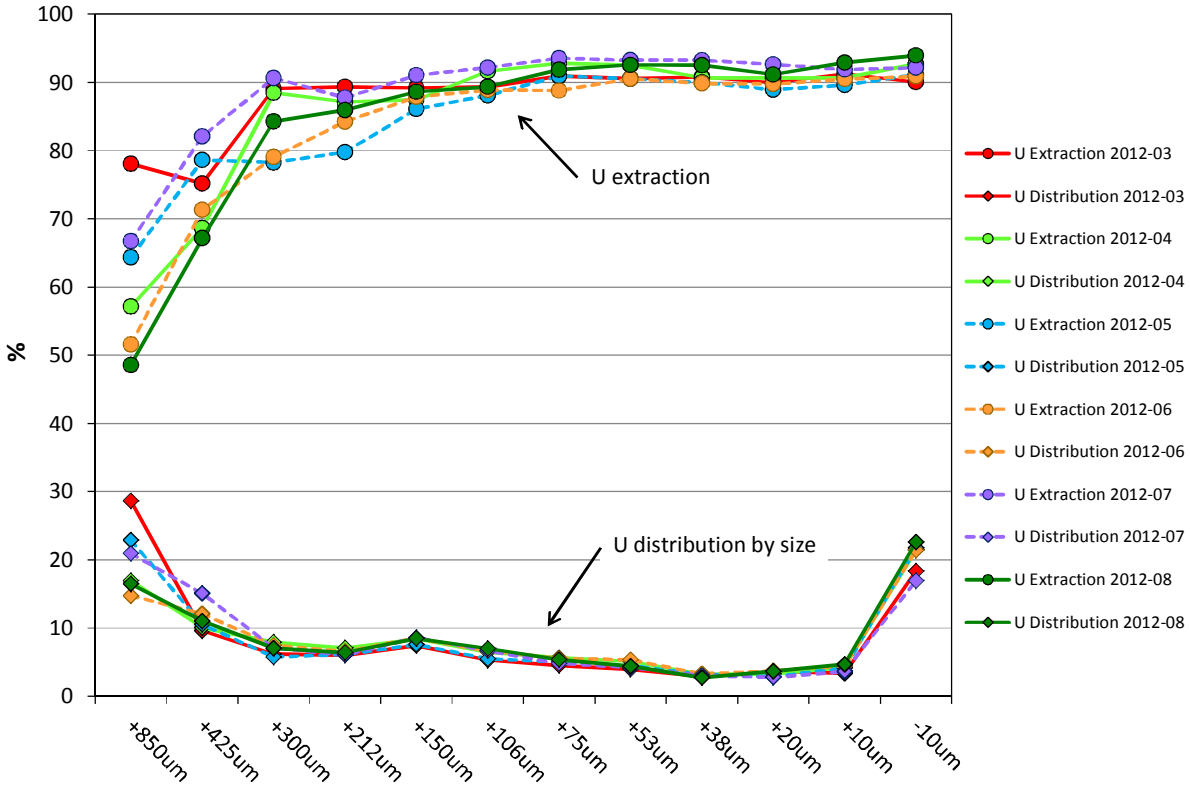

Figure 2.7: Uranium extraction and distribution by size fraction across seven months (Ryan, 2013)

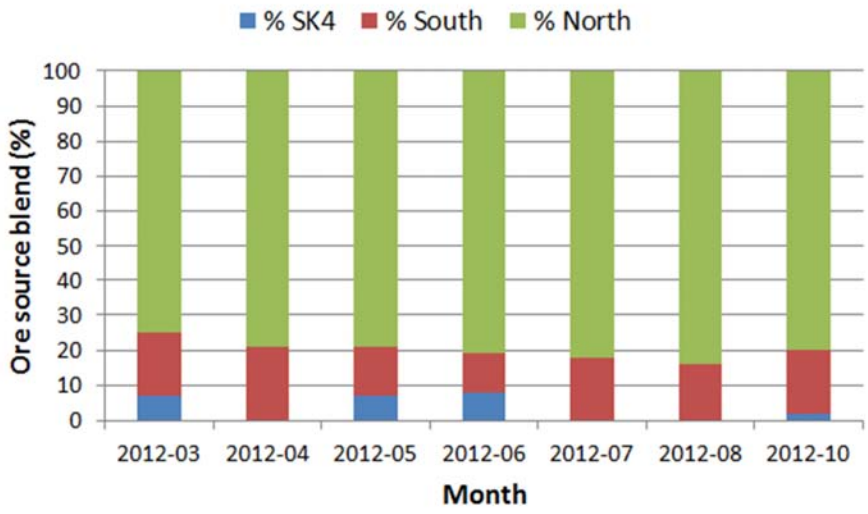

Figure 2.8: Blend of ore sources sent to leaching plant across seven months (Rössing, 2013b)

Of the monthly composites analysed (seven in total), the % extraction of uraninite and uranophane was estimated to be on average 89 % and 86 %, respectively (the average concentration of these minerals in the residue samples was 30 and 20 ppm, respectively).

An SEM-based petrography analysis of a pair of matched samples (April 2012 feed and residue composites) revealed the following. Fully-liberated, unleached uraninite (Figure 2.9) was found in the tailings samples. The same is expected for all the other months analysed due to the grain size of the uraninite and the concentration of uranium remaining in the -10 µm size fraction (Figure 2.7). This could have been due to non-optimal leach conditions (Figure 2.9), i.e. non-ideal redox conditions, incomplete leaching in the normal residence time or galvanic hindrance (association with other more leachable minerals). On the other hand, little to no traces of fully-liberated uranophane was found in the tailings samples, suggesting sufficient dispersion of acid in the leach tanks for the time that these samples were taken. Both uraninite and uranophane locked grains (<10% liberated) were found in the tailings samples (uranophane to a larger extent).

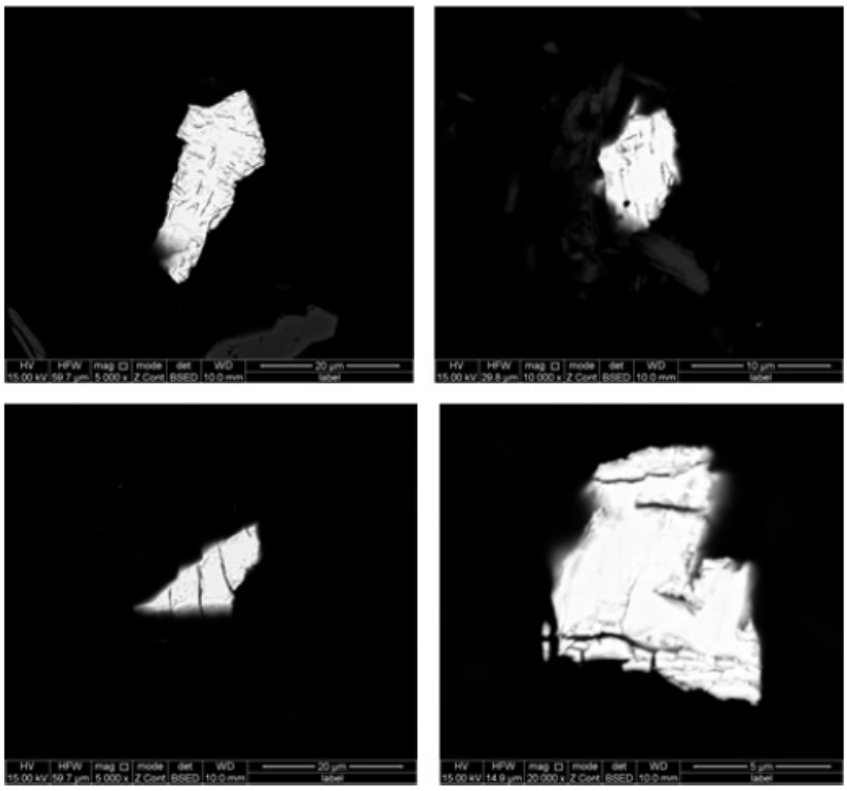

Figure 2.9: BSE images of fine-grained, fully liberated Uraninite grains in April feed and residue samples (Ryan, 2013)

2.4.3 Comparison with earlier mineralogical investigations

During the early years of operation at Rössing (1977 – 1984), "North" material (Nosib) was predominantly treated in the plant (refer to Figure 1.4). In 1985, the proportion of "Hakos"[12] (South material) began to increase. A detailed mineralogy examination of the tailings over the period 1985 to 1989 revealed that not only had the proportion of refractory uranium minerals increased but that there was a strong indication that the liberation size for uraninite from the Hakos ore was finer than the liberation size for the Nosib ore, i.e. an increase in the Hakos type ore would, therefore, require a finer grind size to properly expose the uraninite to help ensure the same level of extraction as achieved with the Nosib ore (Johnson, 1990).

[12] The Hakos Group refers to rock types that are similar to those found in the Rössing deposit, but have a few other lenses that are not found in the western regions such as anorthosites and ferruginous quartz stringers related to gold and minor copper occurrences. The term seems more commonly used to describe the geology in the area around Otjiwarongo, and Rehoboth and is likely thought to be different from the Swakop group due to the presence of the mentioned rock types and ubiquitous presence of skarns and gossans (Murasiki, 2013). It is, therefore, assumed that the author (Johnson, 1990) actually referred to the Swakop group depicted in figure 1.4 in his paper. Both terms do, however, refer to ore located in the Southern region of the Rössing deposit (different in mineralogical composition from the Northern region, i,e, Nosib group).

The information on liberation presented in Ryan's (2013) report corresponds to the assessment conducted by Johnson in 1990 in that it is not surprising that locked uraninite grains were found in the residue samples, as the proportion of "South" material sent to the leach plant has always been higher than that received pre-1984 and the Rössing leach feed grind size remains relatively constant (d_{80} = 1.1 ±0.1 mm (28 ±3 % < 850 µm) (Ismet, 2013). It is also important to note that no significant changes were made to the Rössing crushing and milling plants after 1990.

2.5 Techno-economic modelling

Techno-economic modelling can be used to optimize a process or product design with the goal of optimizing the value gained from the process. For metallurgy, the process chemistry is generally modelled (this could be based on results from laboratory based test work or on first principles) and combined with the revenue generated and cost (reagent cost, maintenance cost, labour, etc.) of the process to provide a robust model that can be used to run different scenarios (e.g. increase throughput rate, change in reagent price, change in ore type, etc.) and predict outcomes. Techno-economic modelling becomes an invaluable, direction-steering and decision making tool for metallurgists and chemical engineers (Bartilson, 2010). This approach to process design and optimization is used extensively in different industries, e.g. plastics, chemicals, food, minerals processing, metal fabrication etc. (Bush, 2005; Stange, 1991 and Olateju and Kumar, 2011).

A basic example of techno-economic modelling is the selection of an acid concentration set point for a leaching process. As discussed in section 2.3.4, a plant trial conducted in the Rössing leach plant in 1988 revealed that uranium extraction decreased by 0.26 % and acid addition decreased by 1.3 kg/t when the terminal acid concentration was reduced from 3.2 to 2 g/L. To decide whether there was value in reducing the terminal acid concentration, the economics of the process were considered, in particular the acid price and the uranium price. Acid addition and uranium extraction would have been converted into monetary values and the net impact on the bottom line then calculated. In this case in 1988, the reduction in acid addition (i.e. financial saving) was found to be worth more than the financial loss in uranium extraction. In 2014, however, the outcome may be significantly different, depending on the relative prices of the two commodities.

Given the uranium market when this work was done (January 2014), i.e. uranium prices as low as US$ 35.75/lb U_3O_8 (UxC, 2014) last seen in 2005, the need to reduce the cost of

uranium production is very high. The ability to model a leach process and determine the optimal plant set points that will result in maximised profit is, therefore, very important. At Rössing, uranium sales are, however, generally based on long term contracts, i.e. uranium sales are pre-committed for the year and are based on the long term price rather than the spot price. The long term price is, however, affected by the spot price and it therefore, remains important to be able to determine improved set points that will result in maximised production (to meet contracted uranium sales) and the efficient use of expensive reagents such as sulphuric acid and pyrolusite.

2.6 Summary and thesis focus

From the literature review, it is clear that several factors can impact the efficiency of the uranium leaching process. pH, ORP and to a limited extent, pulp density and residence time are process parameters that can be altered to effect a change in leach extraction and/or reagent consumption with limited capital plant modifications. Mixing efficiency, leach feed particle size distribution and temperature can also be altered to influence leach extraction and reagent consumption. Altering these factors would, however, require capital expenditure, for example by installing an additional mill.

Value delivered by the leaching circuit at RUL is highly dependent on the economic efficiency of the leach process, i.e. the ability to extract uranium from the ore (revenue is generated through sale of the final uranium oxide product) and the variable cost at which it is extracted (which includes the cost of reagents added to the leach circuit, maintenance costs etc.). For a low grade uranium oxide producer in the current economic uranium market it is therefore, essential that maximum value is obtained through the uranium production process, i.e. maximise revenue and minimize costs. The need to constantly improve and adapt the process to consistently maximise value as the uranium price, reagent prices and ore types vary is, therefore, of great importance. A test facility and techno-economic leaching model that enable Rössing metallurgists to select economically improved set-points to increase value in the leach circuit as a function of the external economic environment, ore type and plant operability (e.g. number of tanks online) are therefore, essential tools. Neither of these has been available up until now.

A key objective of this project will be the development and execution of a leach program and the development of a techno-economic model that can be used to determine improved set-points for the Rössing leach circuit. Although both the literature review and the mineralogical

investigation of RUL leach tails samples indicated that there is potential value to be gained in making major (capital intensive) physical modifications to the plant (e.g. increase leach temperature and/or tighten PSD by modifying the milling circuit), the scope of this project will be limited to process changes that can be effected at as low a cost as possible due to cost constraints at RUL. The mineralogical investigation also indicated that a certain portion of *liberated,* but yet unleached, uraninite remains in the leach tails suggesting the potential to increase leach extraction to an extent, without further grinding.

A leach optimization test work program that aims to improve leach value by varying pH, ORP and total iron will thus be developed. The focus of this particular study will be on the effect of ORP, total iron and to a limited extent pulp density and temperature (seasonal temperature changes could potentially result in different optimum leaching conditions during summer and winter) on uranium extraction and reagent consumption and consequently, leach value. ORP was selected as the main focus as it is expected to have the greatest impact on uranium leach extraction from uraninite bearing ores (Ram et al., 2011 and 2013).

The main objectives for this project are as follows:

1. Determine the impact of varying ORP and total iron concentration on uranium extraction and reagent consumption for different RUL ore types.
2. Determine whether operating at an ORP higher than currently implemented at RUL will be economically viable.

As presented in the Introduction, section 1, the key outcomes for this project will be as follows:

1. The development of a laboratory scale, batch, agitated leach test.
2. The development of a techno-economic model that fits batch leach data to empirical models and combines this with the exit age residence time distribution function and RUL operational data to determine the impact of set point changes on overall leach value.
3. The development of a method that can be used to select improved set points for the Rössing leaching plant for a given ore type, equipment availability and economic environment.

3 Materials and Methods

The effect of pulp density, ORP, total iron and temperature on leach extraction and reagent addition were investigated by conducting an agitated batch leach experiment for each set of test conditions. The results thereof were modelled and were combined with Rössing leach plant operational data and economic inputs to establish the effect on overall leach value.

Section 3.1 describes the ore samples used, the mineralogy of the samples and the reagents utilised in the agitated leach test. Section 3.2 describes the apparatus used. Section 3.3 describes the methods used to prepare and leach the samples and an error analysis of the method. Section 3.4 describes the Rössing leach circuit techno-economic model used to establish the financial impact of varying process parameters. Lastly, a method for selecting improved set points is summarized in section 3.5.

3.1 Materials

3.1.1 Ore types and mineralogy

Two leach feed samples were acquired from the Rössing leaching plant by sampling the leach feed over several days and then compositing the ore to produce two samples with differing mineralogical characteristics. Ore A (acquired in October 2011) can be classified as a “normal” run of mine ore blend and will be referred to as ROM in this project. Ore B (acquired in March 2012) can be classified as a “high cordierite gneiss” ore blend and will be referred to as CGS in this project. It is expected that both ore blends will be fed to the RUL leaching plant in the future.

The Rössing cordierite gneiss rock type contains significantly higher quantities of biotite and cordierite than other rock types found in the Rössing ore body (such as alaskite, banded gneiss and marble) (Ryan, 2012b). Biotite in the Rössing cordierite gneiss rock type contains ferrous. Empirical mineralogical evidence strongly suggests the reducing nature of biotite. Figure 3.1 shows an example of how secondary uraninite has crystallized along the grain boundary of biotite grains in a Rössing ore sample (pre-leach). This would have formed via the following mechanism: initial oxidation of uranium in primary uraninite, dissolution and mobilization by oxidized ground water, followed by precipitation of secondary uraninite when it encounters a redox barrier such as biotite (containing ferrous) (Ryan, 2012b). Biotite is soluble in sulphuric acid solutions and may result in reducing conditions in the leaching circuit as a result of the release of ferrous into solution. This would increase the oxidant

requirement for this rock type (cordierite gneiss), required to oxidize the ferrous to ferric to obtain the required oxidation levels (ORP) in the leach circuit.

The percentage of cordierite gneiss in a run of mine ore blend to the leaching circuit can vary between 2 and 10 %. Ore blends containing more than 7 % cordierite gneiss are classified as “high cordierite gneiss” ore blends. A high cordierite gneiss ore blend (8 – 10 %) is expected to exert a higher oxidant demand than a normal run of mine ore blend (2 - 7 %) due to the reductive properties of the cordierite gneiss rock type. Obtaining an ore blend with a high concentration of cordierite gneiss (between 8 - 10 %) was, therefore, important for this study, to establish whether the order of results obtained with the “normal” ore type (ROM) was preserved for another ore type (CGS), especially an ore type that may have a higher oxidant requirement.

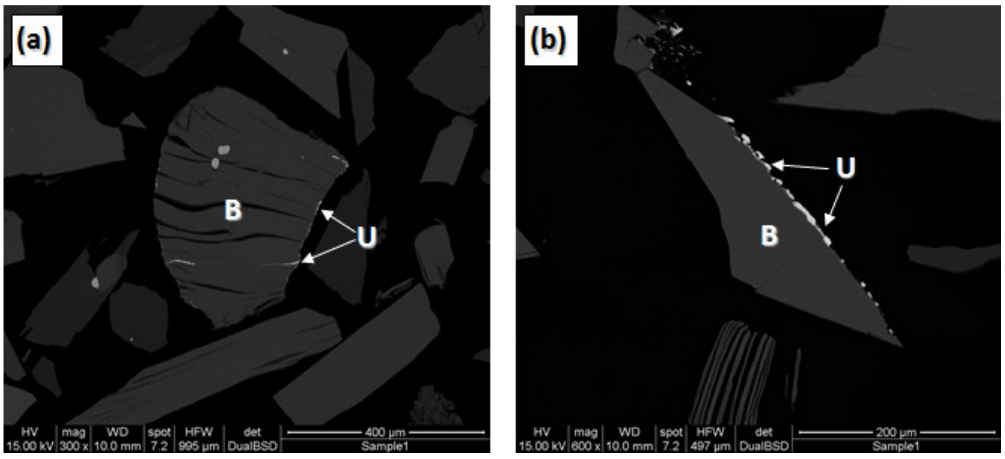

Figure 3.1: Backscattered electron images of dark biotite grans (B) in Rössing ore with bright uraninite (U) which has crystallised along grain boundaries and in biotite cleavage plans (Ryan, 2012b)

Table 3.1 summarizes the characterization of the two ore blends. Figure 3.2 indicates the ore sources for the two blends (this is an estimate, based on the mine geological model), both of which are also potential future blends to be fed to the RUL leaching plant. Both ore types are a blend of North, South and SK4 ore sources but the CGS ore blend contains a greater proportion of South material. The % cordierite gneiss is an estimate provided by the mine geological model. The detailed mineralogy of the two samples is presented in Figure 3.3 and Figure 3.4 and discussed thereafter.

Table 3.1: Ore characteristics

	Ore A (ROM)	Ore B (CGS)
U concentration (Head grade) (ppm)	244 ± 4	218 ± 4
Sulphur content (ppm)	3358	5816
% Cordierite gneiss	3	8
d_{100} (mm)	3350	3350
d_{80} (mm)	1200	1200
% Fines (<75 µm)	14	16

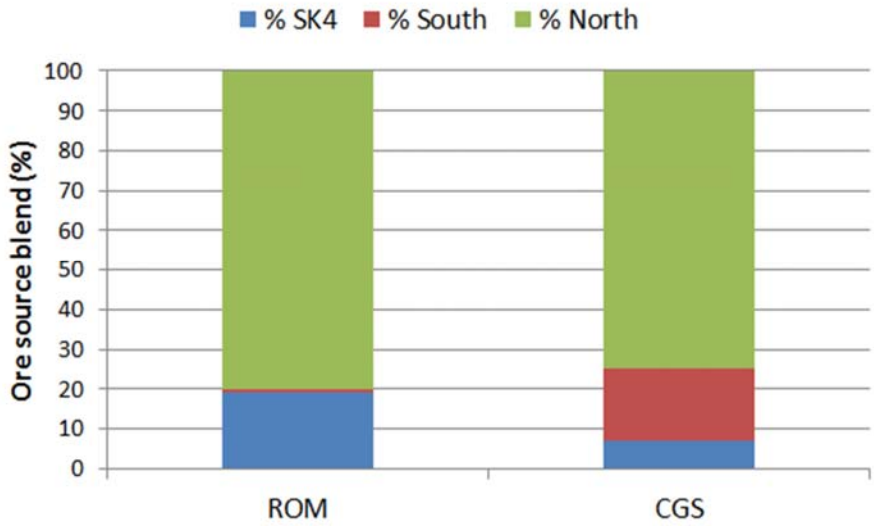

Figure 3.2: Blend of ore sources sent to the leaching plant during the time that the ROM and CGS samples were acquired (Rössing, 2013b)

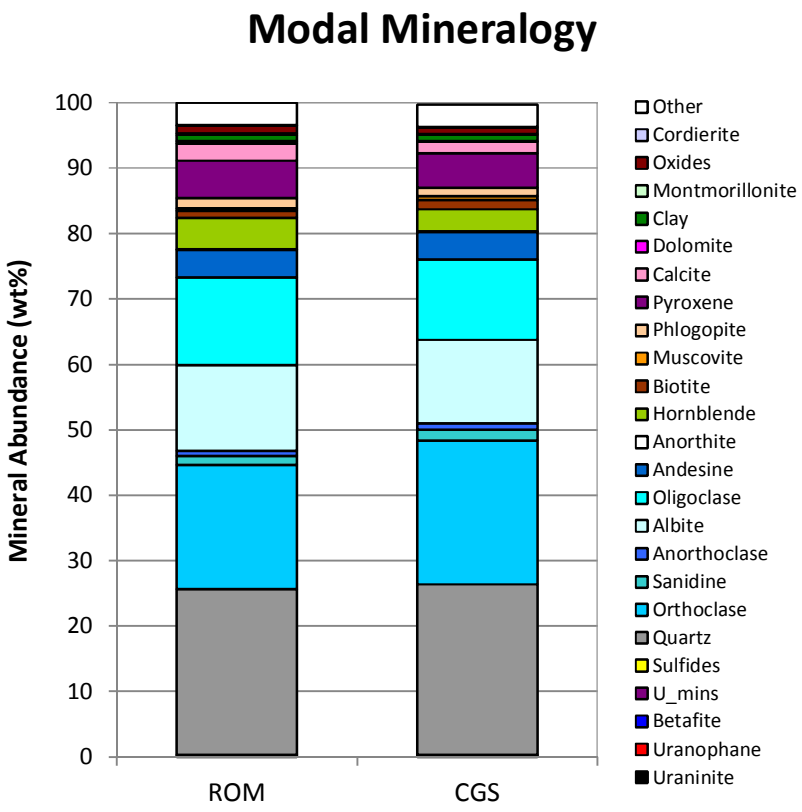

Figure 3.3: Normalised mineral distribution in the -425/+10 µm fraction of the ROM and CGS samples

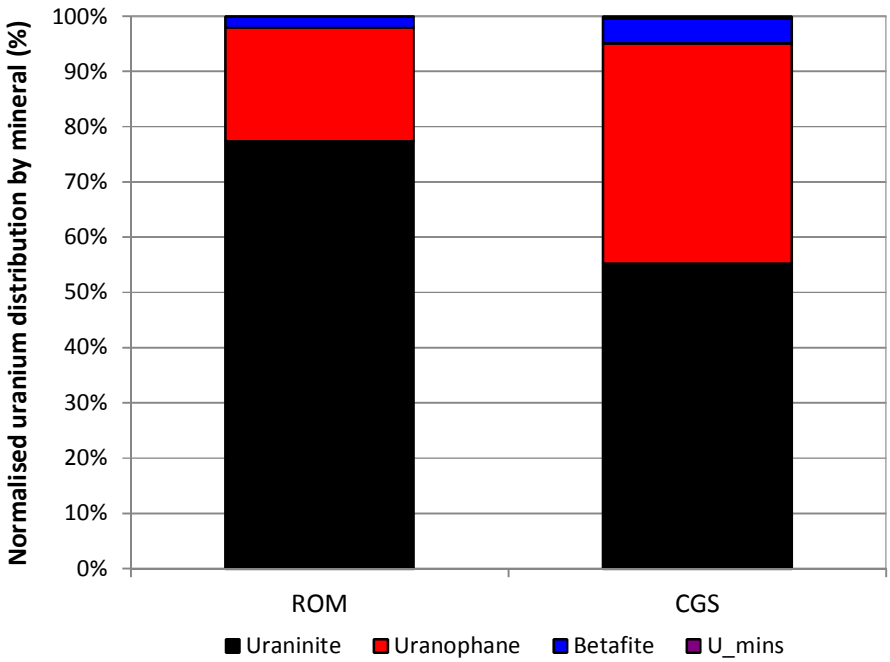

Figure 3.4: Normalised uranium distribution of the ROM and CGS samples

Mineralogical characterization of the two ore blends was conducted by the Rio Tinto Technology and Innovation laboratory in Melbourne, Australia (Ryan, 2012a). Mineralogical characterization (Figure 3.3 and Figure 3.4) of the two ores indicates the following: both ore types consist predominantly of quartz, feldspar, hornblende and pyroxene with minor amounts of mica phases (biotite, phlogopite and muscovite), calcite, clay (and montmorillonite) and oxides. The dominant uranium minerals are uraninite and uranophane with trace betafite. The phase "U_mins" is a grouping used for other uranium minerals (e.g. brannerite, coffinite and carnotite) but no significant concentrations (above detection limits) of these were detected in the samples. Uraninite accounts for ~77.5 % of the total uranium for the ROM sample and ~55 % for the CGS sample. Uranophane accounts for 20.5 % for the ROM sample and ~40 % for the CGS sample.

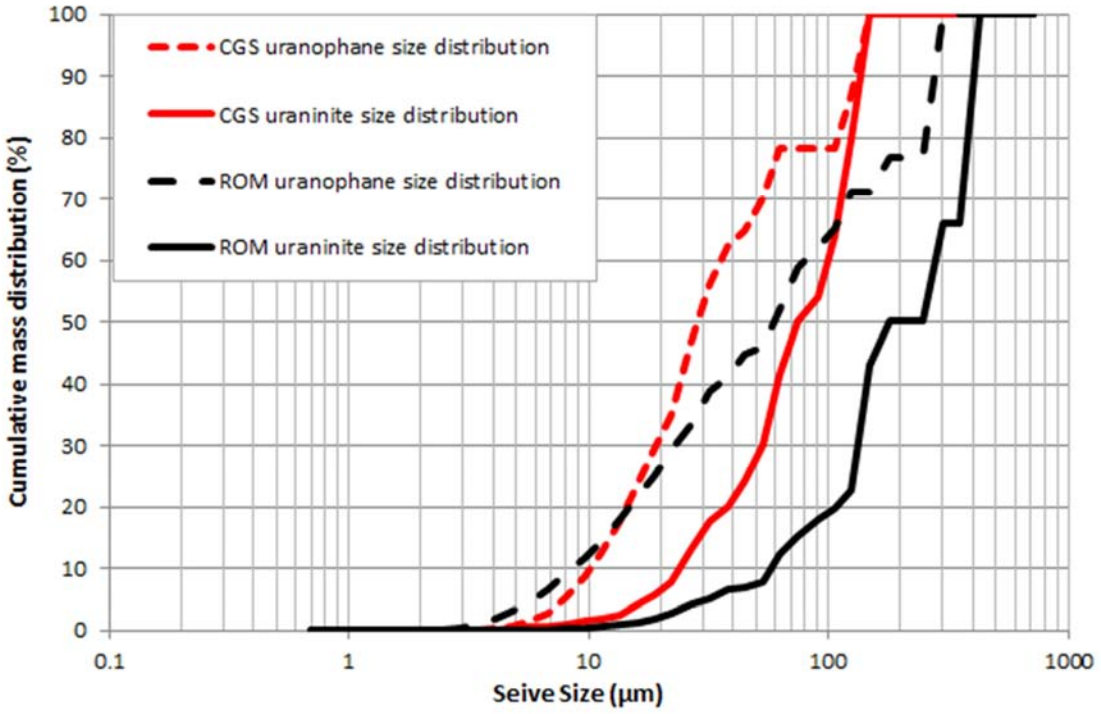

Figure 3.5: Uranium mineral grain size distribution in ROM and CGS samples

Uraninite in the ROM ore is coarser grained than the CGS ore (d_{50} of ~180 µm and 75 µm, respectively) (Figure 3.5). According to Johnson (1990), the uraninite liberation size is smaller for the Hakos (South) ore than the Nosib (North) ore. The % South material in the CGS ore blend is significantly higher (Figure 3.2) than that in the ROM ore blend. It is, therefore, expected that the proportion of finer grained uraninite in the CGS ore blend would be greater than that in the ROM ore blend.

Uranophane is finer grained for both ore types (d_{50} of ~60 µm and 35 µm, respectively). As a result of the difference between the uraninite and uranophane grain size distributions, for the same grind size distribution (<1.1 mm) of the bulk sample, uraninite showed very high degrees of liberation for both ores whereas uranophane was less liberated with more than 70 % of the uranophane grains having less than 60 % of their free surface area exposed (Ryan, 2012a).

The mineralogical analysis suggested that the CGS sample contained a higher concentration of biotite (29 % higher) and cordierite (64 % higher) than the ROM sample which supports the mine model predicted increase in % cordierite gneiss between the ROM and CGS samples. Cordierite gneiss is also believed to be associated with pyrrhotite ($Fe_{1-x}S$) in the Rössing ore body. The higher % sulphur for the CGS sample (Table 3.1) therefore, suggests that it could contain more of this mineral (pyrrhotite was not explicitly analysed in the mineralogical investigation).

3.1.2 Reagents

Agitated Leach reagents

The following chemicals were used in the agitated leach test:

- 98% (wt %) concentrated sulphuric acid (Merck (Pty) Ltd) was used to adjust pH.
- 10% sodium permanganate was used to adjust ORP. This solution was made up by adding 250 g of sodium permanganate monohydrate (Sigma-Aldrich) to 2 L of demineralised water and stirring at 40 °C for 24 hours after which the solution was filtered using a glass membrane funnel before use.
- Synthetic process solution was used to make up the leach slurries for the leach tests. Table A. 1 (Appendix A), indicates the final composition of the synthetic process solution as well as the mass of each chemical added to demineralised water to make up 20 L of synthetic process solution. The aim was to match the average composition of actual recycled process water used in the Rössing leach plant.
- An acidified solution containing a fixed ratio of ferric to ferrous ions was added to the synthetic plant solution to achieve the required ferric and ferrous concentrations (i.e. total iron) for each leach test. An example of the final composition and the mass of chemicals required to achieve this for a 1 L solution is shown in Table A. 2 (Appendix A). For tests conducted at an ORP ≤450 mV (Ag/AgCl), iron was only added in the form of ferrous (i.e. ferrous sulphate) to enable correct ORP control. A combined

platinum ring electrode (Ag/AgCL, 3 M KCl) was used for all ORP measurements and all potentials hereafter listed, were measured with this electrode type. For tests conducted at an ORP > 450 mV, 0.1 g/L iron was added in the form of ferrous and the remainder in the form of ferric. The ferric addition requirement for tests conducted above 450 mV was calculated by subtracting the leachable iron concentration (discussed in section 3.3.3) and the standard ferrous concentration (0.1 g/L) from the total Fe concentration required for the leach test.

- pH 2 wash solution was used to wash any sub-samples or residue samples acquired from an agitated leach test. 98% sulphuric acid was added to demineralised water to achieve a pH with the range of pH 2.0 – pH 2.2.
- Antifoam solution (10,000 ppm) (Senmin) was added to the synthetic plant solution before commencing a leach test at a concentration of ~50 ppm. The addition of antifoam was to prevent foaming of the sample which could cause instability in the test. "Foaming" is usually a result of the reaction between sulphuric acid and gangue minerals in the ore which produce CO_2. Adding antifoam to all tests regardless of sample type was found to have no measurable effect on the leach extraction and was added to all tests as a preventative measure.
- The following buffer solutions were used for pH probe calibration: pH 1 buffer (Merck) and pH 2 (Mettler).
- The following REDOX standard was used for ORP calibration: ~476 mV at 25 °C vs. Ag/AgCl (Associated Chemicals Enterprise)
- A list of the titration reagents used is provided in Appendix A.

Certified reference materials

- Certified reference materials, UREM 3 (UREM 314-912) and UREM 7 (UREM 729-1249) from Mintek were used for equipment calibration purposes when ore uranium concentrations were determined, using a Sodium Peroxide Fusion with ICP-MS detection technique.

3.2 Apparatus

3.2.1 Agitated Leach

All experiments were conducted in a continuously stirred 3.3 L vessel/reactor (Figure 3.8). The reactor was placed in a water bath which allowed for temperature to be controlled. A

Julabo ED (V.2) heater was used to control the temperature within the water bath. A lid (Figure 3.7) was positioned over the reactor to secure a pH probe, ORP probe and other fittings in place to allow for the following to be accomplished:

- Measurement of in-situ pH and ORP during a leach test
- Addition of sulphuric acid and sodium permanganate for pH and ORP control
- Withdrawal of slurry samples from the reactor using a sub-sampling device, i.e. a cylindrical tube connected to a rubber stopper (Figure 3.9). One sub-sample contains 19.4mL of sample (~25g solids at 70% solids).

Stirring was accomplished via the use of an overhead stirrer (paddle impeller, Figure 3.8), set at 450 rpm.

pH and ORP were controlled in the leach vessel via the continuous measurement of pH and ORP in-situ and the dosing of sulphuric acid and sodium permanganate. This was managed via a PID controller (Tiamo software program) coupled to the reagent dosing units (Dosino units). The following pH and ORP probes were used:

- Metrohm Unitrode with Pt1000 temperature sensor (3 M KCl)
- Combined Platinum Ring Metrohm REDOX probe (3 M KCl)

Figure 3.6 illustrates the agitated leach test set-up.

Figure 3.6: Agitated leach test set-up

Figure 3.7: Reactor lid

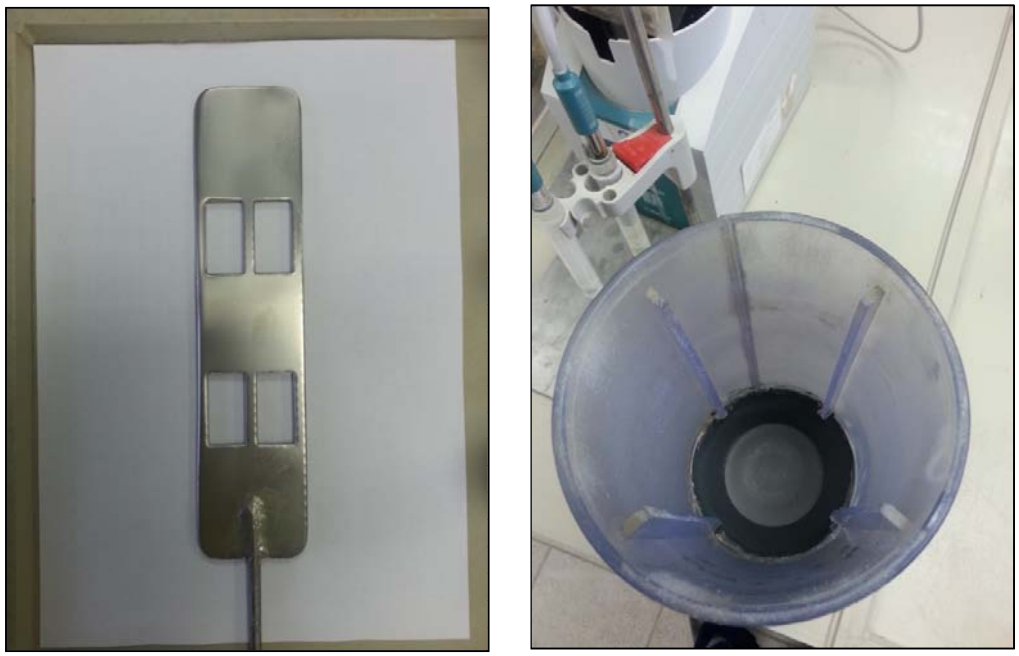

Figure 3.8: Paddle impeller (left), baffles in leach reactor (right)

3.2.2 Other equipment

A rotatory sample divider was used for sample preparation (i.e. splitting out samples for each leach test) to ensure homogeneity between samples for each experiment.

A Centrifuge (Eppendorf AG) and WhatmanTM filter were used to prepare and filter sub-samples taken from the reactor. Once samples had been filtered, Titrando units (Metrohm Dosimat Plus) were used to titrate the filtrate for Fe^{3+}, Fe^{2+} and free acid. A pulverizer (Rocklab ring grinder) was used to prepare dried, solid samples for Inductively Coupled Plasma Mass Spectroscopy (ICP-MS).

Mineralogical characterization of the ores (Ryan, 2012a) was conducted using quantitative mineralogical analyses. A mineral liberation analyser (MLA) and quantitative X-ray diffraction (XRD) device were used.

Figure 3.9: Sub-sampling device

3.3 Method

3.3.1 Health, Safety and Environment

For uranium ore grades lower than 400 ppm, the level of radioactivity emitted is not considered to be hazardous. The RUL laboratory staff is exposed to the same uranium ore grades in their work areas on a daily basis. The average radiation exposure level for laboratory staff at RUL is less than 2 mSv per year. This is much lower than the international occupational exposure limit of 20 mSv per year (set by the International Atomic Energy Agency).

During dry sample preparation stages, a dust mask was worn to prevent inhalation of dust.

All samples used in this project were returned to the processing plant following the completion of the experimental test work and analysis.

3.3.2 Sample preparation

This section describes the sample preparation methodology followed.

Sample collection

Both samples were collected as slurry from the feed box that feeds the mill discharge slurry into the leaching circuit. A sampling scoop (diameter = 10 cm, depth = 15 cm) attached to a

metal handle was used to sample directly from the feed box. It was assumed that the slurry passing through the leach feed box was well mixed due to the high level of turbulence and mixing that occurs within the feed box[13].

Washing

The leach feed samples acquired from the plant were firstly washed with a pH 2 solution, pressure filtered and then washed again with the pH 2 solution. A third wash was conducted with demineralised water.

Drying and rolling

Each sample was then spread out onto a tray and dried in an oven at 105-110 °C for 24 hours. Once cooled, the sample was transferred into a plastic bag. A roller was used to break apart any agglomerates that had formed during the drying stage.

Pre-Screening

The +3.3 mm fraction was removed via a Gilson shaker for the following reasons:

- Having an undefined top-size will not allow estimation of the minimum mass required for representative sample splitting. Screening lowers and defines the top-size thereby allowing this mass to be estimated.
- This size fraction contributes minimally to the overall size distribution of the sample.
- As noted in the mineralogical investigation of Rössing leach feed samples (section 2.4), uranium minerals tend to concentrate in finer fractions and the removal of this size fraction would, therefore, have minimal impact upon the uranium leaching.

Homogenization and splitting

Each sample (~180 kg) was split into 10 sub-samples (A1 - A10) using a rotary sample divider. Sub-samples A1 - A3, A4 - A6 and A7 - A10 were then recombined and sent through the rotary sample divider again to produce 10 sub-samples again (18 kg each). This process was repeated 6 times to ensure that the sample was adequately homogenised.

[13] The particle size distributions for both samples (taken on different days) were very similar, which supports the assumption that the slurry within the leach feed box is well mixed.

Each sub-sample was split further into 10 sub-samples (1.8 kg) using the rotary sample divider. One sample was used for particle size distribution analysis, one for uranium assay and one for any other analysis required (e.g. sulphur content or mineralogy). At the end of the splitting process for each ore type, 10 samples were submitted for PSD analysis, 10 for uranium assay and a composited sample was submitted for mineralogical analysis.

For each phase of test work, several sub-samples were again recombined and split into 2.5 kg samples, e.g. 14 sub-samples (each 1.8 kg) were recombined to ~25 kg and then split into 10 x 2.5 kg samples. A schematic which illustrates the homogenization and splitting process can be found in Appendix G.

Sample characterization

Each 1.8 kg sub-sample was screened to determine the average particle size distribution of the bulk sample. A Pascal shaker and the following screens were used: 3.35, 1.7, 1.18, 0.850, 0.425, 0.212, 0.075 and 0.045 mm. Each 1.8 kg sub-sample was analysed for uranium concentration. A Sodium Peroxide Fusion with ICP-MS detection technique was used. This analysis (using ICP-MS) was conducted by the Bureau Veritas Laboratory in Swakopmund, Namibia.

Mineralogical characterization of the ore samples was conducted by the Rio Tinto Technology and Innovation Laboratory in Melbourne, Australia (Ryan, 2012a).

3.3.3 Pre-leach iron dissolution test

Both ores contained naturally occurring iron. Total iron concentration in solution was selected as a parameter to be varied in this study. It was therefore, important to assess the extent of iron dissolution for both ore types so that the total iron concentration in the starting solution (synthetic plant solution) could be made up correctly to achieve the desired total iron concentration in the leach test. A pre-leach iron dissolution test was conducted for each ore type. This involved the following steps:

- The water bath was preheated to 29 °C. A 2500 ± 100 g ore sample was added to 905 g synthetic plant solution and demineralised water (target % solids = 70 %) in the reactor. The initial agitation speed was set at 350 rpm and then increased to 450 rpm once the solids had been added. Once the ore and solution were added to the reactor, the leach was started (i.e. Tiamo automatic sulphuric acid dosing software

program engaged) and the water bath temperature was increased to 35 °C. The delayed increase in the temperature set point was a precautionary measure taken to ensure that the required leach temperature was not exceeded. The exothermic reaction between sulphuric acid and water naturally increases the temperature of the leach slurry and the surrounding water bath. This heat of reaction is not sufficient to maintain the temperature at 35 °C in the laboratory environment, hence the use of the water bath and heater. The target temperature set point was achieved within 10 to 15 minutes. The leach was run for 2.5 hours and controlled at a pH of 1.4. ORP control was switched off for this pre-leach.

- An initial sub-sample was taken from the reactor once leaching had commenced (target mass of sample = 200 g solids). The sample was spun in a centrifuge and then filtered twice (gravity filtration and then syringe filtration). The liquor was retained for Fe analysis. After 2.5 hours, two sub-samples were taken from the reactor. They too were centrifuged and filtered.
- The liquor samples were then titrated for ferric, ferrous and free acid concentration.

3.3.4 Standard Agitated laboratory leach test method

The agitated leach test method proceeded as follows, unless otherwise stated. Figure 3.10 summarizes the method.

- Each leach test comprised of 2 leaches in 2 reactor vessels to provide two residue samples. Leach test A ran for 7 hours and leach test B ran for 13 hours. Test vessel A was sampled at 2, 4 and 6 hours and test vessel B was sampled at 6, 9 and 11 hours. A “2-leach” method was used to decrease the error associated with the analysis of the results. This will be explained in further detail in section 3.3.6.
- The water bath was preheated to 29 °C. A 2500 ± 100 g ore sample was added to 905 g synthetic plant solution and 5.5 mL anti-foam solution (target % solids = 70 %) in each reactor. The initial agitation speed was set at 350 rpm and then increased to 450 rpm once the solids had been added. Once the ore and solution were added to the reactor, the leach was started (i.e. Tiamo automatic sulphuric acid dosing software program engaged) and the water bath temperature was increased to 35 °C.
- pH control was enabled from the start of the test. The Rössing leach plant operates at a pH between 1 and 2. The second tank in each module is controlled at pH ~1.45 and the resultant terminal tank pH is pH ~1.82. However, the leach techno-economic model is set up to model test results from test work conducted at a *constant* pH. A

constant pH set-point was thus applied to all tests. An average pH of 1.6 was selected for this purpose.

- The first 10 minutes of the leach test was used to stabilize the pH of the slurry at 1.6. This was achieved via the continuous measurement of pH and the dosing of sulphuric acid (PID controller). This initial period of stabilization was required to prevent ferric loss via precipitation (ferric precipitates as ferric hydroxide above a pH of 2.5). During these first 10 minutes, no sodium permanganate was added, i.e. the ORP was allowed to drift naturally. The dosing of sodium permanganate (via the PID controller) was then started at 10 minutes to achieve the required in-situ ORP throughout the rest of the leach. As described in section 1.3, in the RUL leach circuit, oxidant is added to the second leach tank in series, i.e. ± 23 minutes after the slurry first enters the leach circuit (i.e. the residence time of the leach slurry in the first tank in series is on average 23 minutes).
- All sub-samples (target mass = 200 g) were spun in a centrifuge and then filtered twice (gravity filtration and then syringe filtration). The liquor was titrated for Fe^{3+}, Fe^{2+} and free acid. The solids were washed with pH 2 solution wash solution four times, vacuum filtered and then dried in an oven at 110 °C for 24 hours. After drying, the samples were pulverised and assessed for their uranium content.
- The leach slurry remaining after 13 hours was pressure filtered and the liquor collected for analysis. The residue was then washed 3 times with 4 L of a pH 2 solution and dried in an oven at 110 °C for 24 hours. The entire residue sample was pulverised (250 g at a time), recombined and then split into 10 sub-samples 6 times using the rotary sample divider. A 100 g sample was then split from the residue sample and assessed for uranium. A Sodium Peroxide Fusion with ICP-MS detection technique was used.

The batch leach tests were conducted with the techno-economic modelling objective in mind, i.e. to assess the impact of process variables on extraction, reagent consumption and overall predicted value for a specified number of leach tanks online (residence time). The Rössing leach plant does not operate with less than 3 leach tanks online (<4 hours). For this key objective, it was therefore, not necessary to assess the initial 2 hours of leaching in great detail. The first sub-sample for each experiment was taken from the laboratory leach vessel after 2 hours of leaching and every 2 hours thereafter. Determining the kinetic rate constants for the uranium dissolution reactions, was not part of the scope of this project (this would have required more frequent sampling during the first 30 minutes of leaching).

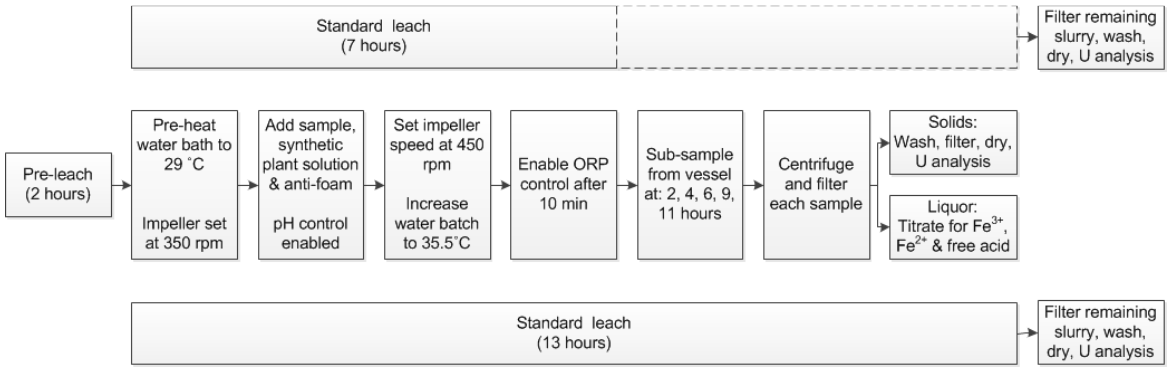

Figure 3.10: Schematic of Agitated Batch Leach Test method

3.3.5 Effect of oxidant

For the agitated batch leach tests, sodium permanganate was used to oxidize ferrous to ferric according to the following reactions:

$$MnO_4^- + 8H^+ + 5e^- \rightarrow Mn^{2+} + 2H_2O \quad [32]$$

$$5Fe^{2+} \rightarrow 5Fe^{3+} + 5e^- \quad [33]$$

$$[32] + [33]: \; MnO_4^- + 8H^+ + 5Fe^{2+} \rightarrow Mn^{2+} + 2H_2O + 5Fe^{3+} \quad [34]$$

In the Rössing leaching circuit, MnO_2 is used (in the form of pyrolusite) to oxidize ferrous to ferric according to the following reactions:

$$MnO_2 + 4H^+ + 2e^- \rightarrow Mn^{2+} + 2H_2O \quad [35]$$

$$2Fe^{2+} \rightarrow 2Fe^{3+} + 2e^- \quad [36]$$

$$[35] + [36]: \; MnO_2 + 4H^+ + 2Fe^{2+} \rightarrow Mn^{2+} + 2H_2O + 2Fe^{3+} \quad [37]$$

$NaMnO_4$ (10%) is used in the laboratory as an oxidant due to the ease with which it can be continuously added to a batch leach reactor and the fact that smaller volumes of this chemical are required to achieve the same oxidation efficiency as MnO_2 (which is in the form of pyrolusite). A $NaMnO_4$ addition rate, determined via the batch leach test would, therefore,

need to be converted into an equivalent MnO_2 requirement and further to an equivalent plant pyrolusite addition rate for these results to be meaningful to the Rössing leaching circuit.

The reactivity of MnO_2 in the pyrolusite reagent used in the Rössing leaching circuit is approximately 70%. Reactivity is defined as the mass fraction of pyrolusite available as reactive MnO_2 to oxidise ferrous to ferric (for a specific pyrolusite particle size distribution). This has been established through several standard MnO_2 reactivity experiments conducted at Rössing over the past 20 years (Rössing, 1990).

For this project, an experiment was also conducted, to confirm that the chemical efficiency with which $NaMnO_4$ oxidizes ferrous to ferric is equivalent to the efficiency at which MnO_2 does the same. This hypothesis was proven to be true. The results from this test work can be found in Appendix E.

In the results sections the $NaMnO_4$ addition rate has therefore, been converted into an equivalent pyrolusite addition rate. The equivalent pyrolusite addition rate will be referred to as the 'oxidant' addition rate from this point onwards.

3.3.6 Error analysis of the agitated laboratory leach and methods used to minimize variation

To establish the repeatability of the agitated leach test method, an error analysis was conducted. The analysis revealed that the largest contributor to error was due to in-situ sub-sampling from the leach vessel (i.e. to determine intermediate points on a uranium extraction versus time curve). This error was improved by changing to a "2-leach" methodology, i.e. using a sample split out from the entire final residue of a 7 hour leach and a 13 hour leach instead of in-situ sub-samples taken during the leach at these points in time. To minimize error over the length of the leach experiment and to allow for interpolation between data points (for use in the techno-economic modelling exercise discussed in Chapter 5) the raw leach data was fitted to empirical models. This section details the error analysis of the agitated leach method, improvements made to minimize error, the fitting of raw data to the empirical models and the subsequent expected error associated with the results presented in Chapter 4.

Initial error analysis of the agitated leach test method

The standard deviation (σ) for the in-situ sub-sampling method (Table 3.2) was determined to be ±1.7 % uranium extraction (determined by taking 6 sub-samples from the vessel at the end of the leach using the sampling tube (Figure 3.9) and analysing each sample for uranium concentration, five times). The standard deviation for the residue sampling method was determined to be ±0.7 % uranium extraction (determined by sampling the dried, pulverized leach residue 6 times and analysing each sample for uranium concentration, five times). Refer to Appendix F for the raw data (Table F. 1 and Table F. 2).

Table 3.2: Standard deviation in % U extraction for different sampling techniques

	68% confidence interval	**95% confidence interval**
Sigma level	σ	2σ
In-situ sub-sampling	±0.9 %	±1.7 %
Residue sub-sampling	±0.3 %	±0.7 %

To determine the proportion of the sub-sampling error attributed to analytical error, the standard deviation in the analytical method was determined. This was determined to be 0.2% uranium extraction (Table 3.3). The data from the analysis for sub-sampling error was used to determine the analytical error in the average 5 repeat assays (Table F. 3).

Table 3.3: Standard deviation in % U extraction for analytical method

	68% confidence interval	**95% confidence interval**
Sigma level	σ	2σ
Analytical error	±0.1 %	±0.2 %

Using the improved "2-leach method", a series of repeat leach tests (4 tests) were conducted under the same conditions[14], to establish the overall error associated with each point in time. The errors in % uranium extraction, acid addition and oxidant addition were determined. The standard deviations in acid and oxidant addition were determined directly from the total volume measurement of reagent added at each point in time.

Figure 3.11 illustrates the mean % uranium extraction curve (red data points) as well as the standard deviation (95% confidence) for each data point (black error bars). The data points

[14] ORP=525 mV, pH=1.6, 35 ˚C, 70% solids, head grade (U concentration) = 317 ppm, mineralogy similar to Ore A

at 7 and 13 hours were obtained through residue sampling and the remaining data points were obtained through in-situ sub-sampling. The overall error for each point consists out of the sub-sampling error, analytical error and “other” error. “Other” refers to all other errors that could contribute towards the overall error at different points in time, such as the level of control (pH, temperature and ORP) and other system inputs such as the degree of sub-sample washing. The type and extent of each of these potential contributing factors was not measured explicitly. Table 3.4 provides a summary of the overall error analysis for the 4 repeat leaches, including the error analysis in reagent addition. The analytical error was measured for each point in time and was found to remain relatively consistent for all points (indicating the consistency of the analytical method). In this exercise, the sub-sampling error for each point in time was not measured explicitly. The results do, however, indicate that the error for the residue sample points was lower than the error for the in-situ sample points. The leach control (pH, ORP and temperature) for all tests was well maintained. The fluctuations in overall error are expected to be due to other system inputs such as sub-sample washing (which has not been quantified but appears to have a greater effect on the earlier points in time, <4 hours). A further improvement to the agitated leach test would be to conduct an assessment of the washing method used and establish whether the use of a more rigorous washing method is able to lower the overall error. The largest error was seen at the 2 hour sampling point. The rate of increase in uranium extraction over the first 2 hours of leaching was faster than the rate of increase in uranium extraction over the subsequent 2 hour intervals. A sample taken incorrectly at the 2 hour sampling point (e.g. a five minute deviation from the sampling time) would be expected to have a greater effect on the calculated uranium extraction (Equation 38), compared to a sample taken incorrectly at the 6 hour sampling point.

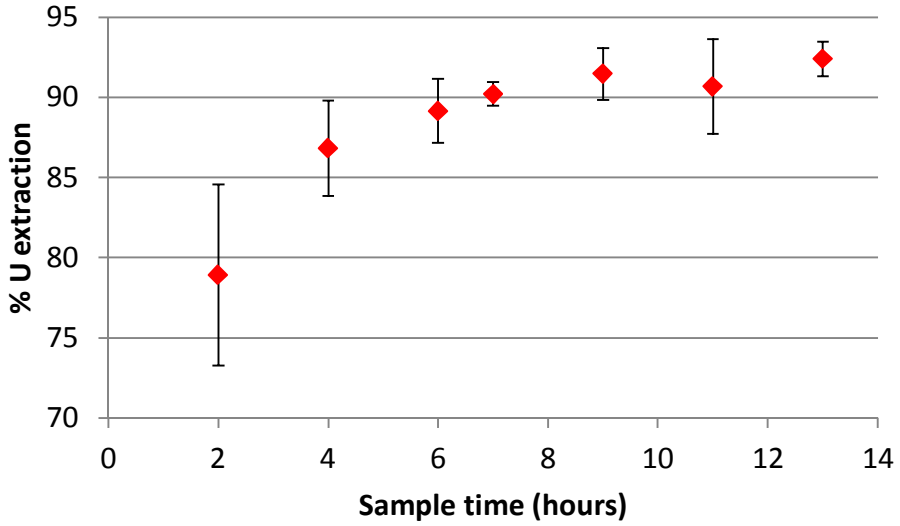

Figure 3.11: Overall error (2 σ) in % uranium extraction for different points in time on a leach curve

Table 3.4: Overall and analytical error (2 σ) for different points in time on a leach curve

Time (hours)	**2**	**4**	**6**	**7**	**9**	**11**	**13**
Sub-sample type	In-situ	In-situ	In-situ	Residue	In-situ	In-situ	Residue
Overall error in % U extraction (2SD)	5.7	3.0	2.0	0.8	1.6	3.0	1.1
Analytical error in uranium determination (2SD)	0.2	0.1	0.2	0.2	0.1	0.2	0.1
Overall error in acid addition (kg/t) (2SD)	0.46	1.65	0.42	0.34	0.30	0.45	0.46
Overall error in oxidant addition (kg/t) (2SD)	0.007	0.012	0.019	0.020	0.009	0.004	0.007

Fitting batch leach test data to empirical models to minimize error

In the analysis of the batch agitated leach test data for this project (results presented in Chapter 4), the raw data was fitted to an empirical model using a weighting technique to account for the degree of error associated with the type of sub-sample, i.e. more confidence was placed in the residue sub-samples. This minimizes error over the length of the experiment and also allows for interpolation between data points (for different residence time scenarios).

Uranium extraction was firstly calculated at different time intervals (2, 4, 6, 7, 9, 11, 13 hours) through the determination of the concentration of uranium remaining in the solids (equation 38):

$$\%\ \text{U extraction} = \frac{U_H - U_S}{U_H} \times 100 \qquad [38]$$

Where U_H = Uranium concentration in the original ore sample (Head grade) and
U_S = Uranium concentration in the sub-sample (in-situ and residue).

Acid and oxidant addition rates were determined for the same points in time and were based on the mass of acid or oxidant added to the leach at each point in time.

The data was then fitted to empirical models (equations 39, 40 and 41) using a least squares method. The models are purely empirical and were selected based on the best fit to the data. An article by McConville (2008) provided the starting point for selecting the empirical models that best fitted the extraction and reagent addition data[15].

$$\%\ \text{U extraction}\ (t) = \frac{at}{b + t} \qquad [39]$$

$$\text{Acid addition}\ (t)\ \left(\frac{kg}{t}\right) = \frac{ct}{d + t} + et \qquad [40]$$

$$\text{Oxidant addition}\ (t)\left(\frac{kg}{t}\right) = \frac{ft}{g + t} + ht \qquad [41]$$

a – h are empirical constants and t = time (hours).

[15] This article provides a summary of 52 common one-, two- and three-parameter binary functions that cover a wide range of behaviour that can be used to model experimental data.

All sample data points were used to fit the batch leach data to the % uranium extraction empirical model. Fitting the data to the model was, however, weighted according to the error associated with the sample type, i.e. the final residue sample points (7 hours and 13 hours) were weighted higher than the sub-sample sample points (2, 4, 6, 9 and 11 hours). Acid addition and oxidant addition data points were fitted to their respective empirical models without weighting them as the standard deviation at each point in time was found to remain relatively constant.

Table 3.5 summarizes the results from the sampling error analysis. The weighting for each data point type was determined by taking the inverse of the variance (fourth column in Table 3.5).

Table 3.5: Weighting of data points according to error

Sample Type	Variance	Weighting (Inverse of variance)
Subsample	0.76	1.3
Residue	0.11	8.9

Example – Batch leach test results fitted to % uranium extraction model

Table 3.6, Table 3.7 and Figure 3.12 summarize an example of the results from a batch test experiment fitted to the % uranium extraction model (Equation 39). The data in column A was fitted to equation 39 using Excel Solver and a least squares method, i.e. the difference between the actual (A) and modelled data points (B) was squared, multiplied with the weighting for each sample type and then summed for all data points. This value was minimized by changing the constants for the model to achieve the best fit to the experimental data. The model constants are presented in Table 3.7 and the model output in column B (Table 3.6) and Figure 3.12.

Table 3.6: Example of batch leach test results fitted to the % U empirical model

t (hr)	Sample Type	% Uranium extraction (batch test)	% Uranium extraction (model)	Error $(A-B)^2$	Weighting
		A	B	C	D
0	NA	0	0		
2	Subsample	74.0	75.5	2.3	1.3
4	Subsample	82.5	82.8	0.1	1.3
6	Subsample	84.5	85.6	1.2	1.3
6	Subsample	84.9	85.6	0.5	1.3
7	Residue	88.0	86.4	2.6	8.9
9	Subsample	86.1	87.5	2.0	1.3
11	Subsample	89.3	88.2	1.2	1.3
13	Residue	87.7	88.7	1.0	8.9
			Sum of least squares Σ(C x D)		42.5

Table 3.7: Model information for example (% U extraction)

Model Constants:	
a	91.7
b	0.429
Model fit:	
Least squares	42.5
R^2	0.9986

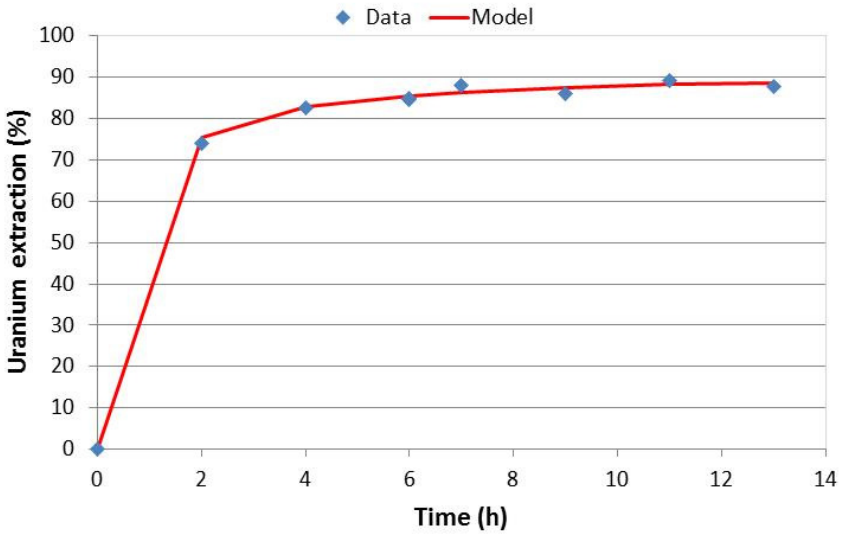

Figure 3.12: Example of batch leach test results fitted to the % uranium empirical model

Example – Batch leach test results fitted to acid & oxidant addition models

Table 3.8 contains the raw results for acid and oxidant addition over time for the same leach test used in the % uranium extraction example. Sodium permanganate addition was converted into an equivalent MnO_2 addition as follows:

$$\text{Equivalent } MnO_2 \text{addition (g)} = \frac{NaMnO_4 \text{ addition (mL)} \times \text{density}\left(\frac{g}{mL}\right)}{\text{Molecular mass of } NaMnO_4\left(\frac{g}{mol}\right)} \times \frac{5 \text{ moles } Fe^{3+} \text{ generated per mole of } NaMnO_4}{2 \text{ moles } Fe^{3+} \text{ generated per mol of } MnO_2} \text{ x Molecular mass of } MnO_2\left(\frac{g}{mol}\right) \quad [42]$$

In the laboratory leach, acid is consumed by gangue minerals in the ore and by the leach oxidant ($NaMnO_4$) according to equation 34. In the RUL leach plant, however, acid will be consumed by gangue minerals in the ore and by the leach oxidant (MnO_2) according to equation 37. Acid consumed by the oxidant will, therefore, differ between the laboratory and plant scenarios. The acid added to the laboratory leach test was converted into an adjusted acid addition rate for the plant scenario, as follows:

$$\text{Acid consumed by } NaMnO_2 \text{ (g)} = \frac{NaMnO_4 \text{ addition (mL)} \times \text{density}\left(\frac{g}{mL}\right)}{\text{Molecular mass of } NaMnO_4\left(\frac{g}{mol}\right)} \times \frac{8 \text{ moles } H^+ \text{ consumed per mole of } NaMnO_4}{2 \text{ moles } H^+ \text{ generated per mol of } H_2SO_4} \text{ x Molecular mass of } H_2SO_4\left(\frac{g}{mol}\right) \quad [43]$$

$$\text{Acid consumed by minerals (g)} = H_2SO_4 \text{ addition (mL)} \times \text{density}\left(\frac{g}{mL}\right) - \text{Acid consumed by } NaMnO_2\text{(g)} \quad [44]$$

$$\text{Acid consumed by } MnO_2 \text{ (g)} = \frac{\text{Equivalent } MnO_2 \text{ addition (g)}}{\text{Molecular mass of } MnO_2\left(\frac{g}{mol}\right)} \times \frac{4 \text{ moles } H^+ \text{ consumed per mole of } MnO_2}{2 \text{ moles } H^+ \text{ generated per mol of } H_2SO_4} \text{ x Molecular mass of } H_2SO_4\left(\frac{g}{mol}\right) \quad [45]$$

$$\text{Adjusted acid addition(g)} = \text{Acid consumed by minerals(g)} + \text{acid consumed by } MnO_2\text{(g)} \quad [46]$$

The reagent addition results presented in chapter 4 are the equivalent MnO_2 and adjusted acid addition rates.

Table 3.8, Table 3.9, Figure 3.13 and Figure 3.14 summarize an example of the results from a batch test experiment fitted to the acid and oxidant addition models (Equations 40 and 41).

The data in column A and D were fitted to equations 40 and 41 using Excel Solver and a least squares method, i.e. the difference between the actual (A) and modelled data points (B) was squared and then summed for all data points. This value was minimized by changing the constants for the model to achieve the best fit to the experimental data. The model constants are presented in Table 3.9 and the model output in column B and E (Table 3.8) and Figure 3.13 and Figure 3.14.

Table 3.8: Acid and MnO_2 addition data for example

t (hr)	Adjusted acid addition (batch test) (kg/t) A	Acid addition (model) (kg/t) B	Error $(A-B)^2$ C	Equivalent MnO_2 addition (batch test) (kg/t) D	MnO_2 addition (model) (kg/t) E	Error $(D-E)^2$ F
0	-	-	-	-	-	-
2	30.8	30.7	0.0	0.59	0.59	0.000
4	32.8	33.1	0.1	0.73	0.73	0.000
6	35.4	34.9	0.2	0.87	0.80	0.001
6	34.2	34.9	0.4	0.78	0.80	0.002
7	36.5	35.7	0.6	0.91	0.88	0.002
9	36.9	37.2	0.1	0.91	0.91	0.001
11	38.5	38.7	0.1	0.98	0.98	0.000
13	40.3	40.2	0.0	1.05	1.05	0.000
		$\Sigma(A-B)^2$	1.497		$\Sigma(D-B)^2$	0.007

Table 3.9: Model information for example (reagent addition)

	Acid addition	MnO_2 addition
Model Constants:		
	c = 91.671	f = 0.836
	d = 0.429	g = 1.057
	e = 0.70	h = 0.02
Model fit:		
Least squares	1.497	0.007
R^2	0.9988	0.9914

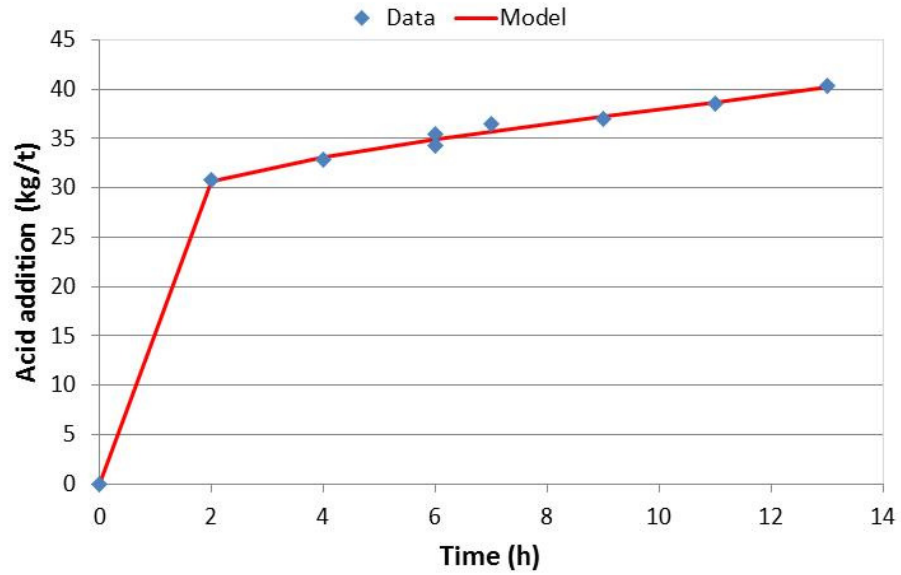

Figure 3.13: Example of batch leach test results fitted to the acid addition empirical model

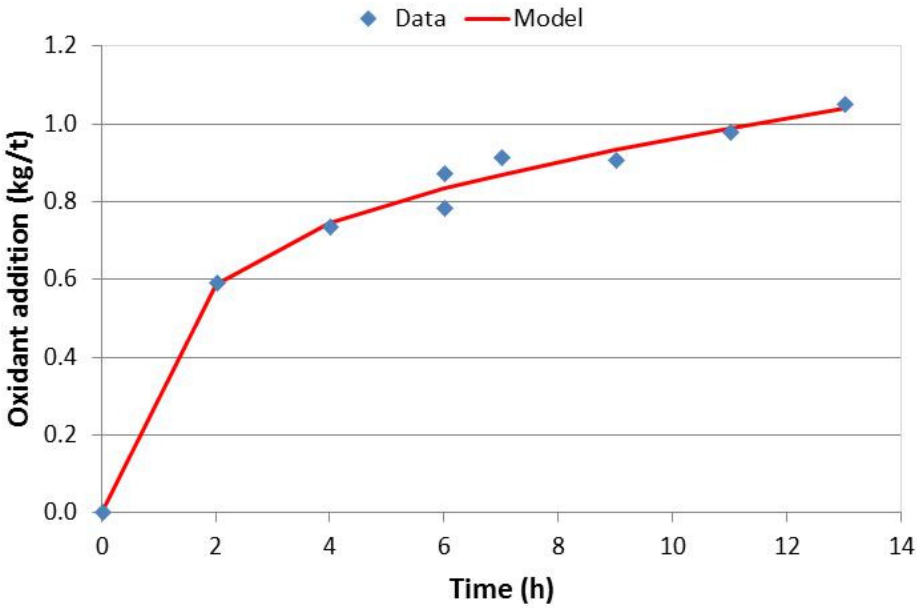

Figure 3.14: Example of batch leach test results fitted to the oxidant addition empirical model

Overall error in the agitated batch leach test method

The data from the 4 repeat experiments that were conducted to establish the error in the overall leach method were fitted to the empirical models. The standard deviations in final uranium extraction, acid addition and oxidant addition (13 hours) were then determined (Table 3.10). The error associated with the final acid addition and oxidant addition was low

for both reagents, indicating a good level of repeatability in terms of the overall reagent control for the leaches. The standard deviations (2σ) displayed in Table 3.10 are relevant to the discussion of the results presented in Chapter 4.

Table 3.10: Standard deviation for modelled final uranium extraction and reagent addition

Standard deviation at 13 hours	% U extraction	Acid addition (kg/t)	Oxidant addition (kg/t)
σ	0.6	0.22	0.001
2σ	1.2	0.45	0.003
		2σ as % of mean = 2.2%	2σ as % of mean = 0.6%

3.4 Rössing leach circuit techno-economic model

3.4.1 Background

The agitated leach tests were carried out as batch leaching tests, i.e. all of the ore particles were exposed to the leach reagents for the same leaching period. The Rössing leaching process, is however, a continuous leaching process, i.e. leach slurry is continuously transferred from one stirred reactor (CSTR) into another. According to CSTR theory (Nicol, 2011) the effluent stream of a CSTR (leach tank) would, at any instant, comprise of fluid and solid particles that had spent various lengths of time in the reactor. The distribution of exit ages of the particles is referred to as the residence time distribution (RTD) and is a function of the mixing and flow distribution patterns within the reactor vessel. For mineral leach slurry, the average residence time of large particles is likely to exceed that of small particles (Nicol, 2011). A number of phenomena contribute to this, e.g. short-circuiting propensity (small), settling and re-suspension (large) and slower relative upward velocity in leach tank upcomers (large).

To adequately assess the impact of different process variables on the economics of a leach process, it is best practise to take the exit time distribution of slurry in a CSTR into account. The batch kinetic results from the leach experiments conducted in this study were, therefore, combined with the standard exit time distribution (Equation 48) for a CSTR and relevant information about the residence time of Rössing leach tanks to model the effect of ORP and total iron on leach extraction and reagent consumption. Thermographic imaging (Figure

3.15) was used to determine the average fillet height build-up in the leach tanks. Residence time distribution tests were also carried out to confirm the calculated residence times.

Figure 3.15: Example of thermographic image of leach tank wall (Meyer, 2008). (Red indicates the warmer active slurry and blue indicates the cooler stagnant zone, i.e fillet build-up in the tank).

This section provides an overview of the development of this model, i.e. the Rössing leach circuit techno-economic model (Hamilton, 2010)[16]. Each set of data from an experiment was inserted into the model to determine the predicted overall %U extraction and reagent addition rate for the Rössing leach plant and subsequently the overall value predicted for the specific set of parameters that the laboratory leach was conducted at. The results of this techno-economic modelling exercise are presented in Chapter 5. Figure 3.16 provides a schematic of how the model functions.

[16] The Rössing leach circuit techno-economic model was originally created by Erin Hamiliton (Rio Tinto Technology and Innovation) for the purpose of optimizing the Rössing leaching process. It was later validated with batch leach test work data in 2011.

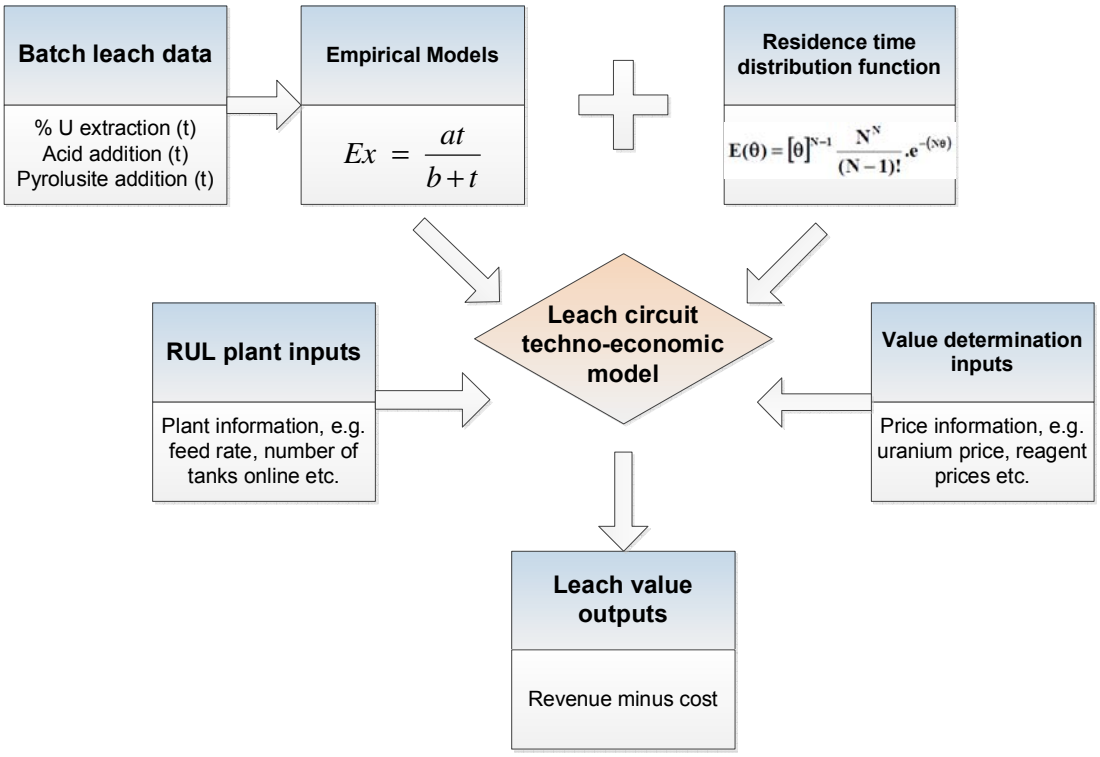

Figure 3.16: Schematic of Rössing leach circuit techno-economic model

Inputs into the model, i.e. RUL plant data such as leach feed rate, number of tanks online, etc. and value determination inputs such as the uranium price, reagent prices, etc. are detailed in Appendix B.

3.4.2 Batch kinetic data combined with residence time distribution function

The batch kinetic data was fitted to the empirical models described in section 3.3.6 and combined with the residence time distribution function, E(t), for a CSTR (Nicol, 2011) to determine the overall % uranium extraction for a specific scenario and for a given number of leach tanks online. This was calculated according to equations 47, 48 and 49.

$$\text{Overall \%U extraction} = \frac{\sum[\%\text{U extraction(t)} \times \text{E(t)}]}{\text{Cumulative E(t)}} \quad [47]$$

$$\text{E(t)} = \frac{t^{N-1} exp(-Nt/\bar{t})}{(N-1)!(\bar{t}/N)^N} \quad [48]$$

Where t = time (hours)

N = number of tanks in series

$\bar{t}$ = total average residence time = Total tank volume (m^3) / Leach flow rate (m^3/h)

Total tank volume = Σ(Tank volume – Sand fillet volume)

Table 3.11 uses the results from the example in Table 3.7 from the previous section, to determine the overall % uranium extraction for a specific residence time. In this example, a 5 tank scenario was modelled, i.e. $\bar{t}$ = 7.8 hours. The sand fillet (determined via thermographic imaging) for the different leach tanks was zero for tank 1, 39.1 m^3 for tank 2, and 61.3 m^3 for tanks 3 to 5.

$$\bar{t} = \frac{[\,(296\,m^3 - 0\,m^3) + (1449\,m^3 - 39.1\,m^3) + (1449\,m^3 - 61.3m^3) \times 3\,]}{748\,m^3/h}$$

Empirical model (using constants from Table 3.7):

$$\%\ \text{U extraction (t)} = \frac{91.671\ \text{t}}{0.429 + \text{t}} \qquad [49]$$

Table 3.11: Batch leach kinetic data combined with exit time distribution function (N = 5) to determine overall % uranium extraction

Column	A	B	C	D
t (h)	E(t) *Equation 48*	Cumulative E(t)	% U extraction (t) *Equation 49*	E(t) x % U extraction (t) *A x C*
0.015	3.3E-12	3.3E-12	3.1	1.0E-11
0.030	5.2E-11	5.6E-11	6.0	3.1E-10
0.045	2.6E-10	3.2E-10	8.7	2.3E-09
0.060	8.2E-10	1.1E-09	11.3	9.2E-09
.	.	.	.	.
.	.	.	.	.
.	.	.	.	.
25.17	2.8E-06	1.0	90.1	2.6E-04
25.19	2.8E-06	1.0	90.1	2.5E-04
		$\frac{\sum[\%\text{U extraction(t)} \times \text{E(t)}]}{\text{Cumulative E(t)}}$		85.9

E(t) (column A) and % U extraction (column C) were calculated at each time (t) value in increments of 0.015 hours using equation 47 and 49. The resulting E(t) and % U extraction at each time (t) were multiplied with each other and summed (column D). The sum was then

divided by the final cumulative E(t) value (equation 47). The overall % U extraction for a 5 tank scenario was determined to be 85.9 %.

The overall acid requirement was calculated similarly using equations 50, 48 and 51. It is important to note that in the Rössing leaching plant, acid and oxidant are only added up front (mixing and control tanks). This is gradually consumed with time as the leach slurry progresses through the leach train. The overall acid requirement (equation 50) and oxidant requirement (equation 52) therefore, refer to the total acid and oxidant that would need to be added up front in the real plant process.

$$\text{Overall Acid requirement } (\text{kg/t}) = \frac{\sum[\text{Acid addition(t)} \times \text{E(t)}]}{\text{Cumulative E(t)}} \quad [50]$$

Empirical model (using constants from Table 3.9):

$$\text{Acid addition f(t)} \left(\frac{\text{kg}}{\text{t}}\right) = \frac{91.671\text{t}}{0.429 + \text{t}} + 0.70\text{t} \quad [51]$$

Table 3.12: Batch leach kinetic data combined with exit time distribution function (N = 5) to determine overall acid requirement.

Column	A	B	C	D
t (h)	E(t) *Equation 48*	Cumulative E(t)	Acid addition f(t) *Equation 51*	E(t) x acid addition f(t) *A x C*
0.015	3.3E-12	3.3E-12	2.98	9.8E-12
0.030	5.2E-11	5.6E-11	5.45	2.9E-10
0.045	2.6E-10	3.2E-10	7.53	2.0E-09
0.060	8.2E-10	1.1E-09	9.30	7.6E-09
.	.	.	.	.
.	.	.	.	.
.	.	.	.	.
25.17	2.8E-06	1.0	48.92	1.4E-04
25.19	2.8E-06	1.0	48.93	1.4E-04
			$\frac{\sum(\text{Acid addition(t)} \times \text{E(t)})}{\text{Cumulative E(t)}}$	36.2

The overall oxidant requirement was calculated using equations 52, 48 and 53. The source of MnO_2 in the Rössing leaching process is pyrolusite. For the purposes of conducting financial evaluations with the Rössing leach circuit techno-economic model, the MnO_2 addition rate was converted into a pyrolusite addition rate by dividing the MnO_2 addition rate by the percentage of reactive MnO_2 in the Pyrolusite reagent (equation 52).

$$\text{Overall oxidant requirement (kg/t)} = \frac{\sum[\text{Oxidant addition(t)} \times \text{E(t)}]}{\text{Cumulative E(t)}} \Big/ \frac{\%\ \text{reactive } MnO_2 \text{ in Pyrolusite}}{100} \quad [52]$$

Empirical model (using constants from Table 3.9):

$$\text{Oxidant addition (t)} \left(\frac{\text{kg}}{\text{t}}\right) = \frac{0.836\text{t}}{1.057 + \text{t}} + 0.02\text{t} \quad [53]$$

Table 3.13: Batch leach kinetic data combined with exit time distribution function (N = 5) to determine the overall oxidant requirement.

Column	A	B	C	D
t (h)	E(t) *Equation 48*	Cumulative E(t)	Oxidant addition f(t) *Equation 53*	E(t) x oxidant addotion f(t) *A x C*
0.015	3.3E-12	3.3E-12	0.0120	4.0E-14
0.030	5.2E-11	5.6E-11	0.0237	1.2E-12
0.045	2.6E-10	3.2E-10	0.0351	9.2E-12
0.060	8.2E-10	1.1E-09	0.0462	3.8E-11
.	.	.	.	.
.	.	.	.	.
.	.	.	.	.
25.17	2.8E-06	1.0	1.3185	3.7E-06
25.19	2.8E-06	1.0	1.3188	3.7E-06
	$\frac{\sum[\text{Oxidant addition(t)} \times \text{E(t)}]}{\text{Cumulative E(t)}} \Big/ \frac{\%\ \text{reactive } MnO_2 \text{ in Pyrolusite}}{100}$			1.22

Iron addition (added once-off as an initial dose) was not fitted to a model as iron was only added at the start of each test. This was calculated by subtracting the concentration of iron in the starting solution from the required total concentration of iron (i.e. total iron set point) and multiplying this difference with the liquor portion of the leach slurry that would have been presented to the leach circuit at a given mill throughput rate. The iron requirement was then converted into a Conarc reagent requirement based on the availability of iron in the Conarc reagent.

Overall uranium extraction and reagent addition requirements for a specific residence time (number of tanks online) were then converted into economic indicators (revenue and cost). The Rössing plant inputs, value determination inputs and leach value output formulae used to calculate the economic indicators in the techno-economic model can be found in Appendix B. The net financial value for a given scenario could then be determined (revenue minus

cost). The net financial value for the RUL leaching process is referred to as “leach value” in this work.

The results and recommendations from this laboratory based test work and techno-economic modelling exercise provide direction for selecting improved set points for the RUL leaching plant. The model is used to determine the relative impact of changing a process variable, on the overall leaching value, i.e. it is not expected that the absolute extractions and reagent consumptions predicted by the model would be achieved in the plant. The model is used to predict an improved scenario. Any recommendation made through this work would first need to be trialled (i.e. validated) in the plant before fully implementing it. A method for quantifying an improvement via a plant trial is described in section 5.3.2.

3.4.3 Error in techno-economic modelling exercise

The overall error associated with the *predicted* uranium extraction and reagent requirement numbers (for a 5-tank residence time) was determined. The data used in the error analysis (4 repeat leach tests) in section 3.3.6 was fitted to the empirical models and combined with the residence time distribution function for a CSTR for a 5-tank scenario. Table 3.14 summarizes the error. This error is applicable to the results presented in Chapter 5.

Table 3.14: Standard deviation in the output from the techno-economic model (4 repeats)

Standard deviation (5 tanks)	% U extraction	Acid requirement (kg/t)	Oxidant requirement (kg/t)
σ	0.4	0.13	0.006
2σ	0.7	0.25	0.013

3.5 Method for selecting improved set-points

One of the objectives of this work was to develop a method that can be used to select improved set points for the Rössing leaching plant. This section describes the method developed through this work, which can be used to select improved set-points for a specific ore type. Figure 3.17 summarizes the steps in the method. Further details of the test work section are summarized in Figure 3.18. The scope of the experimental work covered in this thesis is highlighted in orange, steps 1 to 5 (Figure 3.17) and steps 1 to 3 (Figure 3.18).

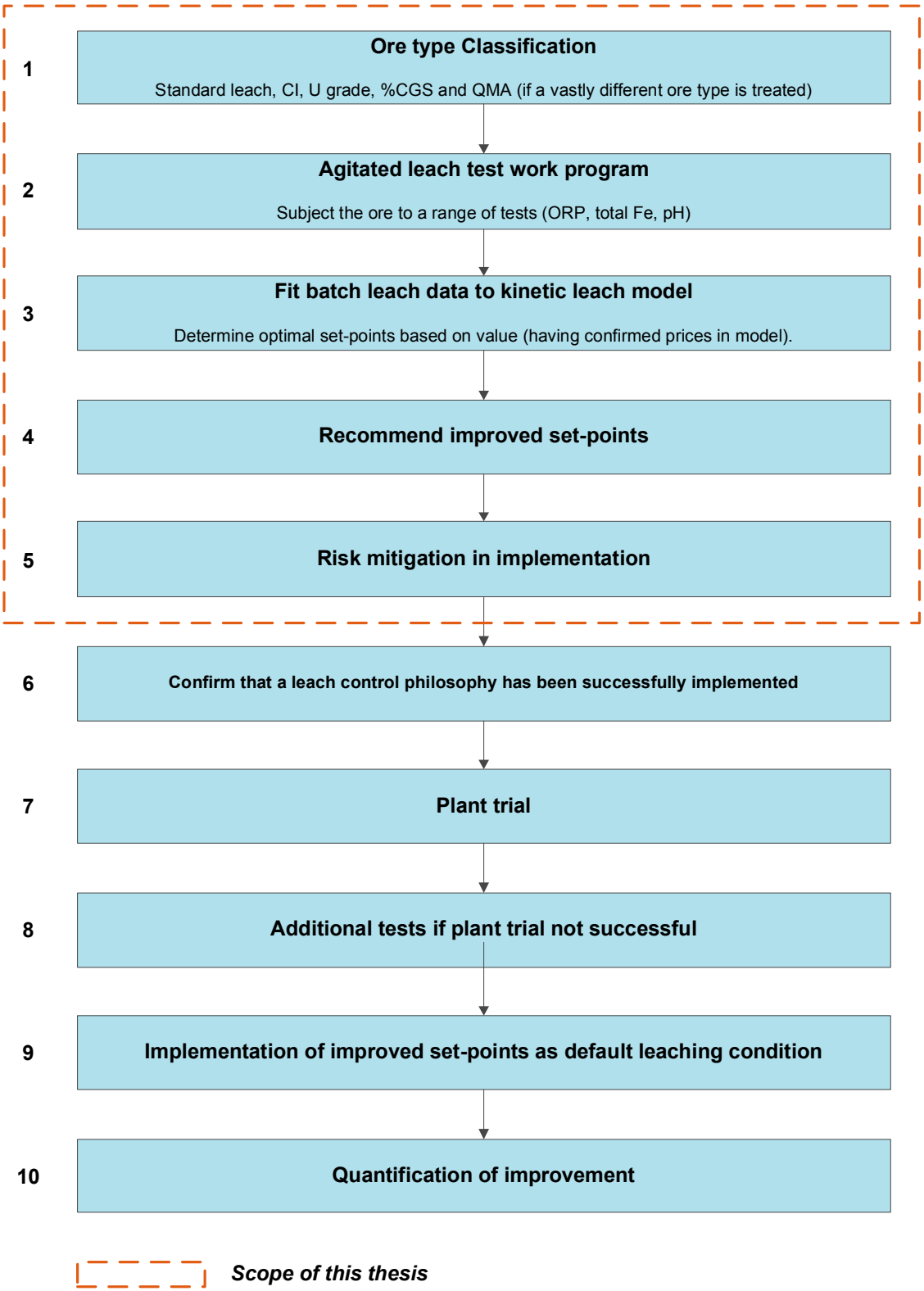

Figure 3.17: Method for selecting improved set-points

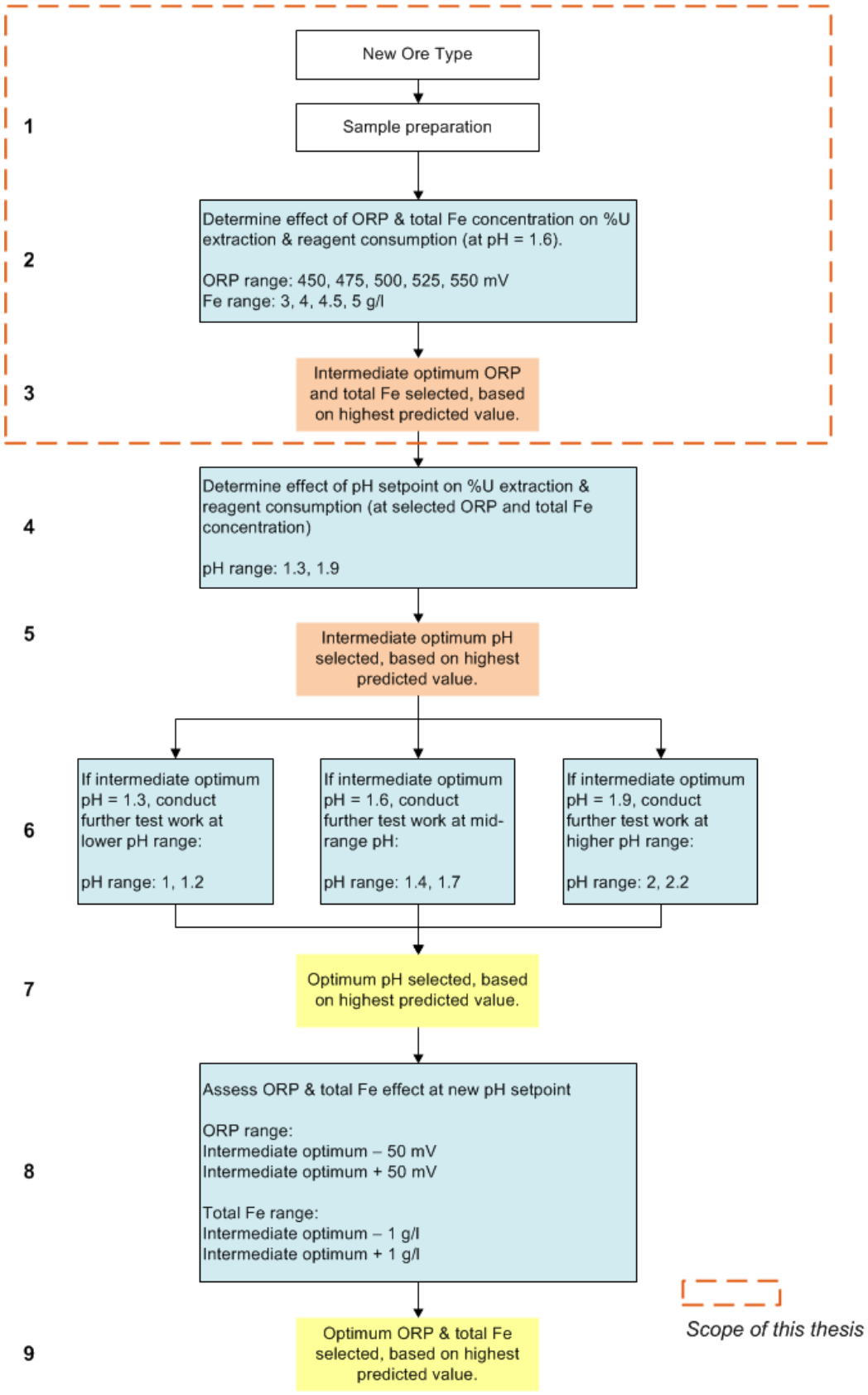

Figure 3.18: Test work required to determine improved set-points

4 Experimental results

4.1 Introduction and overview

The results from the batch leach tests are presented and discussed in this chapter. The results are then further interpreted through the use of a techno-economic model to determine improved operating set points for the Rössing leaching plant in chapter 5.

Table 4.1 provides an outline of the experiments conducted. Tests 1 and 2 studied the effect of pulp density on uranium extraction for the ROM ore type. Tests 3 to 8 studied the effect of ORP on uranium extraction and reagent addition for the ROM ore type. Tests 9 to 11 were conducted to establish the effect of ORP at a lower total iron concentration. The effect of ORP on uranium extraction and reagent addition was then assessed for a different ore type (CGS) in tests 12 to 15. A single test at a higher temperature (test 16) was conducted to provide an indication of the value to be gained from operating at a higher leach temperature. Further optimization of total iron concentration at a higher ORP set point was then conducted in tests 17 to 19 (these results are presented in chapter 5 under the modelling section).

All raw data from the batch leach tests were fitted to the empirical models described in section 3.3.5. The extraction and reagent addition curves presented in this chapter are the modelled curves. All raw data and model constants can be found in Appendix C.

The Rössing leach plant operates at a pH between 1 and 2. The second tank in each module is controlled at around pH 1.45 and the resultant terminal tank pH is on average 1.82 (i.e. a decaying pH profile philosophy is currently used). The average pH in the leach circuit is pH 1.6. All batch leach tests were, therefore, controlled at a *constant* pH of 1.6 throughout the leach to minimize the risk of introducing pH as a variable. It is recommended that further test work is conducted to establish the effect of running a leach at a constant pH versus a decaying pH (as is the current RUL control philosophy). With the introduction of the automated online pH control system at RUL, to be commissioned in 2014, the flexibility to control at a constant pH profile versus a decaying profile will exist which could improve the process further.

The Rössing leach plant currently operates at an ORP between 420 and 500 mV (average = 475 mV (Ag/AgCl)). A selection of ORP setpoints within this range and above this range, were, therefore, tested. The current total iron concentration target in the RUL leach plant is a

range, i.e. 4.0 – 5.2 g/L. A total iron concentration of 4 g/L was selected as the starting point for the test work and also the base case.

Table 4.1: Outline of experiments

Number	Ore type	ORP (mV)	Total Fe (g/L)	pH	Temperature (˚C)	% Solids
1	ROM	450	4	1.6	35	70
2	ROM	450	4	1.6	35	75
3	ROM	440[17]	4	1.6	35	70
4	ROM	450	4	1.6	35	70
5	ROM	475	4	1.6	35	70
6	ROM	500	4	1.6	35	70
7	ROM	525	4	1.6	35	70
8	ROM	550	4	1.6	35	70
9	ROM	450	3	1.6	35	70
10	ROM	500	3	1.6	35	70
11	ROM	550	3	1.6	35	70
12	CGS	450	4	1.6	35	70
13	CGS	475	4	1.6	35	70
14	CGS	500	4	1.6	35	70
15	CGS	550	4	1.6	35	70
16	ROM	525	4	1.6	45	70
17	ROM	525	3	1.6	35	70
18	ROM	525	4.5	1.6	35	70
19	ROM	525	5	1.6	35	70

The error in final % uranium extraction, acid addition and oxidant addition which is relevant to the discussion in Chapter 4 is summarized in Table 4.2 (discussed in section 3.3.6).

Table 4.2: Error analysis relevant to results presented in Chapter 4

Standard deviation at 13 hours	% U extraction	Acid addition (kg/t)	Oxidant addition (kg/t)
2σ	±1.2	±0.45	±0.003

[17] No oxidant was added to this test.

4.2 Effect of pulp density

Before the effect of ORP and total Fe on % uranium extraction and reagent addition could be tested using the laboratory agitated leach test method, it was necessary to establish the effect of pulp density on the % uranium extraction profile.

The agitated leach test was designed to operate at a pulp density of 70 % solids. The Rössing leach circuit operates at a pulp density between 68 and 74 %. Pulp density is known to affect % uranium extraction (Demopolous, 1985 and Roshani and Mirjalili, 2009). The impact of pulp density was, therefore, assessed. All tests were conducted on the ROM ore type, at a pH of 1.6, ORP of 450 mV, temperature of 35 ℃ and total iron concentration of 4 g/L.

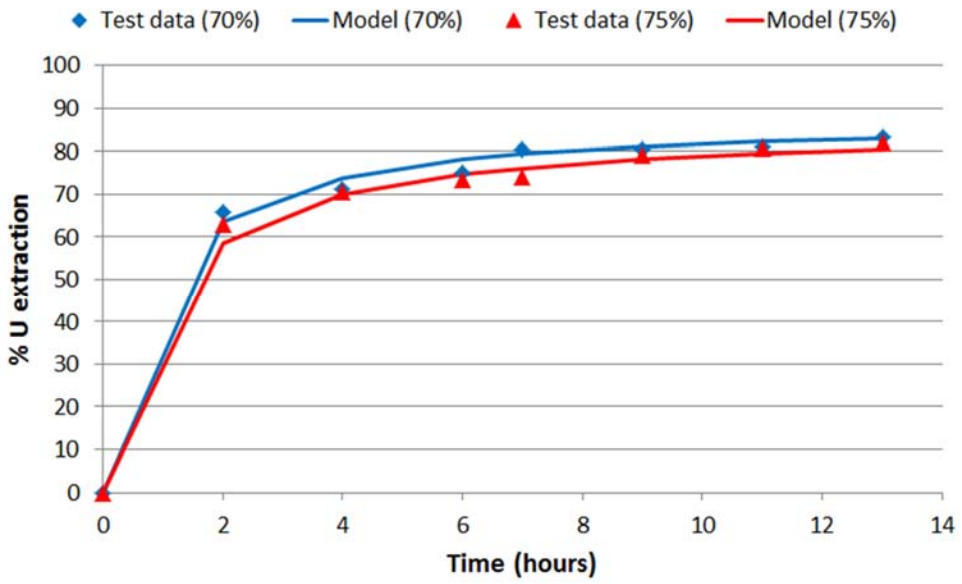

Figure 4.1: Effect of pulp density on % U extraction

The results in Figure 4.1 show that for the first 2 hours of leaching, the rate of uranium extraction was higher for the lower pulp density test. Beyond this point, uranium extraction increased at similar rates for both leaches. After 13 hours of leaching (final data point) the lower pulp density test achieved a uranium extraction 2.6 % greater than the higher pulp density test. The difference falls outside of the accepted experimental error (1.2 %) (section 3.3.6) and is therefore, considered to be significant. This result is in agreement with the trend noted by Roshani and Mirjalili (2009). The increase in % uranium extraction at the lower pulp density could be explained by an enhancement of mass transfer between the reactants and reaction surface at the lower pulp density, i.e. lower pulp viscosity (Vagias et al., 2010). A

high viscosity slurry, could result in the leaching rate being controlled by diffusion instead of being controlled by reaction which would result in a slower rate of leaching (Merrit, 1971).

Pulp density is also expected to impact the extent of uranium extraction as a result of chemical equilibrium. For higher pulp density tests, after a certain amount of time, the higher concentration of uranium leached into solution could result in the suppression of any further uranium leaching. Although it is beyond the scope of this thesis to establish at which uranium concentration (in solution) equilibrium is reached, it is important to note that this could influence the extent of uranium extraction at higher pulp densities.

The leach tests were only run for 13 hours and it is, therefore, unclear whether both the rate and extent of extraction were affected by pulp density. Had the leach been run for a longer period of time, the higher density test may have caught up to the lower density test. The residence time of the Rössing leach circuit varies between 6 and 10 hours (depending on the number of leach tanks online). For Rössing purposes it is, therefore, suggested that the lower pulp density test resulted in a higher % uranium extraction (within 13 hours of leaching).

ORP and pH control were well maintained for both tests. Although only a single test at each pulp density was conducted, the quality control check leach was within range for the week that these tests were conducted[18]. This suggests that the observed differences in % uranium extractions are likely to be significant.

It could not with certainty be said that the same trends (uranium extraction and reagent addition) with leach conditions, such as pH and ORP, would still hold at both pulp densities.

Operating the leach test at 70 % solids (according to the original design specification) was noted to be physically more manageable. To allow a more efficient test work program, it was decided to continue the leach test program at 70 % pulp density with the following provisos:

- Further test work would then need to be conducted to determine whether the change in extraction when variables such as ORP and pH are altered, is consistent at different pulp densities.
- Assess whether the order of leach results and subsequently the optimum set of conditions are preserved.

[18] One quality control leach test was conducted per week for the duration of the experimental test work program (under the same leaching conditions as the original repeatability test work, explained in section 3.3.6). The results thereof had to fall within the set control limits (±2SD) for the test work results to be accepted.

Should the result indeed be an indication of the effect of pulp density on leach extraction, a recommendation to tighten the leach plant pulp density control to the lower end of the range (i.e. 68 to 70 %) could potentially result in increased leach value. A trade-off study between the lower ore throughput rate at the lower pulp density and the improved uranium extraction would, however, need to be conducted to optimize leach value. Furthermore, it is recommended that any final decisions regarding a change in operating pulp density are underpinned by a series of tests with multiple repeats to ascertain the differences noted in this initial test work.

Key findings:

- It appears that final % uranium extraction increased (2.6 %) when pulp density was lowered from 75 to 70 %.
- The results indicate that there is potential value to be gained by tightening up the pulp density control in the Rössing leach plant to the lower end of the range (i.e. 68 – 70 %). This, however, requires further test work to confirm this observation. A trade-off study between a lower ore throughput rate at the lower pulp density and the improved uranium extraction would, however, need to be conducted to optimize value.

4.3 Pre-leach iron dissolution test results

Both ore types were pre-leached to determine the quantity of iron that would leach into solution. The resulting total iron concentration in solution was 2.7 g/L for the ROM ore type and 2.8 g/L for the CGS ore type (2.5 hour leach). It was expected that the leaching of the CGS ore would result in a higher total iron concentration due to the higher cordierite, biotite and potential iron sulphide content of this ore. The difference was, however, marginal. Over a longer period of leaching time, the difference may have become more prominent.

4.4 Effect of ORP (Ag/AgCl)

The effect of ORP over the range 440 to 550 mV was investigated. The results are presented in Figure 4.2, Figure 4.3, Figure 4.4 and Table 4.3. The ORP, pH and temperature profiles for these tests are presented in Appendix D. All tests were conducted on the ROM ore type, at a pH of 1.6, temperature of 35 ℃ and total iron concentration of 4 g/L.

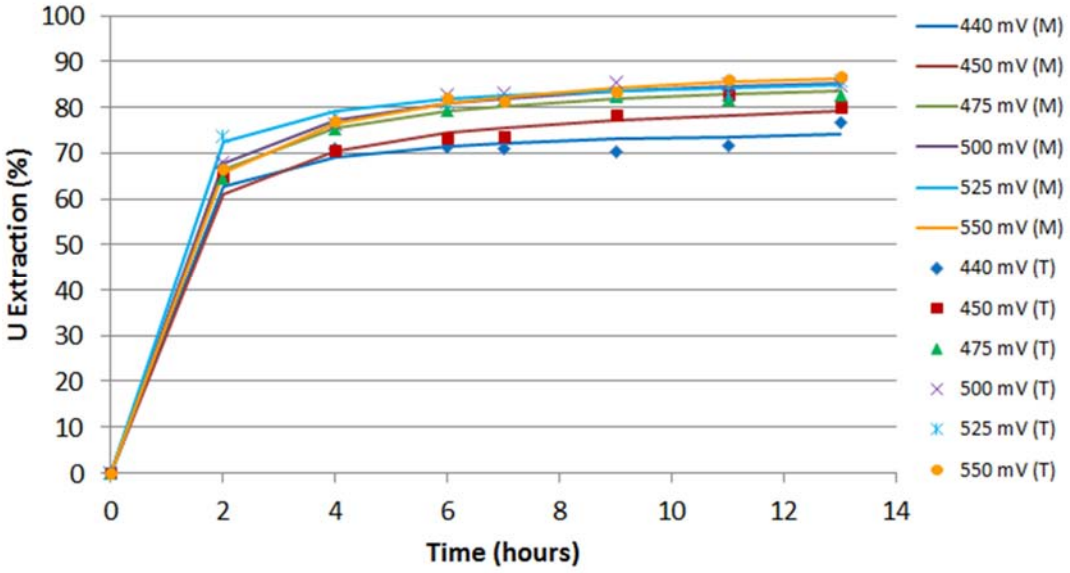

Figure 4.2: Effect of ORP on % U extraction (Total Fe = 4 g/L, ROM ore type)[19]

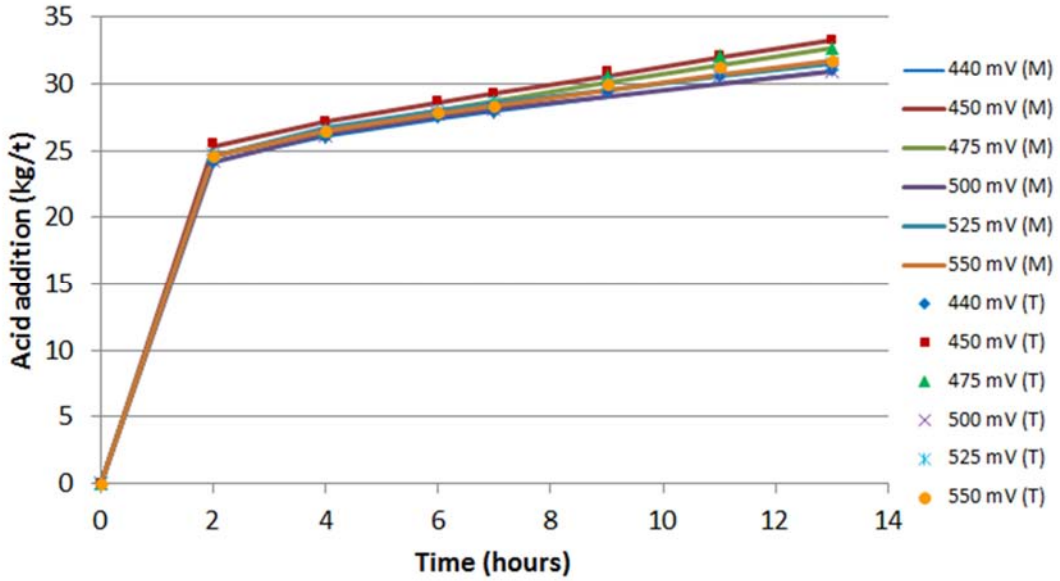

Figure 4.3: Acid addition profiles at various ORP set points (Total Fe = 4 g/l, ROM ore type)

[19] 'T' refers to the raw batch leach test data and 'M' refers to the model fitted to the data

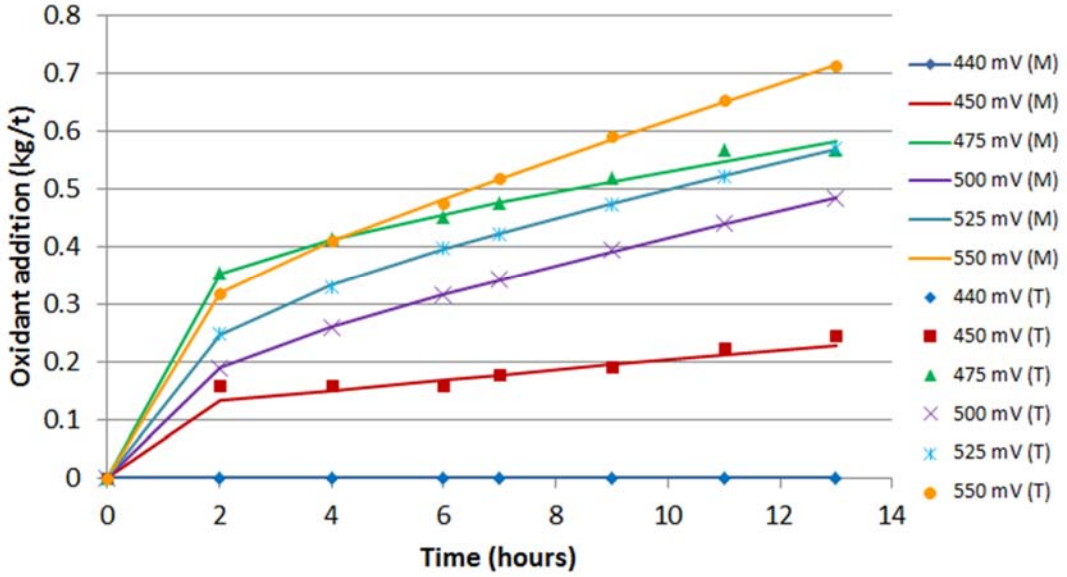

Figure 4.4: Oxidant addition profiles at various ORP set points (Total Fe = 4 g/l, ROM ore type)

Table 4.3: Results of ORP tests at Fe = 4 g/L (ROM ore type)

ORP (Ag/AgCl, 3M KCl)	% uranium extraction (at 13 hr)	Acid addition (kg/t) (at 13 hr)	Oxidant addition (kg/t) (at 13 hr)	Iron addition (kg/t) (at 13 hr)
440	74.1	31.0	0.00	1.64
450	79.0	33.2	0.23	1.64
475	83.5	32.7	0.58	1.64
500	85.3	30.9	0.48	1.64
525	84.8	31.5	0.57	1.64
550	86.3	31.7	0.71	1.64

Within the first 2 hours of leaching, 61 – 72 % of the uranium contained within the ore was dissolved into solution. The increases in % uranium extraction after 7 hours of leaching were fairly marginal. The final % uranium extraction (after 13 hours) ranged between 74 and 86 %. As only ~2 % of the uranium contained within the ore is refractory (betafite and coffinite), a higher % uranium extraction would be expected from this ore type. As discussed in section 3.1.1, around 70 % of the uranophane grains in the original ROM ore type sample were, however, determined to have less than 60% of their free surface area exposed (feed sample). Uranophane accounts for 20.5 % of the uranium in the ROM ore. The lower than expected uranium extraction (after 13 hours) could, therefore, be attributed to the limited exposure of uranophane to the leaching reagent. After several more hours of leaching, the % uranium extraction could, however, increase as gangue minerals are further digested by acid and thus exposing the free surface area of the uranium bearing mineral. The acid addition profile in Figure 4.3 suggests that gangue mineral dissolution will still proceed after 11 hours

of leaching, albeit at a rate slower than that noted in the first 2 hours of leaching. As expected, ORP appeared to have no effect on acid addition, i.e. the acid addition profiles and final acid addition rate were fairly similar for all 5 tests.

The influence of ORP on % uranium extraction is evident from the batch leach test results, i.e. after 13 hours of leaching % uranium extraction was highest at the highest ORP and decreased as ORP was decreased (apart from the test conducted at 500 mV). The correlation coefficient between ORP and final uranium extraction data sets (including the 500 mV data point) was 0.870 (statistically significant at the 90% confidence interval[20]). The same trend was noted in the studies conducted by Ram et al. (2013) and Roshani and Mirjalili (2009). An increase in 50 mV had a greater impact on uranium extraction in the lower ORP range than in the higher ORP range (an increase from 450 to 500 mV resulted in a 6.3 % increase, whereas an increase from 500 mV to 550 mV resulted in a 1.0% increase).

Within the first 2 hours of leaching, the relationship between ORP and uranium extraction is less clear, i.e. no statistically significant correlation. In fact, the fastest rate of uranium dissolution was seen for the test conducted at 525 mV. It was, however, expected that the test conducted at 550 mV would have had the fastest reaction rate within this time period (Ram, 2013). For this test, the target ORP of 550 mV was, however, only achieved after 20 minutes (Figure 4.5). Ram (2013) studied the rate of reaction for synthetic uraninite dissolution over a period of 90 minutes. Within the first 30 minutes, 55-60 % of the uranium had dissolved for tests conducted above 530 mV whereas only ~25 % had dissolved for a test conducted at 420 mV. This illustrates the effect of ORP on the rate of pure uraninite dissolution within the first 30 minutes of leaching and therefore, the potential effect thereof on the leaching of uraninite bearing ore (although not to the same degree, given other factors such as mineral liberation and galvanic hindrance that would need to be taken into account). The failure to meet the target ORP within the first 20 minutes of leaching could have limited the rate of uranium dissolution for the 550 mV test resulting in a lower than expected result for this test. Had the initial rate of uranium dissolution for the 550 mV test indeed been faster during the first 2 hours of leaching, it may well have resulted in a much higher final uranium extraction (after 13 hours or even after 7 hours of leaching). If the 550 mV result is increased by 5% extraction, the correlation between initial uranium extraction and ORP becomes statistically significant. The lack of correlation between the initial rate of uranium extraction and ORP could be attributed to experimental error. It is also possible that

[20] Degrees of freedom = 4

side reactions, favoured at a higher ORP could have competed for ferric, resulting in a lower uranium dissolution rate for the test conducted at 550 mV.

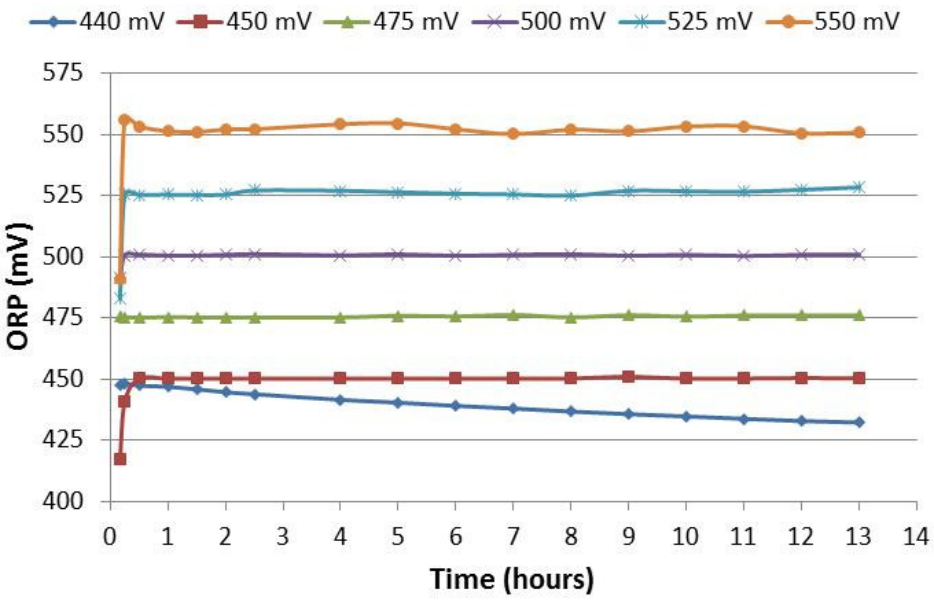

Figure 4.5: ORP profiles for batch leach tests conducted at Fe = 4 g/L

Figure 4.5 illustrates the ORP profiles for the leach tests conducted at different ORP set points. No oxidant was added to the leach test conducted at 440 mV. It is interesting to note that the ORP decreased consistently throughout the leach test. This indicates that reducing leach reactions progressed throughout the duration of the leach. The main contributor to lowering the ORP is expected to be the reduction of ferric to ferrous via uraninite (equation 1). As mentioned in section 1.3, the dissolution of gangue minerals such as biotite (the ROM ore type contains 1.07% thereof) and the subsequent release of ferrous into solution would also have the potential to lower the ORP during the leach. It is also important to note that although no oxidant was added to this test, the starting ferric, ferrous ratio of the synthetic process solution (resulting in a starting ORP of 450 mV) was sufficient to leach 63% of the uranium into solution within the first 2 hours of leaching. For the 440 mV test, although the rate of uranium extraction decreased after 2 hours of leaching, the ORP continued to drop at the same rate. This supports the suggestion that ORP was affected by the leaching of another reducing species (such as ferrous) into solution.

Final oxidant addition increased with an increase in ORP apart from the test conducted at 475 mV, where the oxidant addition rate was 0.18 kg/t higher than the test conducted at 500 mV. This could not be explained as the ORP control and total Fe control for this test were

within range. The correlation coefficient between overall oxidant addition and ORP was 0.872, indicating a statistically significant relationship between the 2 data sets. The oxidant addition profiles in Figure 4.4 also indicate that oxidant had to be constantly added to all leaches (apart from the 440 mV test) to combat the change in ORP as the leach reactions proceeded with time. Both the initial rate of oxidant addition (first 2 hours) and the rate for the remainder of the leach (2 – 13 hours) could be correlated to ORP, i.e. oxidation addition rate increased with an increase in ORP. The initial rate in all instances was greater than the second rate. This is likely due to the presence of a competing reductant, which leaches more rapidly at a higher ORP.

In the experiment, oxidant addition was controlled via a feedback control loop (i.e. oxidant continuously added to maintain the target ORP via a PID controller). The oxidant addition rate reflects the oxidant requirement of the ore (to maintain a targeted ORP set point). The initial rate (first 2 hours) of oxidant addition (Figure 4.4) for all tests was greater than the oxidant addition rate for the remainder of the leaching time. The rate of uranium extraction was also higher during the first 2 hours of leaching but there was, however, no statistically significant correlation between the initial rates of oxidant addition and initial rates of uranium extraction for the different tests. This could be a direct result of experimental error (standard deviation in % modelled uranium extraction at the 2 hour point is expected to be in the region of 5.6 %).

Between 2 to 10 hours, the rate of uranium extraction decreased significantly. Uranium leaching came to near completion within 10 hours. Oxidant addition rate also decreased after 2 hours, but continued in a linear fashion, even after 10 hours. This again suggests the leaching of ferrous or another reducing species into solution, which would require a continuous supply of oxidant to maintain the target ORPs.

In the Rössing leach circuit, ORP is only adjusted in the second tank and then allowed to decrease as the slurry progresses through the leaching circuit. The results in this section suggest that for a similar ore, this current approach to ORP control is correct (for an ore containing a specific species that, when leached into solution, would have the potential to reduce the ORP). Maintaining a target ORP throughout the leach would only increase the overall oxidant demand for the leach process and have little impact on increasing the rate of uranium extraction and consequently, the leaching value, further. Further test work and a financial evaluation would, however, need to be completed to confirm this.

Key findings:

- For the ROM ore type the maximum % uranium extraction (86.3 %) was achieved at 550 mV (Ag/AgCl) after 13 hours of leaching. The remaining unleached uranium in the ore is thought to be refractory betafite or coffinite and poorly liberated uranophane (i.e. 70 % of the uranophane grains in the feed sample had less than 60 % of their free surface area exposed).
- All leach curves started to plateau at 7 hours (i.e. marginal increases in % uranium extraction after 7 hours).
- Final % uranium extraction (after 13 hours) was found to increase with an increase in ORP, i.e. a strong correlation between the 2 data sets was established.
- A change in ORP in the 450 – 500 mV range had a greater effect on % uranium extraction than a change in ORP in the 500 – 550 mV range.
- ORP had no effect on acid consumption.
- It was possible to leach 67 % of the uranium into solution for a system where ORP was not controlled, i.e. starting at an ORP of 480 mV and declining to 430 mV after 11 hours.
- The oxidant demand could be categorised into two distinct regions, an initial, accelerated oxidant addition rate during the first 2 hours of leaching and a slower, but linear rate during the remaining 11 hours of leaching.
- Although the initial rate of uranium extraction was also much faster than the remainder of the leach, no correlation between the initial rate of uranium extraction and the initial oxidant addition rate was found. This is suggested to have been a result of experimental error.
- Oxidant was continuously added to all leaches (apart from the 440 mV test). This suggested that other reducing species, such as ferrous, leached into solution throughout the entire leach.
- The results supported the current Rössing leach plant ORP control philosophy. Changing this to a constant ORP control philosophy appears to hold little benefit as a result of the increased oxidant demand. Further test work and a financial evaluation would, however, need to be completed to confirm this.

4.5 Effect of total iron

Further test work was conducted to establish the effect of total iron on uranium extraction and reagent addition. The objectives were (i) to assess whether the same trends (ORP versus uranium extraction and oxidant addition) established at a total iron of 4 g/L held for a total iron of 3 g/L and (ii) to assess the impact of higher total iron concentrations at a higher ORP. The results are presented in Figure 4.6, Figure 4.7, Figure 4.8 and Table 4.4. All tests were conducted on the ROM ore type, at a pH of 1.6, temperature of 35 °C and total iron concentration of 3 g/L.

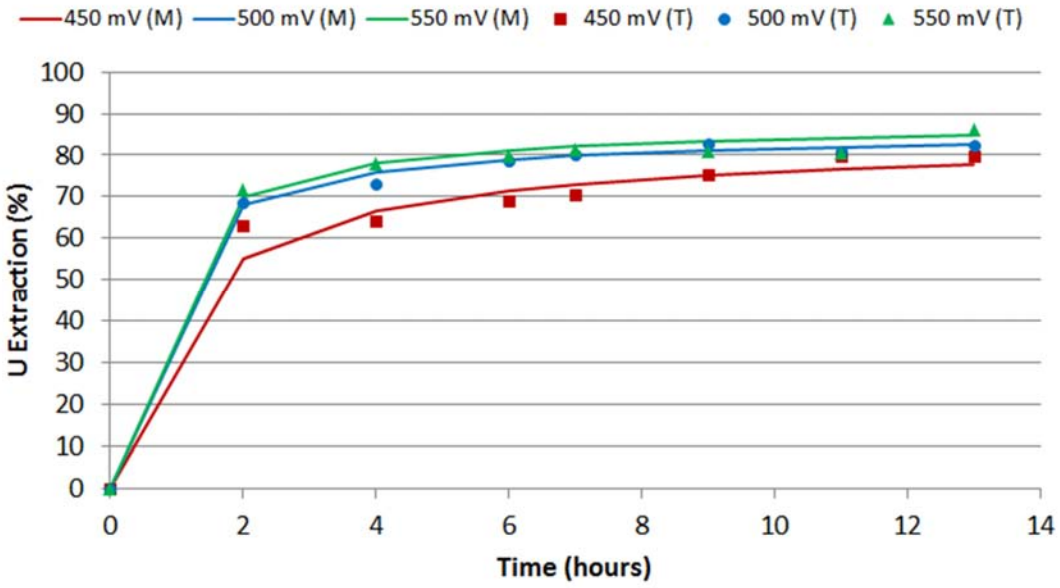

Figure 4.6: Effect of ORP on % uranium extraction (Total Fe = 3 g/L, ROM ore type)

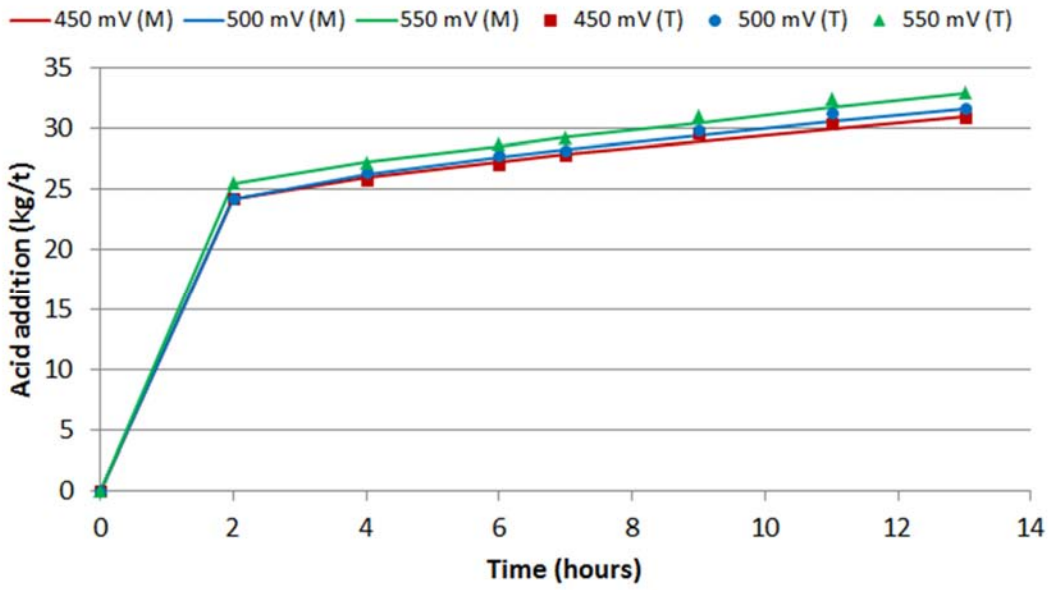

Figure 4.7: Acid addition profiles at various ORP set points (Total Fe = 3 g/l, ROM ore type)

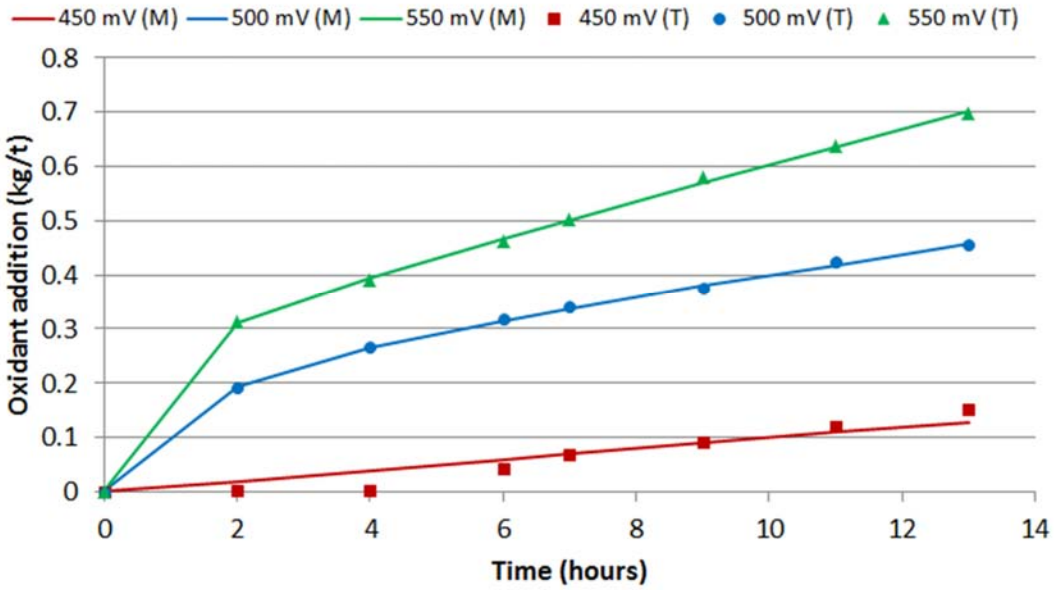

Figure 4.8: Oxidant addition profiles at various ORP set points (Total Fe = 3 g/L, ROM ore type)

Table 4.4: Results of ORP tests at Fe = 3 g/L (ROM ore type)

Total Iron (g/L)	ORP (Ag/AgCl, 3M KCl)	% U Extraction (at 13 hr)	Acid addition (kg/t) (at 13 hr)	Oxidant addition (kg/t) (at 13 hr)	Iron addition (kg/t) (at 13 hr)
3	450	77.7	30.9	0.13	0.38
3	500	82.4	31.6	0.46	0.38
3	550	84.8	32.9	0.70	0.38
4	450	79.0	33.2	0.23	1.64
4	475	83.5	32.7	0.58	1.64
4	500	85.3	30.9	0.48	1.64
4	525	84.8	31.5	0.57	1.64
4	550	86.3	31.7	0.71	1.64

Similarly to the experiments conducted at a total iron concentration of 4 g/L, the majority of uranium had dissolved into solution within the first 2 hours of leaching (55 – 70 %). The results indicate that the initial rate of uranium dissolution (first 2 hours of leaching) is slightly affected by the ORP at a total iron of 3 g/L. The trend is more definite with the 3 g/L tests compared to the 4 g/L, suggesting that at Fe = 3 g/L, ORP has more of an impact on the rate of uranium extraction than at Fe = 4 g/L. For the 3 g/L total Fe experiments, the % uranium extracted at 2 hours, increased with an increase in ORP from 450 to 500 mV (13.0 % increase). When ORP was increased from 500 to 550 mV, no significant change in the % uranium extracted at 2 hours, was seen (i.e. within experimental error).

For the 3 g/L tests, the increases in % uranium extraction were again fairly marginal after 7 hours for the 500 and 550 mV tests. The 450 mV test curve only plateaued at 11 hours, indicating much slower leaching kinetics for this test.

The results indicated that final % uranium extraction (at 13 hours) increased with an increase in total iron concentration, i.e. at specific ORP setpoints, 450, 500 and 550 mV, % uranium extraction increased with an increase in total iron (the differences fall outside of the acceptable error, 1.2 %). This finding is supported by work conducted by Ram et al. (2013).

From the results presented in Table 4.4, it can be seen that a similar % uranium extraction can be obtained for a system at a lower ORP than a system at a higher ORP, if sufficient iron is added at the lower ORP. This reflects the importance of both ORP and iron concentration in the dissolution of uraninite and the potential value to be gained from further optimizing the ORP set point at a high total iron[21] concentration (given the lower cost

[21] Iron added in the form of Conarc which contains 70 % ferric, i.e. a higher ferric concentration.

associated with adding more iron rather than adding more pyrolusite to the Rössing leach plant).

For the 3 g/L total Fe tests, acid addition increased marginally with an increase in ORP. This is different to the finding from the previous section where no trend was found between ORP and acid addition. Oxidant addition rate increased with an increase in ORP for the 4 g/L and 3 g/L total iron tests. One would expect higher acid consumption rates at higher oxidant consumption rates according to equations 34 and 37, i.e. 1 mole of sodium permanganate requires 4 moles of sulphuric acid. This indicates that the change in the acid addition rate for the different tests could also have been impacted by other side reactions, i.e. dissolution of gangue minerals. The rate of gangue mineral dissolution could possibly have been impacted by total iron and ORP. Although, further investigation into the explanation for this phenomenon is beyond the scope of work for this thesis, the effect thereof is taken into account in the techno-economic model.

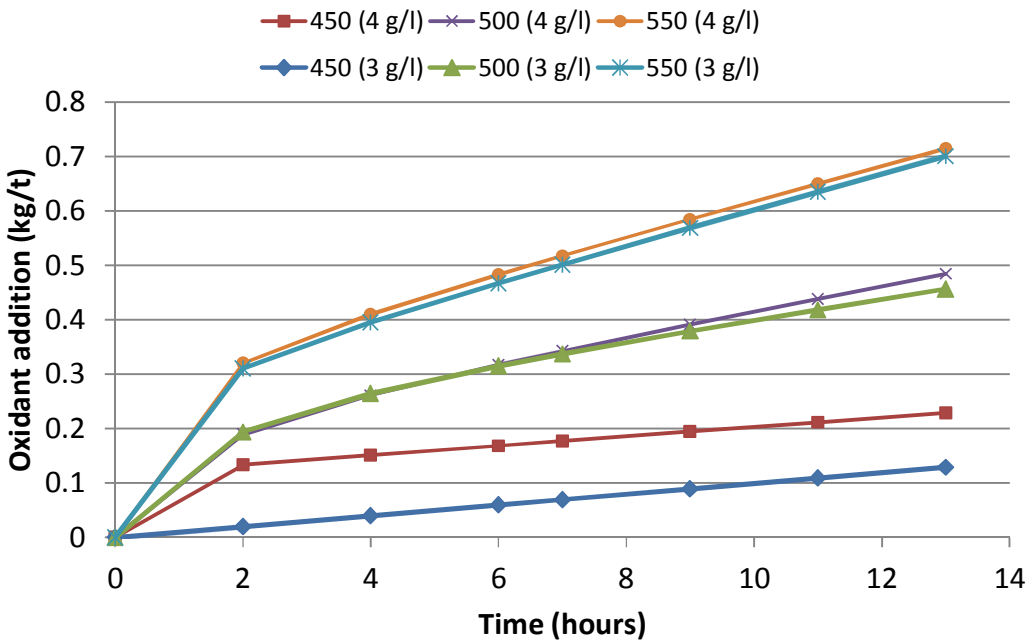

Figure 4.9: Oxidant addition profiles for 3 g/L and 4 g/L total Fe tests (modelled results only)

At an ORP of 500 and 550 mV, the oxidant addition requirement for the 4 g/L experiments was only marginally higher than the 3 g/L experiments. The oxidant addition profiles were in fact very similar (Figure 4.9). At an ORP of 450 mV, however, the test conducted at 4 g/L total Fe required 60% more oxidant than the test conducted at 3 g/L. This was further

investigated through the assessment of the ORP and iron concentration profiles of the two tests (Figure 4.10 and Figure 4.11).

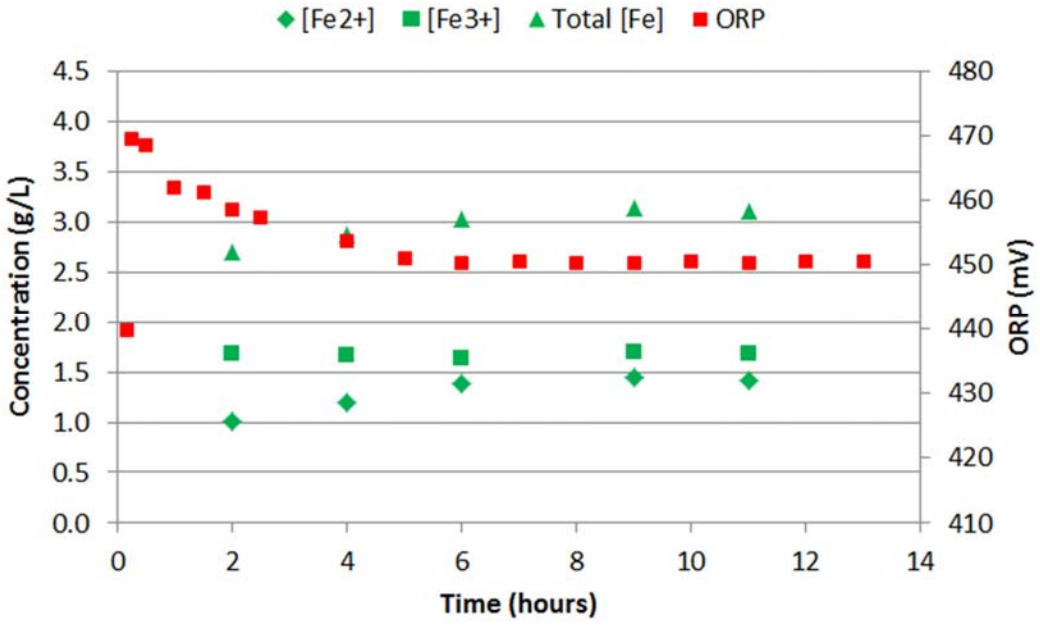

Figure 4.10: Ferric, ferrous, total iron and ORP profiles for leaches conducted at 3 g/L total Fe

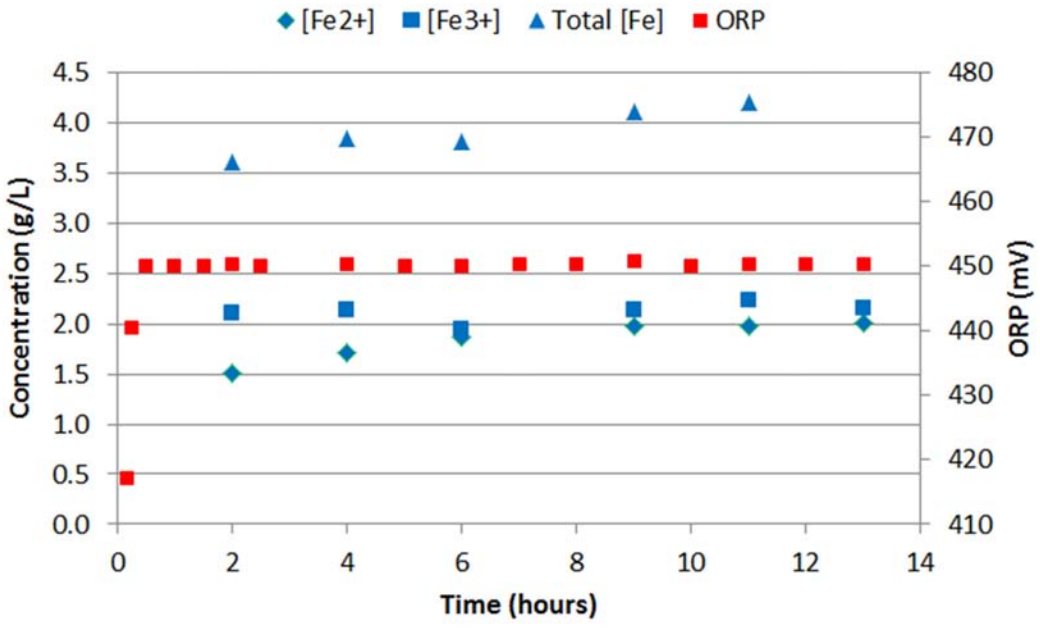

Figure 4.11: Ferric, ferrous, total iron and ORP profiles for leaches conducted at 4 g/L total Fe

Oxidant addition in the agitated leach tests is driven by the need to convert ferrous to ferric to obtain the required ORP set-point (via a PID controller). Figure 4.10 and Figure 4.11 illustrate the ferrous, ferric, total iron concentrations and ORP profiles for the experiments carried out at 450 mV (3 g/L and 4 g/L total Fe). For both tests, iron was added in the form of ferrous at the start to achieve the required total iron concentration. For the test in Figure 4.11, a higher quantity of ferrous was, therefore, added to achieve the higher total iron concentration. ORP control was started after 10 minutes. For the test at the lower total iron concentration (Figure 4.10) it can be seen that the target ORP was initially overshot when ORP control was started (i.e. poor leach control for the first 4 hours of leaching[22]). Although this occurred, the total oxidant addition for this experiment was still lower than the oxidant addition for the experiment at 4 g/L. It is unclear in which form iron leaches from the ROM ore due to the uraninite oxidation reaction that takes place at the same time that iron leaches from the ore (i.e. reducing ferric to ferrous). This data does, however, suggest that it leached in the form of ferric which would have resulted in a higher ferric to ferrous ratio for the experiment where less ferrous was added (Figure 4.10). Apart from the initial overdose of oxidant during the first 30 minutes of leaching, for the remainder of the first 6 hours of leaching, minimal quantities of oxidant were added to the test in Figure 4.10 to allow the ORP to naturally decline to the required set point. This explains the lower oxidant addition rate for this test. This is an interesting observation as it illustrates that for this ore type, iron may leach into solution as ferric, resulting in a lower oxidant requirement. It is, however, unclear which mineral may be responsible for the release of ferric into solution. The ROM ore contains 4.83 % hornblende which has been shown to leach in acidic solutions (Ryan, 2012). The dominant iron species in this mineral is ferrous, with a lesser (but not negligible) amount of ferric. It is, therefore, suggested that the dissolution of hornblende during leaching may have resulted in ferric leaching into solution.

It can also be seen that for both experiments, total iron increased over the duration of the leach tests. The graphs indicate that an increase in ferrous concentration (from 2 to 8 hours) resulted in the increase in total iron concentration. The dissolution of hornblende (containing ferrous) could have been responsible for this. This also explains the continuous oxidant addition requirement to maintain the target ORP for both experiments throughout the duration of the leach, even after uranium extraction had plateaued.

[22] The average ORP for the first 4 hours of leaching was 460 mV. Although this was higher than the target of 450 mV it was still closer to 450 mV than what it was to 500 mV. It was decided to continue to use the results for this test to assess the impact of ORP on % uranium extraction at a total iron of 3 g/l.

The other interesting point to note from this analysis is that total iron appears to have had a greater effect on % uranium extraction than ORP in the lower ORP range (<475 mV), i.e. even though ORP control was higher than target >450 mV for the first 4 hours of leaching (Figure 4.10), the test conducted at the higher total iron concentration (where ORP was well controlled at 450 mV) achieved the higher % uranium extraction.

A further analysis of all of the experimental data for the 3 g/L and 4 g/L tests also suggested that an increase in total iron concentration had more of an effect on % uranium extraction at a lower ORP (Table 4.5) for the first 7 hours of leaching. After 7 hours, the relationship is less prominent as the leach curves start to plateau. The effect on uranium extraction for the first 7 hours of leaching was probably because ferric was the limiting reagent for uranium extraction to take place. At low ORP values the dependence of uranium extraction on ferric concentration would, therefore, be higher than at higher ORP values. This finding corresponds to the conclusion drawn by Ram et al. (2011). They found that over the range 460 to 565 mV, a small change in total Fe was found to significantly increase the rate and extent of % uranium extraction (over 90 min). This effect decreased as ORP was raised from 460 to 565 mV (Figure 2.3). Ram et al. (2011) also found a significantly lower dependency on total Fe in the range 420 to 380 mV (which is below the range of ORP values tested in this work).

Table 4.5: Change in % uranium extraction at 7 and 13 hours over a range of ORP set-points, when total Fe is increased from 3 to 4 g/L

ORP (mv)	Δ% uranium extraction	
	7 hours	13 hours
450	2.5	1.31
500	2.1	2.83
550	0.2	1.51

Key findings:

- % uranium extraction increased with an increase in total Fe concentration:
    - At specific ORP setpoints, 450, 500 and 550 mV, uranium extraction was higher for the tests conducted at 4 g/L Fe compared to tests conducted at 3 g/L.
- Total iron had a real effect on % uranium extraction in the lower ORP range (450 - 500 mV) and less of an effect in the higher ORP range (500 – 550 mV). Total iron also appeared to have more of an effect on % uranium extraction than a change in ORP in the lower ORP range (<475 mV).
- For the ROM ore type, the results suggested that iron leached into solution as ferric and ferrous.
- Similar % uranium extraction was obtained for a system at a lower ORP than a system at a higher ORP, when sufficient iron was added at the lower ORP. This reflects the importance of both ORP and iron concentration in the dissolution of uraninite.
- There is potential value to be gained from further optimizing the ORP set point at a high total iron concentration, given the effect of iron on uranium extraction and the lower cost associated with adding more iron rather than adding more pyrolusite to the Rössing leach plant.

4.6 Assessment of a second ore type

The impact of ORP on uranium extraction and reagent consumption was tested on a second ore type, an ore type which contained a higher concentration of cordierite gneiss, i.e. the CGS ore. This was done to establish whether the order of results obtained for the ROM ore was preserved for another ore type, especially an ore type that may require a greater oxidant addition rate. The results are presented in Figure 4.12 and Table 4.6. The controls achieved for the leach tests are presented in the appendix. All tests were conducted on the CGS ore type, at a pH of 1.6, temperature of 35 °C and total iron concentration of 4 g/L.

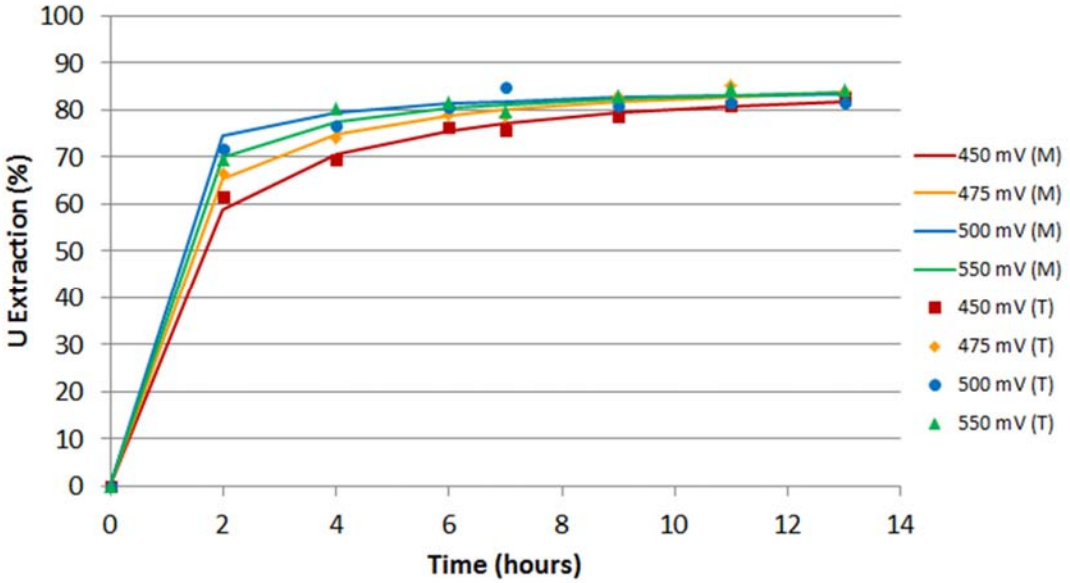

Figure 4.12: Effect of ORP on % uranium extraction (Total Fe = 4 g/L, CGS ore type)

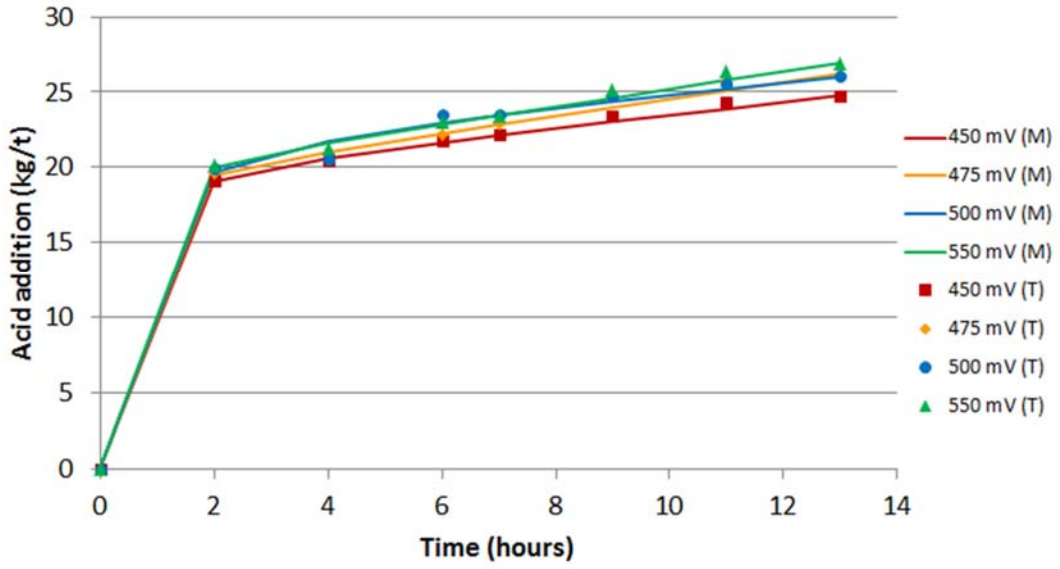

Figure 4.13: Acid addition profiles at various ORP set points (Total Fe = 4 g/L, CGS ore type)

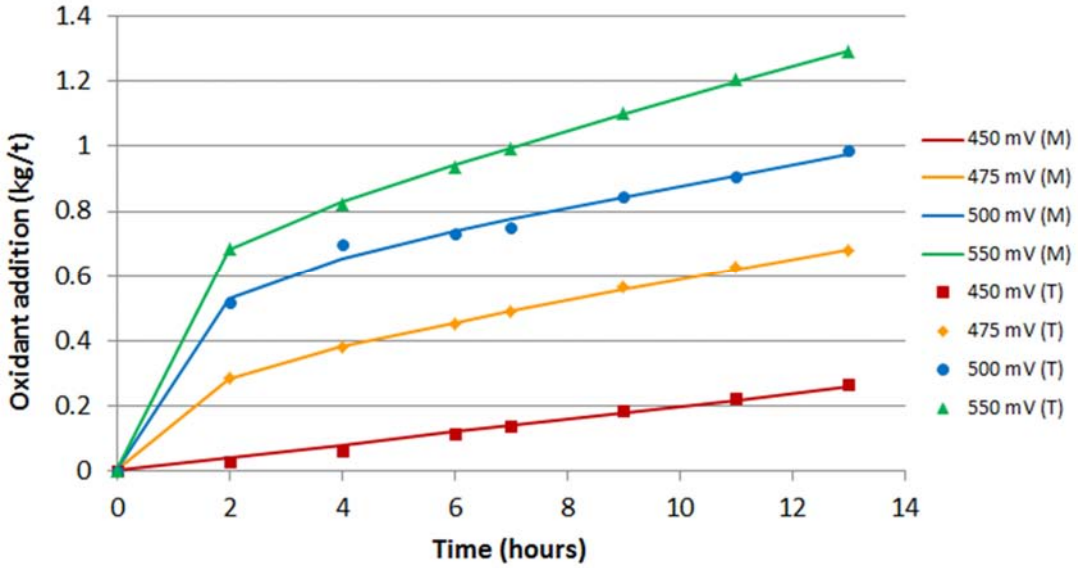

Figure 4.14: Oxidant addition profiles at various ORP set points (Total Fe = 4 g/L, CGS ore type)

Table 4.6: Results of ORP tests at Fe = 4 g/L, CGS ore

ORP (Ag/AgCl, 3M KCl)	% Uranium extraction (at 13 hr)	Acid addition (kg/t) (at 13 hr)	Oxidant addition (kg/t) (at 13 hr)	Iron addition (kg/t) (at 13 hr)
450	81.7	24.77	0.26	1.52
475	83.5	26.22	0.68	1.52
500	83.4	26.06	0.98	1.52
550	83.7	26.90	1.30	1.52

For the CGS ore type 59 – 74 % of the uranium contained within the ore was dissolved into solution within the first 2 hours of leaching. The initial rate of uranium dissolution was affected by the ORP, i.e. the higher the ORP, the higher the initial rate of uranium dissolution. The difference between the % uranium extracted at 2 hours for the 500 and 550 mV tests was within the experimental error (i.e. not significant). It is, therefore, suggested that above 500 mV, the initial rate of uranium dissolution is not impacted by ORP. The shapes of the % uranium extraction curves for the CGS ore type are similar to the shapes of the % uranium extraction curves for the ROM ore type (Figure 4.2). This suggests that the leaching kinetics were similar for both ore types (for a controlled ORP environment).

As the leaches proceeded with time, the difference between % uranium extraction at different ORPs at each point in time decreased. This could be a result of competing reactions within the leach, i.e. oxidative dissolution of iron sulphide minerals such as

pyrrhotite. At higher ORP set-points, this competition is likely to become more significant for the CGS ore type. The curves in Figure 4.14 show that the rate of oxidant addition increased with an increase in ORP (both the initial rate and the second rate), indicating the increased oxidant demand of the ore at a higher ORP. It is unclear in what form iron sulphide was present in the CGS sample. During the leaching experiments, H_2S gas was, however, observed (smelled).

Oxidant addition was significantly higher for the CGS ore, e.g. at 550 mV the CGS ore type required 1.3 kg/t oxidant, whereas the ROM ore only required 0.7 kg/t for the same ORP and total iron set point. Both the initial rate of oxidant addition (first 2 hours) and the rate for the remainder of the leach (2 – 13 hours) were higher for the CGS ore (Table 4.7). The higher the ORP, the larger the difference between the final oxidant requirement for the CGS and ROM ore types. This difference was less prominent at the lower ORP (450 mV). The initial oxidant addition rate for the CGS ore for the 450 mV leach was lower than expected.

Table 4.7: Oxidant addition for the ROM and CGS ores at different ORPs

ORP	**450 mV**		**500 mV**		**550 mV**	
Time	ROM ore	CGS ore	ROM ore	CGS ore	ROM ore	CGS ore
2 hours	0.13	0.04	0.19	0.53	0.32	0.68
13 hours	0.23	0.26	0.48	0.98	0.71	1.30

Table 4.8 summarizes the concentration of iron in solution after 7 and 13 hours for each leach test. This data indicates that between 7 and 13 hours, increased Fe was released into solution. The average total iron concentrations for experiments conducted on the CGS ore also contained 0.34 g/L more total iron in solution when compared to the ROM ore.

Table 4.8: Leach controls (4 g/L Fe, ore B)

ORP (Ag/AgCl, 3 M KCl)	Time (hours)	Total Fe concentration (± 1 SD) (g/L)
450	7	4.1 ± 0.1
	13	4.6 ± 0.3
475	7	4.1 ± 0.2
	13	4.4 ± 0.1
500	7	4.3 ± 0.2
	13	4.4 ± 0.6
550	7	3.9 ± 0.2
	13	4.6 ± 0.1

The higher oxidant addition rate for the CGS ore could be attributed to the dissolution of gangue minerals that contain ferrous. The dissolution of minerals such as biotite and chlorite would increase the overall ferrous concentration in the leach solution. When targeting a specific ORP, the increase in ferrous concentration would require the addition of oxidant to increase the ratio of ferric to ferrous in the leach solution. In the CGS ore type, these minerals could be present in higher concentrations resulting in a higher oxidant demand for this ore type.

Although the concentration of chlorite in the CGS ore type was not explicitly measured in the mineralogical investigation, previous studies have shown that it is present in the Rössing ores (Ryan, 2012). The CGS ore contained ~29% more biotite than the ROM ore (Figure 3.3 and Table 4.9). Biotite and chlorite would release ferrous into solution via the following reactions, lowering the ORP and increasing the overall oxidant demand:

Biotite: $2K(Mg,Fe^{2+})_3[AlSi]_3O_{10}(OH,F)_2 + H_2SO_4 \rightarrow K_2SO_4 + 2(Mg,Fe^{2+})_3[AlSi]_3O_{10}(OH,F)_2$ [14]

Chlorite: $(Mg,Fe)_5Al(Si_3Al)O_{10}(OH)_8 + 8H_2SO_4 \rightarrow 5(Mg,Fe)SO_4 + Al_2(SO_4)_3 + 3SiO_2 + 12H_2O$ [15]

The dissolution of such minerals does not, however, explain the increase in oxidant demand at higher ORPs. The direct oxidative dissolution of minerals such as iron sulphide in the CGS ore type, could, however, explain this observation.

Iron sulphide present in the form of pyrrhotite could be directly oxidised by ferric via equation 20 or dissolved via equation 18 to form ferrous. The H_2S resulting from equation 18 could in turn play a further role in reducing ferric to ferrous via equation 54. Increasing the ferrous concentration of the system, would lower the ORP and therefore, increase the oxidant demand.

$$Fe_{1-x}S + (2 - 2x)Fe^{3+} \rightarrow (3 - 3x)Fe^{2+} + S^0 \quad [20]$$

$$Fe_{(1-x)}S + 2H^+ \rightarrow (1-x)Fe^{2+} + H_2S \quad [18]$$

$$H_2S + 2Fe^{3+} \rightarrow S + 2H^+ + 2Fe^{2+} \quad [54]$$

In a kinetic study conducted by Filippou et al. (1997) on the effect of oxygen partial pressure on pyrrhotite dissolution, experimental data was fitted to a shrinking core model. The reaction order of pyrrhotite with respect to the oxidant was found to be one-half at lower temperatures (353 – 383 K) and first order at higher temperatures (403 – 453 K). This implies the strong relationship between pyrrhotite dissolution rate and oxidant concentration (or ORP) which, therefore, supports the theory that the increased dissolution of pyrrhotite at higher ORPs could be responsible for the higher oxidant demand observed at higher ORPs. Although these tests (Filippou et al., 1997) were conducted at higher temperatures, it is expected that oxidant concentration would still affect pyrrhotite dissolution at a lower temperature, but to a lesser degree.

The increased release of Fe into solution (Table 4.8) supports this hypothesis. It is, however, unclear which of the above mentioned minerals or reactions is responsible for this release and further analysis would need to be conducted to establish this. For the purposes of this project, what is clear from this experimental work is that the CGS ore type requires a higher oxidant addition rate to achieve the same system ORP as the ROM ore type (which can be linked to the difference in mineralogy between the two ore types, i.e. the CGS ore contained a higher concentration of biotite and potentially pyrrhotite). The concentration of iron in solution increased throughout the leach indicating the dissolution of an iron containing mineral.

The acid addition profiles for the CGS ore type were similar in shape for all ORPs. Acid addition did, however, increase slightly with an increase in ORP. Acid addition was significantly lower for this ore type, i.e. ~6 kg/t lower than the acid addition for the ROM ore

(Figure 4.15). This was affected by the initial rate of acid consumption within the first 2 hours of leaching. After the 2 hour mark, both ore types continued to consume acid to the same extent. Table 4.9 provides a summary of the concentrations of potential acid consuming gangue minerals within the two ore types. Considering the difference in calcite concentration between the two ore types alone, stoichiometrically, this equates to an acid consumption difference of 9 kg/t (assuming complete reaction). Complete reaction[23] of dolomite and hornblende adds on an additional difference between the ore types of 7 kg/t. The higher acid consumption for the ROM ore type could, therefore, be explained by the higher concentration of gangue consuming minerals within this ore type.

Table 4.9: Mineral abundance of acid consuming gangue minerals within the ROM and CGS ore types

Mineral	ROM	CGS
	Mineral abundance (%)	
Calcite	2.64	1.74
Dolomite	0.40	0.09
Biotite	1.07	1.38
Hornblende	4.83	3.39

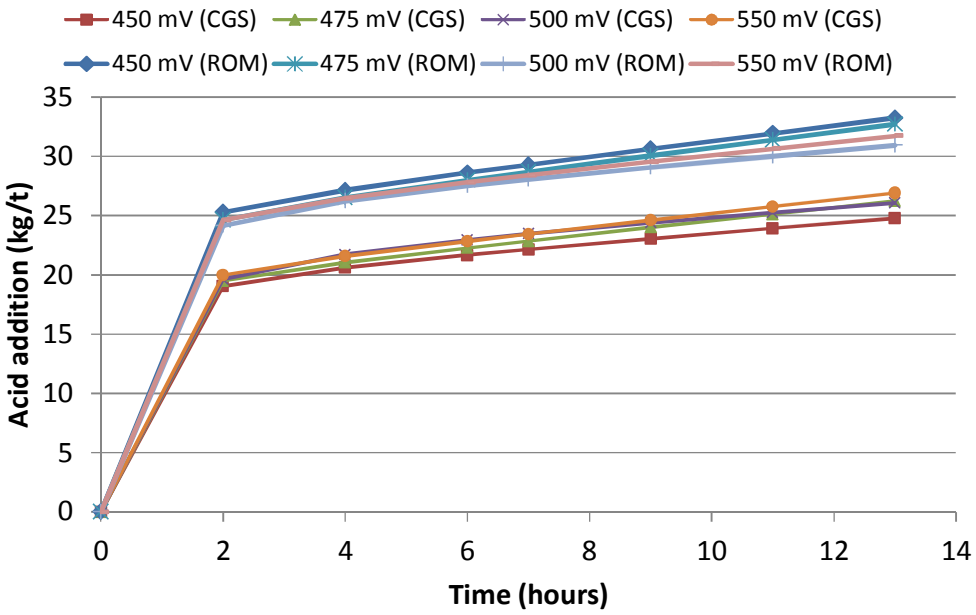

Figure 4.15: Acid addition profiles at various ORP set points for ROM and CGS ore types (modelled results)

[23] It is not expected that complete reaction of these minerals would take place within 7.8 hours of leaching due to various degrees of mineral liberation.

Key findings:

- For the CGS ore type the maximum % uranium extraction (84 %) was achieved at 550 mV after 13 hours of leaching.
- The initial rate of uranium dissolution increased within an increase in ORP (apart from the test conducted at 550 mV which had a lower rate than the test conducted at 525 mV). This may have been a result of competing reactions favoured at higher ORP's.
- The % U extraction curves for the CGS ore were similar in shape to the ROM ore, suggesting similar leaching kinetics for both ore types under constant ORP conditions.
- Oxidant addition increased with an increase in ORP for the CGS ore.
- Oxidant addition was significantly higher for the CGS ore than the ROM ore. The higher the ORP, the larger the differences between the oxidant demand for the CGS and ROM ore types. The higher oxidant demand for the CGS ore may have been a result of the presence of competing reductants (change in mineralogy and gangue content) which leached more rapidly at a higher ORP. The concentration of iron in solution increased throughout the leach indicating the dissolution of an iron containing mineral.
- Acid addition was significantly lower for the CGS ore than the ROM ore. Within the first 2 hours of leaching, the CGS ore consumed ~6 kg/t less acid than the ROM ore. The lower acid requirement for the CGS ore was suggested to have been due to the lower concentration of acid consuming gangue minerals (such as calcite) in the CGS ore type.

4.7 Effect of temperature

As already explained, temperatures in the Rössing leach slurry can vary between 30 and 40 °C depending on the season and the time of day. To answer the question from section 2.3.3 on whether a notable change in uranium extraction and acid consumption can be seen when the temperature is increased by 10 °C, before embarking on an experimental program that studies the effect of temperature, an initial test was conducted. The results from this experiment are presented in Figure 4.16, Figure 4.17, Figure 4.18 and Table 4.10.

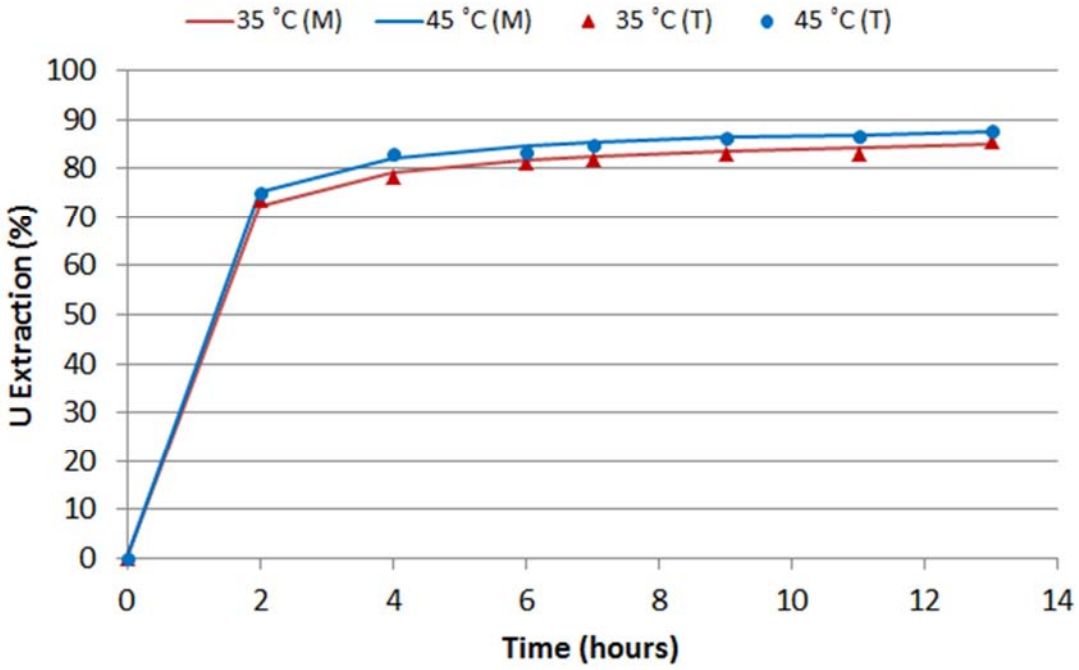

Figure 4.16: Effect of temperature on % uranium extraction (Total Fe = 4 g/L, ROM ore type)

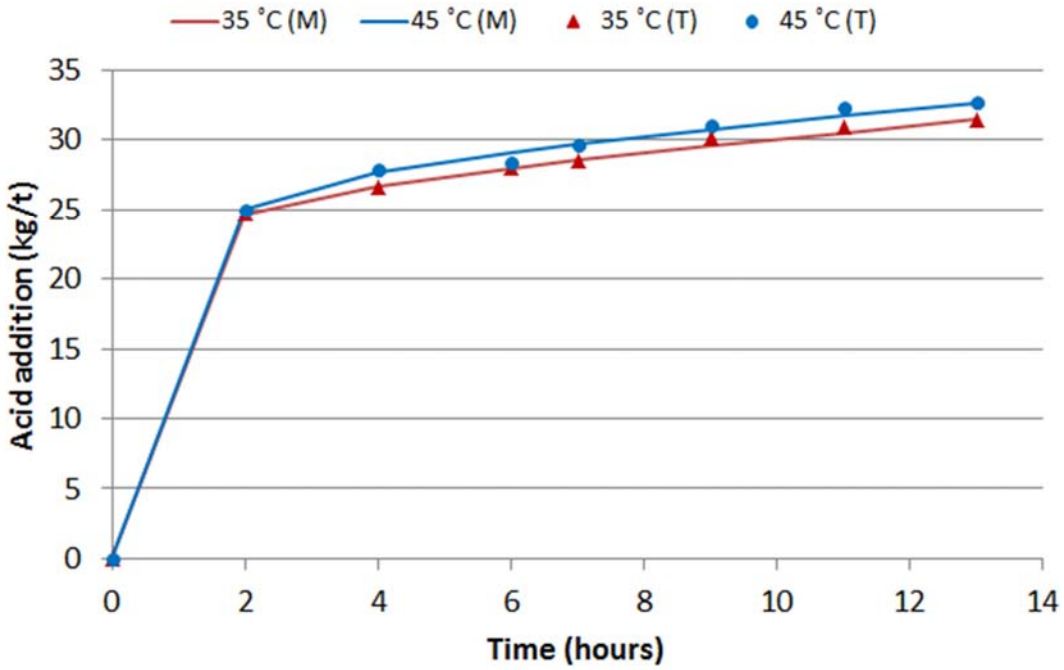

Figure 4.17: Acid addition profiles for different temperatures (Total Fe = 4 g/L, ROM ore type)

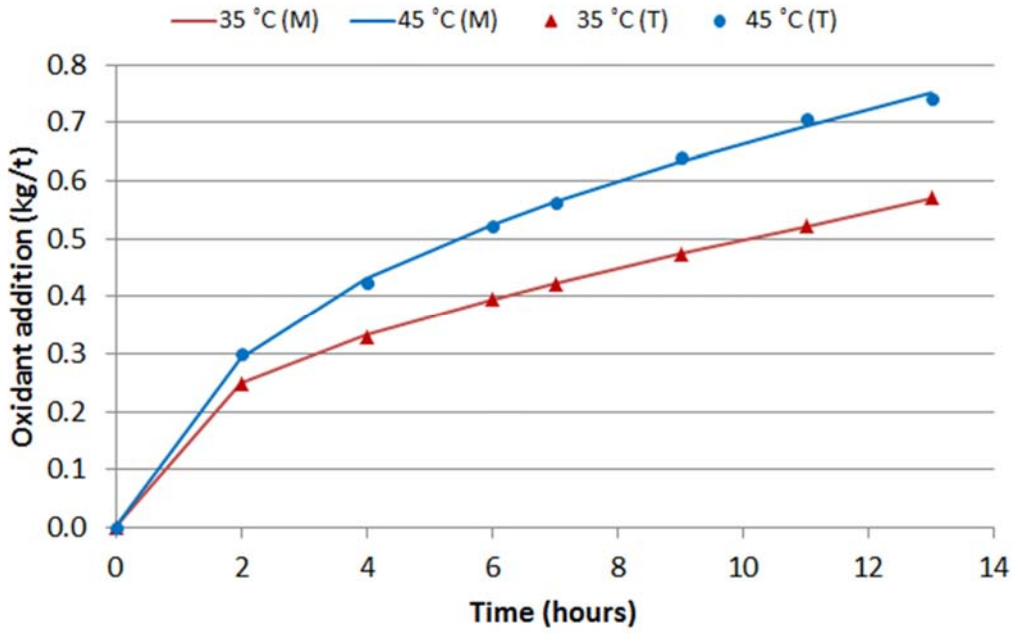

Figure 4.18: Oxidant addition profiles for different temperatures (Total Fe = 4 g/l, ROM ore type)

Table 4.10: Results for temperature tests at 4 g/L, 525 mV

Temperature (°C)	% uranium extraction (t = 13 hours)	Acid addition (kg/t) (t = 13 hours)	Oxidant addition (kg/t) (t = 13 hours)	Iron addition (kg/t) (t = 13 hours)
35	84.8	31.5	0.57	1.64
45	87.3	32.7	0.75	1.64

After 2 hours of leaching, the leach test conducted at 45 ˚C had dissolved 3 % more uranium than the test at the lower temperature, indicating a faster rate for the higher temperature leach. Considering the error associated with the initial stages of the laboratory leach, this does, however, fall within the margin of error. To confirm if there are any differences in leaching rate, these tests would need to be repeated. As expected, the final % uranium extraction was also higher for the higher temperature leach (2.5 % higher after 13 hours). This result is significant as it falls outside of the error margin for the 13 hour point. These results were consistent with the results observed by Ram et al. (2013), Roshani and Mirjalili (2009), Ring (1980) and Demopoulos (1985) who reported an increase in the initial rate and final extraction of uranium for uraninite bearing ores when leaching at higher temperatures.

The temperature profiles for these tests are displayed in Figure 4.19. Although the target temperatures were only achieved after 1-1.5 hours, the difference between the temperatures

of the two leaches was on average 10 ˚C throughout the duration of each leach. These tests can, therefore, still be used to provide an indication of the effect of a 10 ˚C temperature change on uranium extraction and reagent consumption within a 25 to 45 ˚C temperature range. It is important to note that the absolute difference between the extents of uranium dissolution for the two tests at different time intervals is expected to be different over different temperature ranges as it has been shown that the leaching rate of reaction (rate constant) for uraninite does not increase proportionally with an increase in temperature (Ram, 2013). The relationship between temperature and the rate constant can be described by the Arrhenius equation:

$$k = Ae^{-E_a/(RT)} \quad [55]$$

Where k = rate constant, T = Temperature, A = pre-exponential factor, E_a = Activation energy and R = Universal gas constant.

Ram et al. (2013) determined the activation energy and Arrhenius parameter for a uraninite bearing ore (80–85 % uraninite) to be 22.39 kJ/mol and 2.8, respectively for the range of temperatures tested (35 – 90 ˚C).

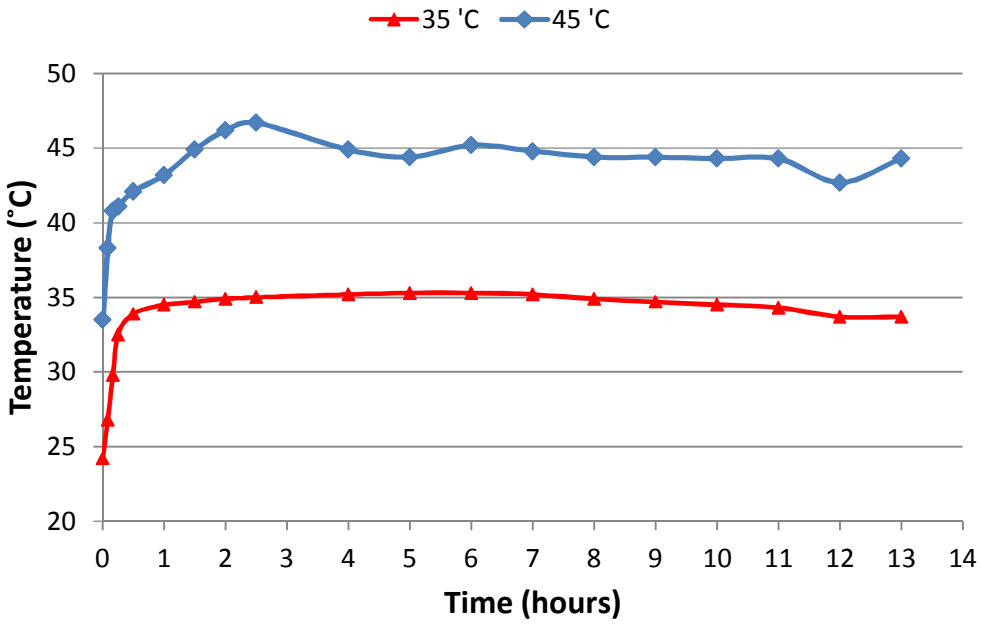

Figure 4.19: Temperature profiles for tests conducted at 35 and 45 ˚C.

After 2 hours of leaching, both tests had consumed similar volumes of sulphuric acid. Between 2 and 13 hours, the 45 ˚C leach required a slightly higher acid addition rate, ending with an overall acid addition of 1.3 kg/t higher than the 35 ˚C leach. A higher acid addition rate was expected for the higher temperature leach due to the potential increased rate of gangue mineral dissolution. Ring (1980) showed an increase in acid consumption for leaches conducted at higher temperatures due to gangue dissolution.

The initial and final rate of oxidant addition was higher for the higher temperature leach. As the rate of uranium dissolution was higher for the higher temperature leach, it was expected that the oxidant addition rate would be higher (due to the conversion of ferric to ferrous during the uraninite dissolution reaction). During the first 2 hours of leaching (when acid addition was the same for both tests) it may also have been an elevation in the *oxidative* dissolution of certain gangue minerals that elevated the oxidant demand during this period. Between 2 to 13 hours, the increase in acid addition for the higher temperature leach (thought to have been a result of an increase in gangue mineral dissolution) may then have resulted in an increased release of reducing species such as ferrous into solution. This would then have contributed to the elevated rate of oxidant addition during this period. The total solution iron concentration increased from 4.0 g/L (2 hours) to 4.8 g/L (13 hours) for the 45 ˚C leach so this is indeed plausible. The total iron concentration for the 35 ˚C leach only increased from 3.7 g/L to 4.0 g/L during the leach.

This test work indicates that there is potential value to be gained from operating the leach at 45 ˚C, i.e. higher uranium extraction with a marginal change in acid addition. The economic effect of the increased oxidant addition rate would, however, need to be considered. The final % uranium extraction achieved for the 45 ˚C was higher than the % U extraction achieved for a test conducted at a higher ORP (550 mV). This indicates that there is potentially more value to be gained by heating the leach circuit than increasing the ORP. The cost of the increased reagent consumption and energy requirement would, however, need to be considered at the higher temperature.

Key findings:

- % uranium extraction increased with an increase in temperature from 35 to 45 ˚C. Acid and oxidant addition were also found to increase over the same temperature range.
- The final % uranium extraction achieved for the 45 ˚C leach was higher than the % uranium extraction achieved for a test conducted at a higher ORP (550 mV).

5 Modelling and application of results to the Rössing leaching plant

5.1 Interpretation of results from techno-economic modelling

The data presented in chapter 4 was combined with the residence time distribution function for a CSTR to establish the impact of varying ORP and total iron on the overall predicted financial value from the Rössing leach process and in so doing select improved set points that maximise predicted financial value (Figure 3.16).

The error in final % uranium extraction, acid requirement and oxidant requirement, relevant to the discussion in Chapter 5 is summarized in Table 5.1 (discussed in section 3.4.3).

Table 5.1: Error analysis relevant to results presented in Chapter 5

Standard deviation (5 tanks, 7.8 hours)	% U extraction	Acid requirement (kg/t)	Oxidant requirement (kg/t)
2σ	0.7	0.25	0.013

An average residence time of 7.8 hours (5 tank scenario) was selected for all modelled scenarios. This is the current average leach residence time in the Rössing leach circuit. All results were compared to a base case scenario to establish the relative change in predicted financial value. The test that resulted in the lowest predicted value was selected as the base case scenario, i.e. 440 mV and 4 g/L total Fe. The outputs from each modelling exercise were predicated extraction, acid requirement, oxidant requirement, conarc addition, revenue, cost and overall value. Predicted revenue, cost and overall value (economic indicators) for each scenario were then compared to the result for the base case scenario to establish a percentage change in revenue, cost and financial value, relative to the base case. The change in revenue, total cost and overall value are presented as a % change for the respective economic indicators due to the confidentiality of this information. An example of how the % change was calculated is presented in Table 5.2.

Table 5.2: Example of how % change in economic indicators is calculated

		A	B	B - A	(B – A)/A x 100
		Base Case	Comparative Case	Difference between base case and comparative case	% Change
R	Predicted revenue	100	130	30	30%
C	Predicted cost	50	60	10	20%
R - C	Predicted overall value (profit)	50	70	20	40%

Due to the confidentiality of Rössing's reagent and uranium contract price information, it is not possible to present these financial indicators in this thesis. To provide an indication of the relative cost of a leaching reagent versus the value of uranium extraction, the global uranium long term price and acid contract prices (available in the public domain) have, however, been used to calculate the relative effect that a change in reagent consumption or uranium extraction will have on cost and revenue. It must be noted that these are not the prices that were used in the techno-economic modelling exercise. For this exercise (Table 5.3), an annual milling production rate of 12,000,000 t and a head grade of 300ppm were assumed. Prices for pyrolusite and Conarc were not available in the public domain.

Table 5.3: Relative cost of reagent versus value of uranium extraction

Uranium price (long term) (UxC, 2014)	50	US$/lb
Revenue generated per 1% uranium extracted	3,968,316	US$/annum
Acid price (contract price) (Argus, 2013)	75	€/t
Exchange rate (16 January 2014)	1.36	€/US$
Cost incurred per 1 kg/t acid consumed (per annum)	1,224,000	US$/annum

5.1.1 Impact of ORP

Table 5.4, Table 5.5 and Figure 5.1 summarise the modelled results for various ORP's for a 5 tank scenario.

Table 5.4: Techno-economic model results of ORP tests at Fe = 4 g/L (5 tank scenario, ROM ore type)

ORP (Ag/AgCl, 3M KCl)	% U Extraction	Acid requirement (kg/t)	Oxidant requirement (kg/t)	Iron addition (kg/t)
440	71.6	28.2	0.00	1.64
450	75.0	29.8	0.25	1.64
475	79.8	29.2	0.68	1.64
500	81.4	28.4	0.50	1.64
525	82.2	28.9	0.61	1.64
550	81.7	28.8	0.76	1.64

Table 5.5: Economic assessment of leach data – predicted value (at 4 g/L Fe)

ORP (Ag/AgCl, 3M KCl)	% Increase in Revenue	% Increase in Cost	% Increase in overall value
	Compared to base case (440 mV, 4 g/L Fe, ROM ore)		
440			
450	4.7	5.9	4.3
475	11.4	10.8	11.7
500	13.7	9.2	15.4
525	14.7	11.1	16.1
550	14.1	11.8	15.0

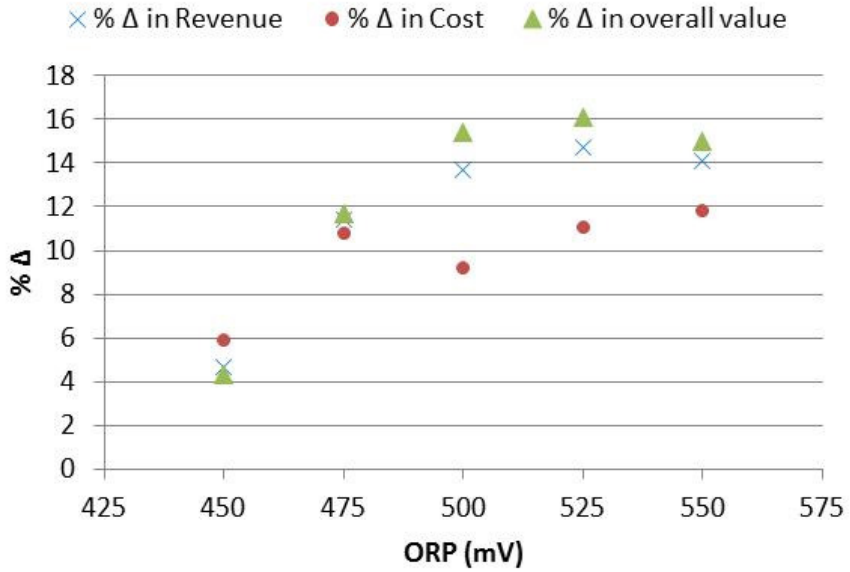

Figure 5.1: Effect of ORP on predicted value generated by Rössing leach circuit (at 4 g/L Fe)

When the data was fitted to the model (Table 5.4) the predicted % uranium extraction results indicated an optimum ORP set point at 525 mV. The experimental results presented in section 4.4 indicated an optimum of 500 mV after 7 hours and 550 mV after 13 hours. Fitting the data to the techno-economic model allows interpolation of the results to different points in time (i.e. different leach residence times). The 5 tank scenario corresponds to a residence time of 7.8 hours. The difference between the extraction result at 550 mV and 525 mV (0.5%) is, however, within the experimental error (0.7%, discussed in section 3.4.3) and it should be concluded that there was no significant change in uranium extraction when ORP was increased from 525 to 550 mV. The reason for this may be that within a higher ORP system, side reactions (such as the oxidation of iron sulphide) start to compete with the uraninite reaction, thus reducing the effect on the extent to which uraninite is leached after 7.8 hours.

The results from the techno-economic modelling exercise (Table 5.5 and Figure 5.1) indicate that an economic optimum exists. Of the conditions tested, the maximum predicted value occurs at an ORP set point of 525 mV. This is largely due to the higher uranium extraction result for this case at this residence time and the lower pyrolusite consumption rate than the 550 mV case.

If the same data is modelled for a 6 tank case (9.7 hours), the preferred ORP set-point changes to 500 mV (green data points in Figure 5.2). Uranium extraction is expected to increase with residence time, i.e. the entire value curve would be expected to shift vertically upwards to a point (as it did from the 4 tank to the 5 tank scenario), maintaining the order of value generated. Increasing the residence time above a certain point could, however, start to shift the value curve down again as gangue acid consumption starts to exert a larger influence than any available remaining extraction. For the 6 tank case, the value curve did indeed shift upwards, but the optimum shifted to a lower ORP set-point. Again, the optimum value generated is mostly affected by uranium extraction which is the highest at 500 mV for the 6 tank case. This highlights the error associated with the batch agitated test work and consequently the modelled extraction (0.7%), i.e. from this test work data, it is difficult to predict the change in value generated over the 500 to 550 mV range where the change in uranium extraction is a lot smaller (and possibly masked by the error) than the change in uranium extraction for the lower ORP tests. What is very clear from the test work is that in all cases (4, 5 and 6 tank scenarios), tests run at ORP's of 440, 450 and 475 mV predict much lower value delivery than tests run in the 500 to 550 mV range.

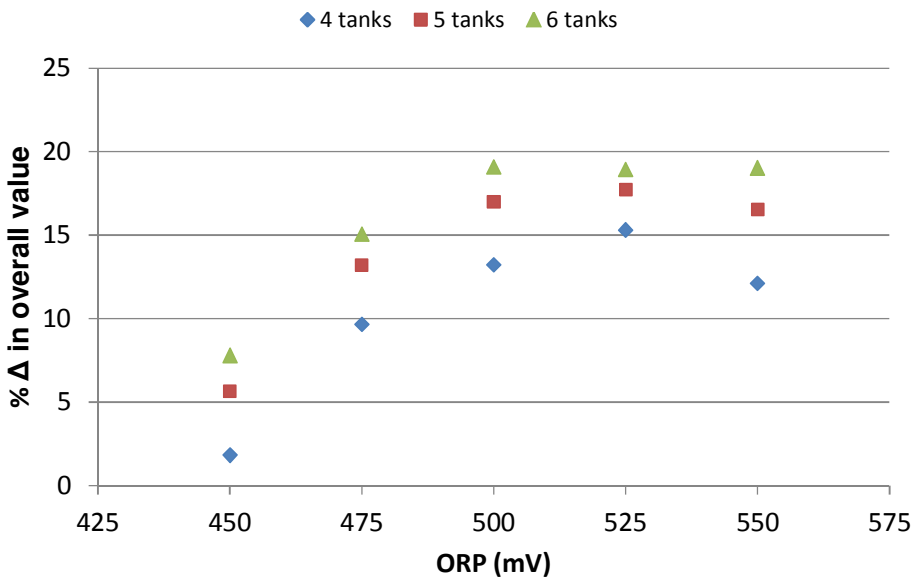

Figure 5.2: Change in overall revenue versus ORP versus number of tanks online

An objective of this work was to determine an improved ORP set point that would result in improved value delivery from the Rössing leaching circuit. For the past 10 years, the leach plant was operated at an ORP set point of 475 mV. This test work suggests that there is potential value to be gained through an increase in % uranium extraction by increasing the plant ORP above 500 mV.

5.1.2 Impact of total iron

In addition to the experimental test work presented in section 4.5, that looked at the effect of ORP on leaching characteristics at a lower total iron concentration, 3 additional leach tests were conducted to establish the effect of total iron concentration at a higher ORP. All results were fitted to the model and are presented in Table 5.6. The overall predicted value results for each set of conditions are presented in Table 5.7.

Table 5.6: Techno-economic model results for ORP tests at total Fe = 3, 4, 4.5 and 5 g/L (5 tank scenario, ore A)

Total Iron (g/L)	ORP (Ag/AgCl, 3M KCl)	% U Extraction	Acid requirement (kg/t)	Oxidant requirement (kg/t)	Iron addition (kg/t)
3	450	72.42	28.2	0.10	0.38
3	500	79.38	28.6	0.49	0.38
3	525	80.64	28.2	0.70	0.38
3	550	81.63	29.7	0.73	0.38
4	450	75.03	29.8	0.25	1.64
4	500	81.42	28.4	0.50	1.64
4	525	82.16	28.85	0.61	1.64
4	550	81.72	28.8	0.76	1.64
4.5	525	83.08	29.3	0.69	2.28
5.0	525	83.21	29.4	0.68	2.91

Table 5.7: Economic assessment of leach data – predicted value (ROM ore type)

Total Iron (g/L)	ORP (Ag/AgCl, 3 M KCl)	% Change in Revenue	% Change in Cost	% Change in overall value
		Compared to base case (440 mV, 4 g/L Fe, ore A)		
3	450	1.1	(1.4)	2.1
3	500	10.8	5.9	12.7
3	525	12.6	7.5	14.6
3	550	14.0	10.4	15.4
4	450	4.7	5.9	4.3
4	500	13.7	9.2	15.4
4	525	14.7	11.1	16.1
4	550	14.1	11.8	15.0
4.5	525	16.0	14.1	16.7
5	525	16.2	15.4	16.4

For the group of experimental results conducted at the lower total iron concentration (total Fe = 3 g/L), the maximum predicted value was achieved at an ORP of 550 mV (compared to the base case). Even though this set point resulted in a higher predicted operational cost (largely due to acid and oxidant requirements), this was overshadowed by the benefit gained via the additional 10 % uranium extraction.

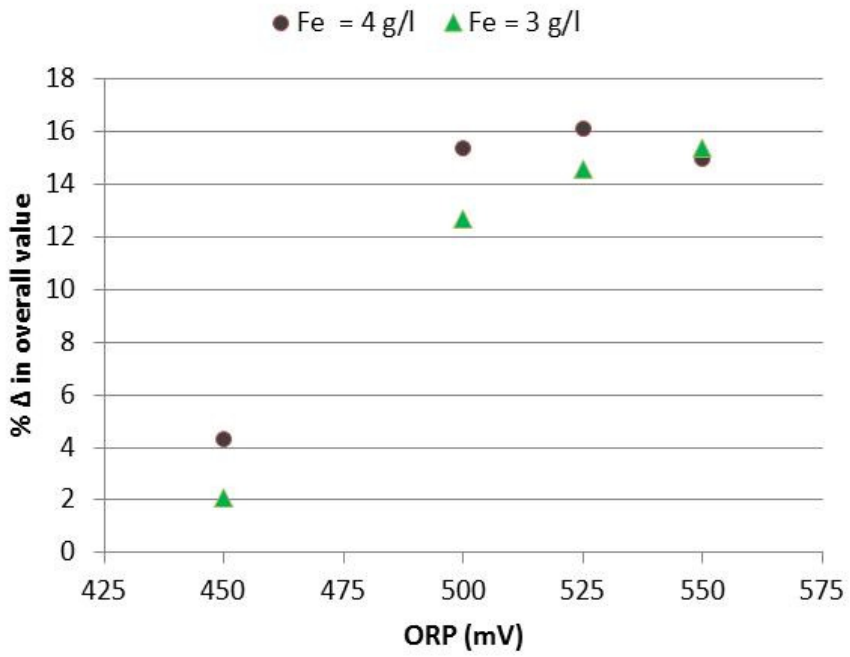

Figure 5.3: Effect of ORP and total iron on predicted value generated by Rössing leach circuit

As indicated in Figure 5.3, results for both the 3 g/L and 4 g/L tests conducted at 550 mV predicted similar value delivery. Below this point, tests conducted at 3 g/L predicted lower value delivery than tests conducted at 4 g/L Fe. In the 3 g/L Fe case, a larger deviation in predicted value is seen between an ORP of 500 and 525 mV when compared to the 4 g/L Fe case. This was probably because ferric was the limiting reagent for uranium extraction to take place, i.e. for the lower total iron scenario, less ferric was available to react with the uranium and a change in ORP from 500 to 550 mV would have had more of an effect on the reaction for the lower ferric scenario than for the higher ferric scenario.

Following this analysis, the recommendation to operate at an ORP greater than 500 mV is still valid.

The results suggested that operating at an ORP higher than 525 mV (at 4 g/L Fe) would not have an impact on overall uranium extraction, i.e. this would provide diminishing value as the plateau is reached. This cannot be said for tests conducted at 3 g/L as uranium extraction was not seen to plateau off over the range of ORP's tested, as it did for the 4 g/L Fe tests. One would not, however, expect it to increase much further than the uranium extraction plateau achieved in the 4 g/L Fe tests, suggesting that the plateau for the 3 g/L Fe tests may very well start at 550 mV (at 3 g/L Fe). Further test work would be required to test this theory.

The recommendation would, therefore, be to constrain the ORP operating range to 500 to 525 mV. This reduces the risk of overdosing pyrolusite to achieve higher ORP targets as an ORP target greater than 525 mV requires mostly ferric in solution, ferrous concentration < 0.1 g/L, even at total iron concentrations of 4.5 and 5 g/L) and also the risk to downstream processes (e.g. Continuous Ion Exchange and Solvent extraction processes).

The effect of total iron concentration on overall leach value is presented in Figure 5.4.

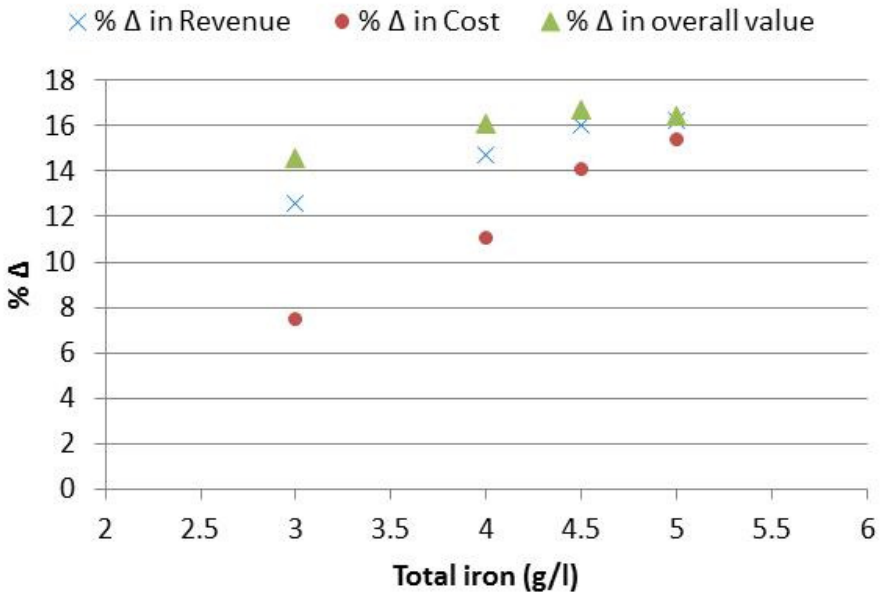

Figure 5.4: Effect of total on predicted value generated by Rössing leach circuit (525 mV, ROM ore)

The highest value (compared to the base case 440 mV, 4 g/L Fe) was achieved at a total iron concentration of 4.5 g/L. Although the highest uranium extraction was achieved at a total iron of 5 g/L, this was only marginally higher than that predicted for 4.5 g/L. The additional cost associated with the higher total iron concentration resulted in a lower predicted value for this point, compared to the predicted value for the test run at 4.5 g/L Fe.

These results were compared to all previous experimental results in this work and are displayed in Table 5.8. The results are arranged in descending order, i.e. highest predicted value delivery to lowest value delivery. Highest predicted values are obtained at an ORP greater than 500 mV and value quickly drops off below an ORP of 475 mV. An economic optimum (highest predicted value delivery) exists at an ORP of 525 mV and total iron

concentration of 4.5 g/L. To increase leach value, a total iron concentration of 4.5 g/L and 525 mV ORP are therefore, recommended for the ROM ore type.

Table 5.8: Comparison of all results

ORP (mV)	Total iron (g/L)	% Δ Value Compared to base case (440 mV, 4 g/L Fe, ROM ore type)
525	4.5	16.7
525	5	16.4
525	4	16.1
525	4	16.1
500	4	15.4
550	3	15.4
550	4	15
525	3	14.6
500	3	12.7
475	4	11.7
450	4	4.3
450	3	2.1
440	4	0

As extraction was seen to increase with an increase in total iron and the cost of the iron is far less than the cost of pyrolusite, it may be that further optimization of ORP (i.e. potentially decreasing it) at a higher total iron[24] set point (to match the uranium extraction that can be achieved at a high ORP set point) could result in higher value delivery than that achieved at a total iron of 4.5 g/L and ORP of 525 mV. Further test work to establish the effect of total iron on leach value at a lower ORP (e.g. 500 mV) is recommended. At a high enough total iron concentration (which would naturally result in a higher starting ORP) non-uranium dissolution side reactions (such as the oxidation of iron sulphide) may, however, start to compete for oxidant resulting in a higher oxidant consumption rate. An optimum total iron concentration (that maximises uranium extraction at the lowest possible oxidant consumption) would, therefore, be expected.

[24] Subject to constraints of downstream operations.

Key findings and application for the ROM ore type:

- The techno-economic modelling exercise indicated that an economic optimum ORP set point exists for the ROM ore type.
    - 525 mV and 4.5 g/L total Fe were determined to be economically improved set points for the Rössing leach plant over the range of set points tested.
    - The results suggested that operating at an ORP higher than 525 mV (at 4 g/L Fe) would result in diminishing value as the uranium extraction plateau is reached and the oxidant requirement is increased.
    - The additional reagent cost associated with operating at a total iron concentration above 4.5 g/l (i.e. at 5 g/l and 525 mV) outweighed the benefit from additional uranium extracted at these set points.
- The predicted value delivery for ORPs less than 500 mV was much lower than the predicted value delivery for ORP's above 500 mV for total iron concentrations of 4 g/l and 3 g/l.
- There is potential value to be gained from further optimizing the ORP set point at a high total iron concentration, given the effect of iron on uranium extraction and the lower cost associated with adding more iron rather than adding more pyrolusite to the Rössing leach plant.

5.1.3 Second ore type

Table 5.9 summarizes the modelled results for the effect of ORP for the CGS ore type (5 tank scenario). Figure 5.5 compares the % uranium extractions with the ROM ore type.

Table 5.9: Techno-economic model results of ORP tests at Fe = 4 g/L, ore B (5 tank scenario)

ORP (Ag/AgCl, 3M KCl)	% U Extraction	Acid requirement (kg/t)	Oxidant requirement (kg/t)	Iron addition (kg/t)
450	76.42	22.45	0.21	1.52
475	79.45	23.30	0.71	1.52
500	81.52	23.71	1.30	1.52
550	80.72	23.90	1.44	1.52

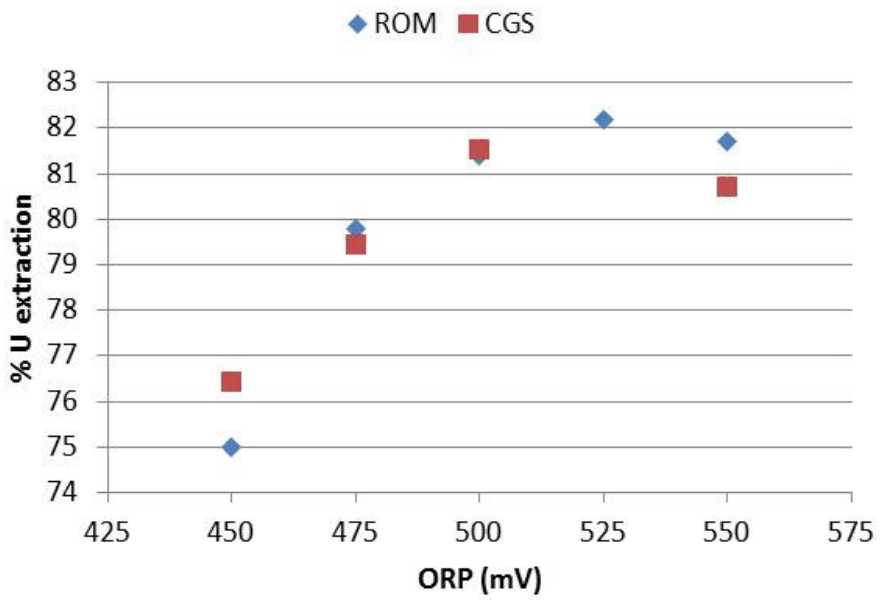

Figure 5.5: Effect of ORP on predicted % U extraction for ROM and CGS ore types

The data suggests that at lower ORP's (<475 mV), % uranium extraction for the ROM ore was more affected by a decrease in ORP than the CGS ore. At higher ORP values (>500 mV), the ROM ore appeared to be less affected by ORP than the CGS ore. This could be attributed to the uranium mineralogy of the different ore types, i.e. the ROM ore contained a higher ratio of uraninite to uranophane than the CGS ore. Uraninite requires an oxidative leach to dissolve uranium whereas uranophane will dissolve in acidic solutions.

The overall predicted value results for each scenario (i.e. each ORP set point) are presented in Table 5.10 and Figure 5.6. All results were compared to a base case (440 mV, 4 g/L Fe, ore A).

Table 5.10: Economic assessment of leach data – predicted value (at 4 g/L Fe, ore B)

ORP (Ag/AgCl, 3M KCl)	% Change in Revenue	% Change in Cost	% Change in overall value
		Compared to base case (440 mV, 4 g/L Fe, ore A)	
450	6.7	(4.3)	11.0
475	10.9	2.1	14.4
500	13.8	7.8	16.1
550	12.7	8.6	14.3

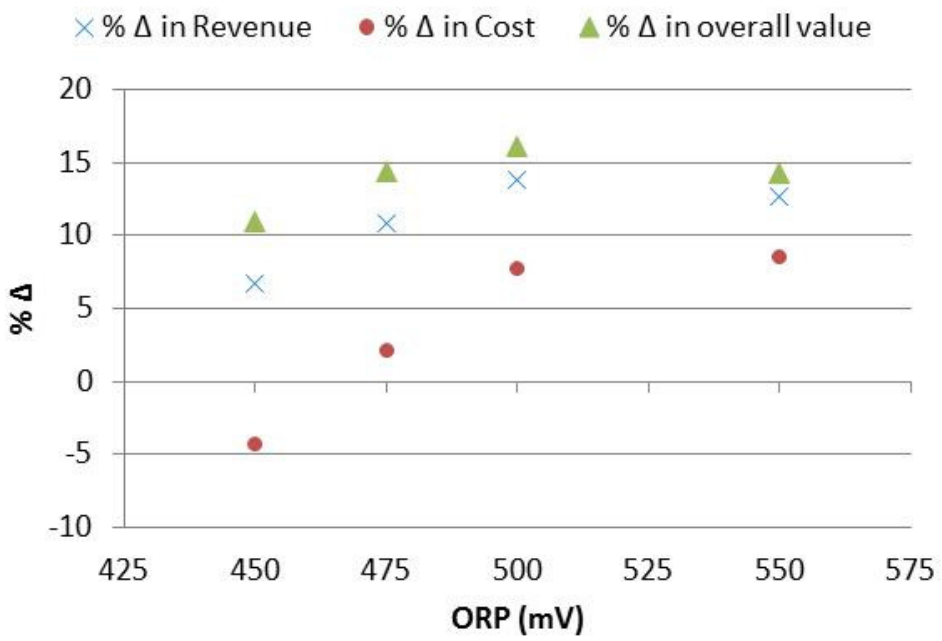

Figure 5.6: Effect of ORP on predicted value generated by Rössing leach circuit (Fe = 4g/L, CGS ore)

Figure 5.6 indicates an economic optimum operating set point at 500 mV. Above this point, value decreased due to the increased reagent cost at a relatively lower uranium extraction. The difference between predicted % uranium extraction at 550 mV compared to 500 mV is 0.80%. Taking the error associated with the model (0.7%) into account, the test conducted at 500 mV would still deliver a higher predicted value. Assuming that predicted % uranium extraction at 550 mV was at least equal to that achieved at 500 mV, the predicted value would not be higher than the value predicted for the 500 mV case due to the increased reagent cost at the higher ORP.

The conclusion from this test work is that the same trend holds for another ore type (CGS), i.e. the leach plant should be operated above 500 mV but not higher than 550 mV to achieve maximum value from the leaching circuit. Leach value was found to decrease rapidly below 500 mV for both ore types.

Key findings for CGS ore type:

- The results from the techno-economic modelling exercise suggested that an optimum ORP could potentially exist between 500 and 550 mV.
- Leach value was found to decrease rapidly below 500 mV.
- At lower ORP set points (<475 mV), the ROM ore was found to be more affected by a decrease in ORP than the CGS ore.

Application:

- The results indicate that even for a reducing ore type, there is potential value to be gained in operating the Rössing leach plant above an ORP of 500 mV.

5.1.4 Temperature

The modelled results for the temperature test work are presented in Table 5.11.

Table 5.11: Techno-economic model results for temperature tests at 4 g/L Fe, 525 mV (modelled results, 5 tank scenario, ore A)

Temperature (°C)	% Uranium extraction	Acid requirement (kg/t)	Oxidant requirement (kg/t)	Iron addition (kg/t)
35	82.2	28.9	0.61	1.64
45	84.8	30.0	0.81	1.64

Predicted % uranium extraction increased by 2.6%, acid requirement increased by 1.1 kg/t and oxidant requirement increased by 0.2 kg/t when temperature was increased from 35 to 45 °C (for a 5 tank scenario). The change in overall predicted value between the 2 scenarios was 3.4%. Although both, acid requirement and oxidant requirement, increased with an increase in temperature, the predicted revenue generated through the additional % U extraction far outweighed this, resulting in a net positive gain for overall leach value. This result suggests that if temperature varies in the Rössing plant, overall value will not be negatively affected by running the plant at a high ORP of 500 – 525 mV. Even if the oxidant requirement were doubled and acid consumption were increased by a further 2 kg/t, overall value would still remain positive, due to the higher % uranium extracted at a higher

temperature. The higher temperature leach (at 525 mV) also resulted in a greater overall predicted financial value than that of the lower temperature leach at a higher ORP (550 mV).

With the experimental test work conducted at 35 °C, an optimum ORP was suggested to lie between 500 and 550 mV. At higher temperatures, this optimum may actually lie lower down the ORP scale. This is an interesting hypothesis and is worth investigating further. Although only one data point and test were conducted at a higher temperature, this work suggests that there is potential to determine the role temperature could play in increasing value.

Key findings:

- Overall predicted value increased by 3.4% with an increase in temperature from 35 to 45°C. Although the acid and oxidant requirement increase over the temperature range, the benefit from the additional uranium extraction outweighed this cost.
- Predicted value for an ORP set point of 525 mV and total iron set point of 4 g/L remained positive for a higher temperature scenario.
- The overall predicted financial value for the higher temperature leach at 525 mV was higher than that of the lower temperature leach at a higher ORP (550 mV).

5.2 Summary of key findings in relation to research objectives

The experimental test work and techno-economic modelling exercise showed that an improved ORP set-point (500-525 mV), which improved economic returns from uraninite ore, exists. When the improved set point was applied to another ore type, this also resulted in improved value when compared to previous performance (ORP = 475 mV).

5.3 Implementation of improved set points

5.3.1 Risk assessment

Prior to the implementation of a new process set point, it is important to conduct a risk assessment to establish the possible knock-on effects that this change may have on the process. This section outlines the potential risks associated with operating the Rössing leaching circuit at higher ORP and total iron set points.

Confirmation of improved set points

As only one test was conducted at each set of parameters, the risk exists that the recommended set points could be incorrect. During the experimental program, this risk was mitigated to a degree (but not eliminated) by conducting quality control tests. Before conducting a plant trial or full implementation, it is recommended that a large set of repeat tests is conducted at the proposed improved set points to verify the modelled parameters and the outcome of the techno-economic modelling exercise.

Practicalities associated with plant implementation

The results have shown that a higher ORP set point required a higher oxidant consumption rate. This was for a controlled leach situation. Process control in the Rössing leach plant is not as steady and is in fact quite variable (ORP, 2 standard deviations in the control tank = 80 mV). The risk that oxidant is overdosed in the leach plant at higher ORPs therefore, exists. If a higher ORP set point is implemented in the Rössing plant, the increase in oxidant consumption would need to be minimized via improved control (such as online ORP measurement coupled to a PID controller and pyrolusite pump) as far as possible, so as not to reduce any value created through increased % uranium extraction.

Figure 5.7 illustrates the relationship between ORP, ferric concentration and total iron in Rössing leach solutions. These curves were derived from equation 29. This relationship indicates that a deviation from the ORP set point at a higher total iron concentration requires a greater change in ferric concentration, especially below 525 mV. A greater change to ferric concentration would in turn require a higher oxidant addition rate in the control tank to re-oxidise ferrous to ferric, as with the CGS ore type. Whilst ORP control is as variable as 80 mV (95% confidence) it would be advisable to set the total iron concentration at a lower set point (4.5 g/L) than the current Rössing plant set point of 5 g/L, to lower the risk of increased pyrolusite addition. The test work also showed that operating at a total iron concentration of 5 g/L at 525 mV would result in a decrease in value delivery due to the increased iron requirement at this level (with a marginal increase in uranium extraction).

Another interesting point to note from Figure 5.7 is that a deviation from set point of say 50 mV at an ORP set point above 500 mV, will require a smaller change in ferric concentration to get back to the target than when operating at an ORP below 500 mV. This is implicit in the nature of the Nernst equation. At an ORP of 450 mV (4 g/L Fe) the ratio of ferric to ferrous concentration is roughly 2.5/1.5 g/L, at an ORP of 500 mV this changes to 3.6/0.4 g/L and at

and ORP of 500 mV this changes to 3.9/0.1 g/L. To increase ORP from 450 mV to 500 mV, 1.1 g/L ferrous will need to be oxidised to ferric, but to increase ORP from 500 mV to 550 mV, only 0.3 g/l ferrous will need to be oxidised to ferric. The implication of this is that at a high ORP, only a small change in ferric is required to change the system ORP (but operating at a high ORP results in higher financial value). At a low ORP, the system is more robust to poor control, i.e. the ferric concentration can change more without undue impact on the system ORP. This is, however, a less profitable place to operate at. This stresses the importance of good control to enable reliable operation in the ORP zone which results in the most value.

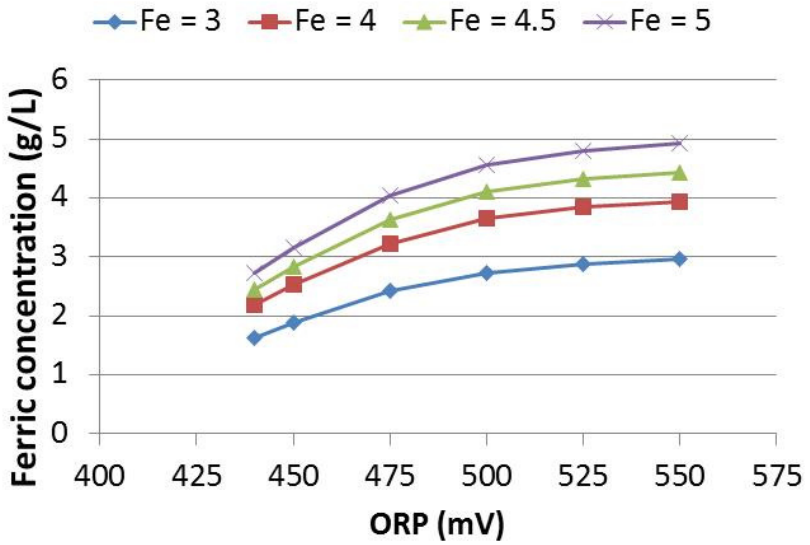

Figure 5.7: Relationship between ORP, ferric and total iron concentration.

The continuous ion exchange (CIX) and solvent exchange (SX) processes at Rössing are sensitive to high concentrations of ferric, i.e. high ORP values. High ORP can affect resin loading in the CIX plant and solvent health in the SX plant. The ORP set point in the leaching circuit would need to be limited to a range that ensures that the exit slurry ORP range is below the critical ORP value to prevent problems for these downstream plants. The ORP in the actual Rössing tank leach process is only dosed up front to achieve the target ORP in the second tank. The ORP in the exit slurry is likely to be lower than the ORP at the start of the leach. It is recommended that a plant sampling campaign and leach tests are conducted to assess the natural decrease of the ORP profile throughout the duration of a leach.

5.3.2 Quantification of improvement

Following the implementation of any improvement, it will be important to be able to quantify the actual value generated by the improvement. A test method, similar to the method described in 3.3.4 was developed to be able to determine the improvement in leach performance. The test method involves the following:

- Conduct a weekly standard 13 hour agitated batch leach test (pH 1.6, 525 mV, 4 g/L Fe) on a weekly composited plant sample (post implementation of improvements). Uranium extraction and reagent consumption are determined.
- Conduct standard 13 hour agitated batch leach tests on weekly composited plant samples from a period before any improvements were implemented in the plant.
- The differences between the standard laboratory leaches and actual plant performance for the plant, pre-improvement are compared to the differences between the standard laboratory leaches and actual plant performance for the plant post-improvement. Equivalent ore characteristics are taken into account when conducting this comparison.
- The noted changes, in the form of uranium extraction and reagent consumption are then converted into overall value improvement.

5.4 Further test work

As illustrated in
Figure 3.18, the test work conducted in this study is the first phase of the method to assess improved set points for the Rössing leaching plant. This section outlines the recommendation for additional test work to be conducted to further optimize the leaching process.

Apart from ORP and total iron, another important variable to consider when selecting improved set points for the plant is pH. This is, however, beyond the scope of this work. For completeness sake, the following tests have been recommended to fully optimize leach set-points for a given ore type:

- After selecting the optimal ORP condition for a specific ore type, test work at 3 different pH set points would need to be conducted to establish the effect on uranium extraction and acid consumption (pH = 1.3, 1.6 and 1.9)

- If it is found that either the rate of uranium extraction or overall uranium extraction are improved at lower pH values with minimal impact on acid consumption continue with the following tests:
    - Assess the impact of further decreasing pH. Select a total iron (e.g. 4.5 g/L) and ORP set point (e.g. 525 mV) and conduct tests at pH values of 1 and 1.2. Results from these tests will need to be inserted into the model to assess predicted plant acid consumptions and whether the plant would physically be able to cope with a higher acid demand (if required). From this work, select preferred pH value to continue test work.
    - Assess the ORP impact at lower pH values (475, 500, 550 mV at selected pH).
    - Assess the total iron impact at lower pH values (3, 4.5, 5 g/L at selected pH).

From this test work, a complete set of leach parameters (i.e. pH, ORP and total iron) that result in the highest predicted value delivery would be recommended for implementation. As recommended in the risk assessment (section 5.3.1), the set of parameters should be verified through a set of repeat tests prior to implementation. The effect of residence time (number of tanks online and throughput rate) would also need to be taken into account when recommending improved set points for the plant. The effect of residence time is quantified by using the leach techno-economic model to predict uranium extraction and reagent consumptions at different residence times.

6 Conclusions and Recommendations

6.1 Key findings

This work was conducted to develop and execute a leach program that assessed the impact of varying leach parameters on different ore types and used techno-economic modelling to select improved set-points (based on maximising net revenue) for plant-scale implementation. The literature review and mineralogical analyses of several Rössing leach feed and tailings samples indicated that, within the constraint of 'no major capital modifications' a change in ORP (or ferric/ferrous ratio) would have the largest impact on % uranium extraction. The focus of this study was, therefore, aimed at studying the effect of ORP and total iron on % uranium extraction and reagent consumption. The key conclusions drawn from this work are summarized within this section.

The extent of uranium leach extraction (13 hours) for the ROM and CGS ore types ranged between 77 % and 88 %. Most of the uranium dissolved into solution within the first 7 hours of leaching with only marginal increases thereafter. The uranium extraction curves for both ore types were similar in shape, indicating similar uranium leaching kinetics over the range of ORP's tested. The remaining unleached uranium in the ore is thought to have remained in refractory minerals (betafite or coffinite) and poorly liberated uranophane.

The final uranium leach extraction (after 13 hours) for the ROM and CGS ore types ranged between 74 % and 87 %. Most of the uranium dissolved into solution within the first 7 hours of leaching with only marginal increases thereafter. The uranium extraction curves for both ore types were similar in shape, indicating similar uranium leaching kinetics over the range of ORP's tested. The remaining unleached uranium in the ore is thought to have remained in refractory minerals (betafite or coffinite) and poorly liberated uranophane.

Final uranium extraction (13 hours) increased with an increase in ORP with the maximum achieved at an ORP of 550 mV for both ore types. The impact of ORP on the initial rate of uranium extraction (2 hours) was more obvious for the CGS ore type than for the ROM ore type. A change in ORP in the 450 – 500 mV range had a greater effect on %U extraction than a change in ORP in the 500 – 550 mV range. The recommendation from this study was, to increase the RUL ORP set point to above 500 mV. When the results of this test work were fitted to the techno-economic model, an improved ORP set point of 525 mV (that maximised financial value for the assessed scenarios) was recommended. An implication of the

relationship between ORP, ferric concentration and total iron concentration (Nernst equation) is that good control will be required to operate within the high ORP zone to prevent overconsumption of oxidant.

Final uranium extraction (13 hours) also increased with an increase in total iron concentration for all tested ORP set points. The results from the test work conducted over a range of ORP and total iron set points were fitted to the techno-economic model and an improved total iron set-point of 4.5 g/l (that maximised financial value for the assessed scenarios) was recommended.

Total iron had a greater effect on % uranium extraction in the lower ORP range (450 - 500 mV) than in the higher ORP range (500 – 550 mV). Total iron also appeared to have more of an effect on % uranium extraction than a change in ORP in the lower ORP range (<475 mV). Similar % uranium extraction was obtained for a system at a lower ORP than a system at a higher ORP, when sufficient iron was added at the lower ORP. This reflects the importance of both ORP and iron concentration in the dissolution of uraninite and the potential value to be gained from further optimizing the ORP set point at a high total iron[25] concentration (given the lower cost associated with adding more iron rather than adding more pyrolusite to the Rössing leach plant). At a high enough total iron concentration (which would naturally result in a higher starting ORP) non-uranium dissolution side reactions (such as the oxidation of iron sulphide) may, however, start to compete for oxidant resulting in a higher oxidant consumption rate. An optimum total iron concentration (that maximises uranium extraction at the lowest possible oxidant consumption) would, therefore, be expected.

Oxidant demand increased with an increase in ORP for both ore types. The oxidant requirement was, however, significantly higher for the CGS ore than the ROM ore. This may have been a result of the dissolution of ferrous from increased concentrations of specific gangue minerals in the CGS ore such as cordierite, biotite and/or iron sulphide.

The oxidant demand could be categorised into two distinct regions, an initial accelerated oxidant addition rate during the first 2 hours of leaching and a slower, but linear rate during the remaining 11 hours of leaching. Oxidant was continuously added to all leaches (apart from the 440 mV test). This suggested that other reducing species, such as ferrous, leached into solution throughout the entire leach. The results supported the current Rössing leach plant ORP control philosophy (i.e. addition of pyrolusite up front to target an ORP set point in

[25] Iron added in the form of Conarc which contains 70% ferric, i.e. a higher ferric concentration.

the second tank). Changing this to a constant ORP control philosophy appears to hold little benefit as a result of the increased oxidant demand. Further test work and a financial evaluation would, however, need to be completed to confirm this.

The acid requirement for the CGS ore type was significantly lower for the CGS ore than the ROM ore. The lower acid requirement was suggested to have been due to the lower concentration of acid consuming gangue minerals (such as calcite) in the CGS ore type.

% uranium extraction increased with an increase in temperature from 35 to 45 ℃. Acid and oxidant addition were also found to increase over the same temperature range. The final % uranium extraction achieved for the 45 ˚C leach (conducted at 525 mV) was higher than the % uranium extraction achieved for a test conducted at a higher ORP (550 mV). The overall predicted financial value for the higher temperature leach at 525 mV was higher than that of the lower temperature leach at a higher ORP (550 mV). This indicates that there is potentially more value to be gained by heating the leach circuit than increasing the ORP. The cost of the increased reagent consumption and energy requirement would, however, need to be considered at the higher temperature.

% uranium extraction appeared to increase when pulp density was lowered from 75 to 70%. The results indicated that there is potential value to be gained by tightening up the pulp density control in the Rössing leach plant to the lower end of the range (i.e. 68 – 70%). This, however, requires further test work to confirm this observation. A trade-off study between a lower ore throughput rate at the lower pulp density and the improved uranium extraction would, however, need to be conducted to optimize value.

In conclusion, this work has successfully achieved the following project objectives:

- Determine the impact of varying ORP and total iron concentration on uranium extraction and reagent consumption for different RUL ore types.
- Determine whether operating at an ORP higher than currently implemented at RUL will be economically viable.

6.2 Recommendation of improved set-point

It is recommended that the Rössing leach ORP set-point is increased to the range 500 - 525 mV and total iron to 4.5 g/L, to realize the predicted increase in % U extraction.

6.3 Recommendations for future work

The following further test work has been recommended to fully optimize the process:

- Determine the effect of high total iron concentrations (>4 g/L) on overall leach value at lower ORP set points. The test work has shown that similar uranium extractions can be achieved at a lower ORP if sufficient iron is added to the system. An optimum total iron concentration is hypothesized due to the potential impact of other reacting reducing species within the ore on oxidant demand and the enhancement thereof at higher total iron concentrations.
- The effect of pH on % uranium extraction and reagent consumption needs to be assessed to optimize this parameter. This should be assessed for a range of different ORP set points. This was beyond the scope of this project.
- Establish the effect of ORP and pH over a range of different pulp densities. As a decrease in pulp density was seen to increase uranium extraction in the test work, the potential exists to further optimize this set point and lower the need for a high ORP set point and hence, the oxidant requirement. The effect of pulp density on other non-uranium side reactions would, however, also need to be assessed.
- Establish the effect of ORP and pH over a range of temperatures.
- Further test work is required to determine the effect of the improved set points on several other ore types (e.g. higher percentage south material).
- As poor liberation of uranophane was hypothesized to be a potential cause for the overall lower than expected uranium extractions for the ores tested, the effect of grind size on uranium mineral liberation and subsequently % uranium extraction and reagent consumption should be established (should the economic climate improve and capital projects be possible).

7 References

Abraham, I.M. (2009). *'Geology and spatial distribution of uranium mineralisation in the SK anomaly area, Rössing area, Namibia'*, A thesis submitted for the degree of Master of Science, University of Witwatersrand, Johannesburg, South Africa, pages 31 - 49

Argus (2013). '*Argus FMB Sulphuric acid'*, Issue 13-42, page 1, Argus Media Ltd., Argus House, London [online] Available at: http://media.argusmedia.com/~/media/Files/PDFs/Samples/Argus-FMB-Sulphuric-Acid.pdf [Accessed 27 January 2014]

Barthelmy, D. (2012). '*Mineralogy Database'*, [online] Available at: http://webmineral.com [Accessed 14 September 2013]

Bartilson, B.W. (2010). '*Techno-economic modelling: An Invaluable Tool for Invention and Investment'*, [online] Algae Industry Magazine, Available at: http://www.algaeindustrymagazine.com/techno-economic-modeling-an-invaluable-tool-for-invention-and-investment/ [Accessed 22 August 2013]

Berning, J., Cooke, R., Heinstra, S.A., Hoffman U. (1976). '*The Rössing uranium deposit'*, South West Africa, Economic geology, 71: 351-368

Berning, J. (1986). '*The Rössing uranium deposit'*, South West Africa/Namibia.Mineral deposits of Southern Africa, 2, page 1819-1832.

Bhappu, R. B., Johnson, P. H., Brierley, J. A., & Reynolds, D. H. (1969). '*Theoretical and practical studies on dump leaching*', AIME Trans, 244, 307-320.

Bush, S. F. (2005). '*A techno-economic model applied to the development of new products and improved processes'*, Chemical Engineering Research and Design, 83(6), 646-654.

Demopoulos, G. P. (1985). *'Acid pressure leaching of a sulphidic uranium ore with emphasis on radium extraction'*. Hydrometallurgy, 15(2): 219-242

Eligwe, C. A., Torma, A. E., and Devries, F. W. (1982). '*Leaching of uranium ores with the H_2O_2-Na_2SO_4-H_2SO_4 system'*, Hydrometallurgy, 9(1): 83-95

Filippou, D., Konduru, R., & Demopoulos, G. P. (1997). '*A kinetic study on the acid pressure leaching of pyrrhotite'*. Hydrometallurgy, 47(1), 1-18

Hamilton, E. (2010). '*RUL leach circuit model'*, Internal publication (MS Excel 2010 workbook), MS Excel model prepared for Rössing Uranium Limited, Rio Tinto Technology and Innovation, Melbourne, Australia

Hayes, P., (2003). *'Process Principles in Minerals and Materials Production'*,
Third ed. Hayes Publishing, pages 227–250

He, M., Wang, Y. and Forssberg, E. (2004). '*Slurry rheology in wet ultrafine grinding of industrial minerals: a review'*, Powder technology. 147: 94-112

He, M., Wang, Y. and Forssberg, E. (2006). '*Parameter studies on the rheology of limestone slurries'*, International journal of mineral processing. 78: 63-77

Hennig, C., Schmeide, K., Brendler, V., Moll, H., Tsushima, S., & Scheinost, A. C. (2007). '*The Structure of Uranyl Sulfate in Aqueous Solution—Monodentate Versus Bidentate Coordination*', In AIP Conference Proceedings, Vol. 882, p. 262.

Huynh, L., Jenkins, P. and Ralston, J. (2000). '*Modification of the rheological properties of concentrated slurries by control of mineral-solution interfacial chemistry'*, International journal of mineral processing. 59: 305-325

IAEA (2013). '*Nuclear Fuel Cycle*, [online] International Atomic Energy Agency, Nuclear Fuel Cycle and Materials, Available at:
http://www.iaea.org/OurWork/ST/NE/NEFW/Technical_Areas/NFC/images/nfc-image-big.jpg [Accessed 23 November 2013]

Infomine (2013). '*Expansion plans'*, [online] Infomine, Mine Sites, Available at:
http://www.infomine.com/minesite/images/Rossing15.gif/ [Accessed 23 November 2013]

Ismet (2013). *Rössing plant data sourced (2009 – 2012)*, Rössing Uranium Limited Ismet database, Swakopmund

Jambor, J.L.(1986). '*Detailed mineralogical examination of alteration products in core WA-20 from Waite Amulet tailings*', CANMET Division Report MSL 86-137(IR), Dept. Energy Mines Resources, Canada.

Johnson, C. C. (1990). '*Economic Leaching at Rössing Uranium Limited'*, Journal of the South African Institute of Mining and Metallurgy, 90(6): 141-147

Kawatra S.W., Bakshi, A.K., Miller Jr., T.E. (1996).'*Rheological characterization of mineral suspensions using a vibrating sphere and a rotational viscometer',* International journal of mineral processing, 44-55:155-165

Kesler, S. B., and Fahrbach, D. O. E. (1982). '*Uranium extraction at Rössing'*, Uranium'82 Symposium, Toronto, Pages 2, 8, 12.

Laxen, P.A. (1973). '*A fundamental study of the dissolution in acid solutions of uranium minerals from South African ores'*, National Institute for Metallurgy, Report NIM-1550.

Lottering, M. J., Lorenzen, L., Phala, N. S., Smit, J. T., & Schalkwyk, G. A. C. (2008). '*Mineralogy and uranium leaching response of low grade South African ores'*, Minerals Engineering, 21(1): 16-22

McConville, F. X. (2008). '*Functions for easier curve fitting*', Impact Technology Consultants, Chemical Engineering, [online] Available at: http://www.che.com/technical_and_practical/Engineering-Practice-Functions-for-Easier-Curve-Fitting_4387.html [Accessed 29 January 2014]

McMaster, S., Ram, R., Charalambous, F., Tardio, J., Bhargava, S. (2012). '*Characterization and dissolution studies on the uranium mineral betafite'*, Chemeca 2012: Quality of life through chemical engineering: 23-26 September 2012, Wellington, New Zealand: 612

Merritt, R. C. (1971). '*The Extractive Metallurgy of Uranium'*, Colorado School of Mines Research Institute. Golden, Colorado, 59-119.

Meyer, N.K. (2008). '*Leach tank build-up: Thermal images'*, Unpublished internal report, Rössing Uranium Ltd., Swakopmund, Namibia, page 8

Morkel, F. (2013). *'Ferric/Ferrous vs redox relationship'*, Unpublished internal report, Rössing Uranium Ltd., Swakopmund, Namibia, page 4

Murasiki, T. (2013). '*Geology question'*, [email] N.K. Jansen van Rensburg (Nicole.JvRensburg@riotinto.com), Sent 1 November 2013, 14:50, Available in: Personal email archive

Nesmeyanova, G. M. and Alkhazashvili, G. M. (1962). '*The effect of certain compounds on the oxidation of uranium in acid media.*' The Soviet Journal of Atomic Energy, 10(6), 583-586.

Ndlovu, B., Forbes, E., Farrokhpay, S., Becker, M., Bradshaw, D., & Deglon, D. (2014). '*A preliminary rheological classification of phyllosilicate group minerals.*' Minerals Engineering, 55, 190-200.

Nicol, M. J., Needes, C. R. S., and Finkelstein, N. P. (1975). *'Electrochemical model for the leaching of uranium dioxide: 1. Acid media*', In: Burkin, A.R. (Ed.), Leaching and Reduction in Hydrometallurgy. Institution of Mining and Metallurgy, London., 1-11.

Nicol, M.J. (1980). *'The Chemistry of uranium leaching'*, Lecture notes, National Institute for Metallurgy, 7: 1-7.

Nicol, M.J. (2011). Hydrometallurgy – '*Theory and Practise (with application to Uranium processing)'*, Lecture notes: Hydrometallurgy course hosted by Rössing Uranium limited, Swakopmund, Modules 6 - 7

Olateju, B. and Kumar, A. (2011). '*Hydrogen production from wind energy in Western Canada for upgrading bitumen from oil sands'*, Energy, 36(11), 6326-6339.

Plysunin, A.M., Mironov, A.G., Belomestrova, N.V., Chernigova, S.Y. (1990). '*Laboratory studies on gold-bearing sulfide oxidation*.' Geokhimiya 1, 51–60.

Prasad, J., Grocott, S., Jansen van Rensburg, N.K. (2012). '*Leach Control Philosophy trial at Rössing', Unpublished internal report*, Rössing Uranium Ltd., Swakopmund, page 1 - 2

Ram, R., Charalambous, F., Tardio, J., Bhargava, S. (2011). *'An investigation on the effects of Fe (FeIII, FeII) and oxidation reduction potential on the dissolution of synthetic uraninite (UO2)',* Hydrometallurgy, 109: 125–130

Ram, R., Charalambous, F. A., McMaster, S., Pownceby, M. I., Tardio, J., Bhargava, S. K. (2013). '*An investigation on the dissolution of natural uraninite ores'*. Minerals Engineering, 50: 83-92

Ram, R. (2013). '*An investigation on the dissolution of synthetic and natural uraninite*', A thesis submitted for the degree of Doctor of Philosophy, School of Applied Science, Applied Science, RMIT University, pages 80 – 94, 100 – 158.

Richardson, J.F., Harker, J. H., Backhurst, J. R. (2002). '*Coulson and Richardson's chemical engineering: Particle technology and separation processes'*, Oxford: Butterworth-Heinemann, pages 502 - 506

Ring, R. J. (1980). *'Ferric sulphate leaching of some Australian uranium ores'*.Hydrometallurgy, 6(1): 89-101

Roesener, H., & Schreuder, C. P. (1992). '*Uranium Mineral resources of Namibia: Nuclear and fossil fuels: Geological Survey of Namibia'*, page 7-1

Roshani, M., and Mirjalili, K. (2009). *'Studies on the leaching of an arsenic–uranium ore'*. Hydrometallurgy, 98(3): 304-307

Rössing (1990). '*Determination of Manganese reactivity*', Analytical Method, Rössing Uranium mine, Swakopmund, Namibia, pages 1 - 4

Rössing (2007). '*Rössing Uranium mine expansion project, Social and Environmental Impact Assessment*', Public information document, Swakopmund, Namibia, Page 6

Rössing (2013a). '*Rössing Uranium's operations'*, [online] Rio Tinto Rössing Uranium Limited, Mining Uranium and the Nuclear Fuel Cycle, Available at: http://www.rossing.com/uranium_production.htm [Accessed 23 November 2013]

Rössing (2013b). '*Ore source blends for 2011 - 2012'*, Data sourced from Rössing MMRS database, Swakopmund, Namibia

Ryan, E., (2010). '*Mineralogy of variable rock types from Rössing'*, Unpublished internal report, Rio Tinto Technology and Innovation, Melbourne

Ryan, E., (2012a). '*Rössing monthly mineralogy reports: October 2011, December 2011, February 2012, March 2012, April, 2012, May 2012, June – August 2012',* Unpublished internal reports, Rio Tinto Technology and Innovation, Melbourne

Ryan, E., (2012b). *'Impacts of amphibole, mica and pyroxene on acid consumption and redox control in the Rössing circuit',* Unpublished internal reports, Rio Tinto Technology and Innovation, Melbourne, pages 3 - 18

Ryan, E., (2013). '*Mineralogical Controls on Uranium Extraction and Acid Consumption at Rössing Uranium Mine, Unpublished internal report'*, Rio Tinto Technology and Innovation, Melbourne, pages 9 - 27

Smith, R.M. and Martell, A. E. (1976). '*Critical Stability Constants'* Volume 4. Inorganic Complexes. Plenum Press.

Sommer, G., Omrod, G.T.W. and Chaix, R.P. (1973). *'Recent developments in the instrumentation and automation of uranium processing plants'*. J. S. Afr. Inst. Min. Metall., (74): 413-420.

Stange, W. (1991). '*The optimization of the CIP process using mathematical and economic models'*, *Minerals Engineering*, *4*(12), 1279-1295.

Steger, H.F. (1982). '*Oxidation of sulfide minerals: VII. Effect of temperature and relative humidity on the oxidation of pyrrhotite*', Chem. Geol. 35, 281– 295.

The Ux Consulting Company. (2014). '*Spot Ux U_3O_8 price*, [online] Available at: http://www.uxc.com/review/uxc_Prices.aspx [Accessed 27 January 2014]

Vagias, N., Zonneveld, A. and Grocott, S. (2010). '*Rössing Uranium Ltd - Improvements to Process Rheology, Mixing, Solid Liquid Separation and Calc Index Tolerence',* Internal unpublished report, Melbourne, pages 9 - 11

Vernon, P.N. and Smit, M.T.R. (1985). '*Engineering and metallurgical improvements at the Rössing uranium treatment plant*', Engineering and metallurgical improvements: Case Studies, Pt. 6, Ch. 42: 440 – 465

Wills, B.A. (1992). '*Mineral Processing Technology*', Pergamon Press, Oxford, England, pg. 7

Appendices

Appendix A: Materials

Table A. 1: Synthetic process solution make-up

Ion	Concentration (g/L)	Compound Added	Manufacturer	Mass of Compound (g)
Mg^{2+}	2.12	$MgSO_4.7H_2O$	Associated Chemicals Enterprise	505.4
Al^{3-}	0.72	$Al_2(SO_4)_3.18H_20$	Merck (Pty) Ltd	210.6
Mn^{2+}	2.30	$MnSO_4.4H_2O$	Merck (Pty) Ltd	221.1
Na^{+}	1.90	Na_2SO_4	Merck (Pty) Ltd	77.1
Ca^{2+}	0.93	$CaSO_4.2H_2O$	Merck (Pty) Ltd	40.7
$Mg^{2+/}NO^{3-}$	2.12/0.08	$Mn(NO_3)_2.6H_2O$	Merck (Pty) Ltd	3.9
Na^{+}/Cl^{-}	1.90/1.50	NaCl	Merck (Pty) Ltd	51.0
$K^{+/}Cl^{-}$	0.22/1.50	KCl	Merck (Pty) Ltd	9.7

Table A. 2: Example of acidified ferric/ferrous ratio solution (at 4.0 g/L total Fe)

Ion	Concentration (g/L)	Compound Added	Manufacturer	Mass of Compound (g)
Fe^{3+}	3.90	$Fe_2(SO_4)_3.6H_2O$	Merck (Pty) Ltd	112.4
Fe^{2+}	0.10	$FeSO_4.7H_2O$	Merck (Pty) Ltd	3.2
H^{+}	0.98	H_2SO_4	Merck (Pty) Ltd	6.4

Table A. 3: Titration reagents used for Fe^{3+}, Fe^{2+} and free acid titrations

Mixed indicator	1g Methylene Blue andg Dimethyl Yellow in one litre Methanol.
Starch solution 1%:	10 g soluble starch and 1L demineralised water.
Sodium Diphenylamine Sulphonate indicator	3.00g Diphenylamine Sulphonate and 1L deionised water
Standard Sodium Thiosulphate	0.0896N (1ml = 0.005g Fe)
Spekker acid	150 ml H_2SO_4, 1L deionised water, 150 ml conc. Phosphoric Acid
Standard Sodium Carbonate	0.102N
Standard Potassium Dichromate	0.0896N

Appendix B: Techno-economic model

Model development - inputs

Rössing plant inputs

The following Rössing plant parameters and operational set points were inputs into the model:

Selection of 1 train or 2 train mode

- The user has the option to study a scenario for a leach circuit operating with both modules in operation (2 train mode) or only one module in operation (1 train mode).
- For this work, the number of tanks online was selected as 5 tanks (unless otherwise stated). The maintenance cost and impeller energy consumption cost associated with a leach tank in operation are included in the model calculations.

Dry ore throughput (t/h) = 1900 t/h (unless otherwise stated)

- Milling throughput rate through both modules

Pulp density (% solids w/w)

- Leach feed pulp density after solution has been added to the mills

Tank information

- Number of tanks online on each module
- Sand fillet bed height in each leach tank (m). This is estimated through the use of thermographic imaging of the leach tanks

Ore moisture (%)

- Inherent moisture in the mill feed resulting from dust suppression through water sprays in the crushing plant

Return dam solution (RDS) density (g/mL)

- Recycled tailings dam solution is added to the mills to achieve the required leach feed pulp density

RDS to CIX Return solution ratio (m^3/m^3)

- Return solution, recycled from the continuous ion exchange (CIX) plant, is added to the leach circuit (this solution contains recycled iron which is used in the leaching process)

RDS ferric concentration (g/L)

- Concentration of ferric in the return dam solution

CIX return solution ferric concentration (g/L)

- Concentration of ferric in the CIX return solution

Leach reagent information

- Pyrolusite: % reactive MnO_2 (established through laboratory dissolution test)
- Iron source: % reactive Fe and % available as Fe^{3+} (established through laboratory dissolution test)

Value determination inputs

The following variables were used to estimate value generated by a specific scenario:

U_3O_8 price (US$/lb)

- Long term price

Ore cost up to leach (US$/t)

- Variable cost of treating an additional ton of ore (mining, crushing, mill rods, power, water)

U_3O_8 incremental cost (US$/lb U_3O_8)

- Downstream processing cost per lb of U_3O_8 treated

Reagent prices (N$/t) have not been included in this report due to confidentiality reasons.

Ore grade (kg U_3O_8/t) = 300 ppm

Operational hours (hours)

- Total hours available per year minus schedule plant maintenance downtime

Value output formulas

For each scenario, total value was calculated using the following equations:

$$\text{Overall value (N\$/h)} = \text{U value (N\$/h)} + \text{Acid value (N\$/h)} + \text{Oxidant value (N\$/h)} + \text{Iron value (N\$/h)} \quad [56]$$

$$\text{U value (N\$/h)} = \text{Ore to leach value (N\$/h)} + \text{Downstream value (N\$/h)} + \text{U production sale value(N\$/h)} \quad [57]$$

$$\text{Ore to leach value (N\$/h)} = \text{Mill throughput (t/h)} \times \text{Ore cost up to leach (US\$/t)} \times \text{Exchange rate (N\$/US\$)} \quad [58]$$

$$\text{Downstream value (N\$/h)} = \text{U from leach (kg/h)} \times \text{U incremental cost (US\$/lb)} \times 2.2046 \times \text{Exchange rate (N\$/US\$)} \quad [59]$$

$$\text{U production sale value (N\$/h)} = \text{U from leach (kg/h)} \times \text{U price (US\$/lb)} \times 2.2046 \times \text{Exchange rate (N\$/US\$)} \quad [60]$$

$$\text{U from leach (kg/h)} = \frac{\text{Overall \%U extraction}}{100} \times \text{Mill throughput (t/h)} \times \text{Ore grade (kg/t)} \quad [61]$$

$$\text{Acid value (N\$/h)} = \frac{\text{Acid addition (kg/t)} \times \text{Mill throughput (t/h)}}{1000} \times \text{Acid price (N\$/t)} \quad [62]$$

$$\text{Oxidant value (N\$/h)} = \frac{\text{Oxidant requirement (kg/t)} \times \text{Mill throughput (t/h)}}{1000} \times \text{Oxidant price (N\$/t)} \quad [63]$$

$$\text{Iron value (N\$/h)} = \frac{\text{Iron consumption (kg/t)} \times \text{Mill throughput (t/h)}}{1000} \times \text{Iron price (N\$/t)} \quad [64]$$

Appendix C: Empirical model constants

Test 1

Table C. 1: Raw batch leach data for test 1

t (hr)	Sample Type	% Uranium extraction (batch test)	Oxidant addition (batch test)	Acid addition (batch test)
0	NA			
2	Subsample	65.8	0.210	27.04
4	Subsample	71.2	0.210	28.56
6	Subsample	74.1	0.240	30.19
6	Subsample	74.9	0.255	30.43
7	Residue	80.3	0.256	30.96
9	Subsample	80.5	0.297	32.33
11	Subsample	81.0	0.330	33.35
13	Residue	83.4	0.360	34.43

Table C. 2: Empirical model constants for test 1

Constant	% Uranium extraction	Constant	Acid addition	Constant	Oxidant addition
a	87.9	c	27.36	f	0.162
b	0.759	d	0.1195	g	0.000
		e	0.5724	h	0.015
Model fit: R^2	0.9943	Model fit: R^2	0.9998	Model fit: R^2	0.9915

Test 2

Table C. 3: Raw batch leach data for test 2

t (hr)	Sample Type	% Uranium extraction (batch test)	Oxidant addition (batch test)	Acid addition (batch test)
0	NA			
2	Subsample	63.0	0.091	26.47
4	Subsample	70.6	0.127	28.94
6	Subsample	71.2	0.164	30.56
6	Subsample	73.3	0.138	29.13
7	Residue	74.0	0.185	31.58
9	Subsample	79.2	0.206	31.75
11	Subsample	80.7	0.231	33.40
13	Residue	82.0	0.261	34.89

Table C. 4: Empirical model constants for test 2

Constant	% Uranium extraction	Constant	Acid addition	Constant	Oxidant addition
a	86.3	c	27.22	f	0.076
b	0.945	d	0.1493	g	0.480
		e	0.6000	h	0.015
Model fit: R^2	0.9921	Model fit: R^2	0.9977	Model fit: R^2	0.9881

Test 3

Table C. 5: Raw batch leach data for test 3

t (hr)	Sample Type	% Uranium extraction (batch test)	Oxidant addition (batch test)	Acid addition (batch test)
0	NA			
2	Subsample	66.8	0.000	24.14
4	Subsample	71.1	0.000	26.03
6	Subsample	71.2	0.000	27.57
6	Subsample	59.2	0.000	27.57
7	Residue	70.9	0.000	26.82
9	Subsample	70.4	0.000	29.36
11	Subsample	71.5	0.000	30.56
13	Residue	76.7	0.000	30.56

Table C. 6: Empirical model constants for test 3

Constant	% Uranium extraction	Constant	Acid addition	Constant	Oxidant addition
a	76.6	c	25.18	f	N/A
b	0.446	d	0.1720	g	N/A
		e	0.4723	h	N/A
Model fit: R^2	0.9607	Model fit: R^2	0.9973	Model fit: R^2	N/A

Test 4

Table C. 7: Raw batch leach data for test 4

t (hr)	Sample Type	% Uranium extraction (batch test)	Oxidant addition (batch test)	Acid addition (batch test)
0	NA			
2	Subsample	65.0	0.159	25.57
4	Subsample	70.5	0.159	27.18
6	Subsample	73.2	0.159	28.71
6	Subsample	71.1	0.159	28.32
7	Residue	73.8	0.140	28.63
9	Subsample	78.4	0.190	30.95
11	Subsample	82.6	0.224	32.16
13	Residue	80.1	0.245	33.21

Table C. 8: Empirical model constants for test 4

Constant	% Uranium extraction	Constant	Acid addition	Constant	Oxidant addition
a	83.5	c	25.22	f	0.116
b	0.731	d	0.1000	g	0.000
		e	0.6314	h	0.008
Model fit: R^2	0.9901	Model fit: R^2	0.9991	Model fit: R^2	0.9310

Test 5

Table C. 9: Raw batch leach data for test 5

t (hr)	Sample Type	% Uranium extraction (batch test)	Oxidant addition (batch test)	Acid addition (batch test)
0	NA			
2	Subsample	64.7	0.354	24.66
4	Subsample	75.2	0.413	26.51
6	Subsample	78.8	0.452	28.02
6	Subsample	79.4	0.465	28.02
7	Residue	81.7	0.458	28.01
9	Subsample	82.3	0.519	30.56
11	Subsample	81.8	0.568	32.09
13	Residue	82.6	0.568	32.09

Table C. 10: Empirical model constants for test 5

Constant	% Uranium extraction	Constant	Acid addition	Constant	Oxidant addition
a	87.6	c	24.62	f	0.381
b	0.635	d	0.1084	g	0.378
		e	0.6369	h	0.016
Model fit: R^2	0.9988	Model fit: R^2	0.9980	Model fit: R^2	0.9956

Test 6

Table C. 11: Raw batch leach data for test 6

t (hr)	Sample Type	% Uranium extraction (batch test)	Oxidant addition (batch test)	Acid addition (batch test)
0	NA			
2	Subsample	67.8	0.189	24.19
4	Subsample	76.3	0.258	26.07
6	Subsample	74.8	0.315	27.79
6	Subsample	82.6	0.343	27.79
7	Residue	82.9	0.316	27.12
9	Subsample	85.6	0.395	29.47
11	Subsample	85.0	0.441	30.52
13	Residue	84.7	0.484	30.52

Table C. 12: Empirical model constants for test 6

Constant	% Uranium extraction	Constant	Acid addition	Constant	Oxidant addition
a	89.5	c	25.95	f	0.216
b	0.643	d	0.2260	g	0.961
		e	0.4175	h	0.021
Model fit: R^2	0.9924	Model fit: R^2	0.9977	Model fit: R^2	0.9917

Test 7

Table C. 13: Raw batch leach data for test 7

t (hr)	Sample Type	% Uranium extraction (batch test)	Oxidant addition (batch test)	Acid addition (batch test)
0	NA			
2	Subsample	73.5	0.248	24.70
4	Subsample	78.2	0.328	26.63
6	Subsample	81.1	0.396	28.00
6	Subsample	84.1	0.423	28.00
7	Residue	81.8	0.394	27.98
9	Subsample	82.8	0.474	30.14
11	Subsample	82.9	0.521	30.99
13	Residue	85.6	0.571	30.99

Table C. 14: Empirical model constants for test 7

Constant	% Uranium extraction	Constant	Acid addition	Constant	Oxidant addition
a	87.5	c	26.30	f	0.309
b	0.421	d	0.2114	g	1.020
		e	0.4303	h	0.022
Model fit: R^2	0.9978	Model fit: R^2	0.9985	Model fit: R^2	0.9930

Test 8

Table C. 15: Raw batch leach data for test 8

t (hr)	Sample Type	% Uranium extraction (batch test)	Oxidant addition (batch test)	Acid addition (batch test)
0	NA			
2	Subsample	66.5	0.320	24.64
4	Subsample	77.1	0.410	26.50
6	Subsample	81.9	0.476	27.93
6	Subsample	82.8	0.509	27.93
7	Residue	81.3	0.491	27.54
9	Subsample	83.3	0.591	30.02
11	Subsample	86.0	0.655	31.23
13	Residue	86.8	0.712	31.23

Table C. 16: Empirical model constants for test 8

Constant	% Uranium extraction	Constant	Acid addition	Constant	Oxidant addition
a	91.5	c	25.32	f	0.318
b	0.778	d	0.1464	g	0.468
		e	0.5138	h	0.031
Model fit: R^2	0.9990	Model fit: R^2	0.9979	Model fit: R^2	0.9957

Test 9

Table C. 17: Raw batch leach data for test 9

t (hr)	Sample Type	% Uranium extraction (batch test)	Oxidant addition (batch test)	Acid addition (batch test)
0	NA			
2	Subsample	63.2	0.001	24.24
4	Subsample	64.1	0.004	25.74
6	Subsample	68.2	0.044	27.05
6	Subsample	69.1	0.062	27.05
7	Residue	70.4	0.038	27.71
9	Subsample	75.5	0.092	29.60
11	Subsample	79.9	0.121	30.29
13	Residue	79.9	0.153	30.29

Table C. 18: Empirical model constants for test 9

Constant	% Uranium extraction	Constant	Acid addition	Constant	Oxidant addition
a	84.0	c	25.04	f	0.000
b	1.04	d	0.1603	g	5.193
		e	0.4730	h	0.009
Model fit: R^2	0.9776	Model fit: R^2	0.9983	Model fit: R^2	0.9102

Test 10

Table C. 19: Raw batch leach data for test 10

t (hr)	Sample Type	% Uranium extraction (batch test)	Oxidant addition (batch test)	Acid addition (batch test)
0	NA			
2	Subsample	68.7	0.191	24.13
4	Subsample	73.2	0.265	26.36
6	Subsample	78.7	0.319	27.82
6	Subsample	80.4	0.342	27.82
7	Residue	80.1	0.303	27.03
9	Subsample	82.9	0.377	29.77
11	Subsample	81.0	0.424	31.17
13	Residue	82.2	0.457	31.17

Table C. 20: Empirical model constants for test 10

Constant	% Uranium extraction	Constant	Acid addition	Constant	Oxidant addition
a	85.7	c	25.24	f	0.252
b	0.515	d	0.1827	g	1.169
		e	0.5167	h	0.017
Model fit: R^2	0.9974	Model fit: R2	0.9969	Model fit: R2	0.9871

Test 11

Table C. 21: Raw batch leach data for test 11

t (hr)	Sample Type	% Uranium extraction (batch test)	Oxidant addition (batch test)	Acid addition (batch test)
0	NA			
2	Subsample	71.5	0.312	25.51
4	Subsample	77.8	0.390	27.18
6	Subsample	79.9	0.461	28.63
6	Subsample	83.5	0.494	28.63
7	Residue	81.3	0.475	28.17
9	Subsample	81.1	0.580	30.92
11	Subsample	80.6	0.638	32.38
13	Residue	86.2	0.697	32.38

Table C. 22: Empirical model constants for test 11

Constant	% Uranium extraction	Constant	Acid addition	Constant	Oxidant addition
a	88.2	c	25.43	f	0.290
b	0.518	d	0.1000	g	0.357
		e	0.5879	h	0.032
Model fit: R^2	0.9951	Model fit: R2	0.9974	Model fit: R2	0.9952

Test 12

Table C. 23: Raw batch leach data for test 12

t (hr)	Sample Type	% Uranium extraction (batch test)	Oxidant addition (batch test)	Acid addition (batch test)
0	NA			
2	Subsample	61.6	0.030	19.11
4	Subsample	69.4	0.061	20.49
6	Subsample	76.2	0.113	21.73
6	Subsample	76.3	0.136	21.73
7	Residue	75.7	0.114	21.70
9	Subsample	78.5	0.183	23.39
11	Subsample	80.9	0.221	24.36
13	Residue	82.7	0.266	24.36

Table C. 24: Empirical model constants for test 12

Constant	% Uranium extraction	Constant	Acid addition	Constant	Oxidant addition
a	87.9	c	19.81	f	0
b	0.984	d	0.1706	g	0.767
		e	0.4009	h	0.019
Model fit: R^2	0.9977	Model fit: R2	0.9984	Model fit: R2	0.9801

Test 13

Table C. 25: Raw batch leach data for test 13

t (hr)	Sample Type	% Uranium extraction (batch test)	Oxidant addition (batch test)	Acid addition (batch test)
0	NA			
2	Subsample	66.6	0.284	19.66
4	Subsample	74.0	0.379	20.86
6	Subsample	79.0	0.449	22.17
6	Subsample	81.9	0.481	22.17
7	Residue	78.6	0.460	22.46
9	Subsample	83.0	0.563	24.59
11	Subsample	85.2	0.626	25.67
13	Residue	83.8	0.680	25.67

Table C. 26: Empirical model constants for test 13

Constant	% Uranium extraction	Constant	Acid addition	Constant	Oxidant addition
a	88.0	c	19.34	f	0.307
b	0.704	d	0.1000	g	0.736
		e	0.5410	h	0.030
Model fit: R^2	0.9971	Model fit: R2	0.9975	Model fit: R2	0.9948

Test 14

Table C. 27: Raw batch leach data for test 14

t (hr)	Sample Type	% Uranium extraction (batch test)	Oxidant addition (batch test)	Acid addition (batch test)
0	NA			
2	Subsample	71.9	0.516	19.94
4	Subsample	76.6	0.700	20.54
6	Subsample	80.6	0.730	23.54
6	Subsample	83.2	0.732	23.54
7	Residue	84.8	0.750	23.02
9	Subsample	80.8	0.844	24.77
11	Subsample	81.4	0.907	25.57
13	Residue	81.5	0.989	25.57

Table C. 28: Empirical model constants for test 14

Constant	% Uranium extraction	Constant	Acid addition	Constant	Oxidant addition
a	85.2	c	21.90	f	0.617
b	0.291	d	0.3158	g	0.619
		e	0.3599	h	0.029
Model fit: R^2	0.9944	Model fit: R2	0.9944	Model fit: R2	0.9950

Test 15

Table C. 29: Raw batch leach data for test 15

t (hr)	Sample Type	% Uranium extraction (batch test)	Oxidant addition (batch test)	Acid addition (batch test)
0	NA			
2	Subsample	69.3	0.682	20.17
4	Subsample	80.3	0.824	21.24
6	Subsample	83.1	0.938	22.96
6	Subsample	81.6	0.989	22.96
7	Residue	79.5	0.948	22.77
9	Subsample	82.9	1.101	25.18
11	Subsample	84.5	1.205	26.34
13	Residue	84.1	1.294	26.34

Table C. 30: Empirical model constants for test 15

Constant	% Uranium extraction	Constant	Acid addition	Constant	Oxidant addition
a	86.8	c	19.83	f	0.699
b	0.490	d	0.1000	g	0.378
		e	0.5554	h	0.047
Model fit: R^2	0.9972	Model fit: R2	0.9970	Model fit: R2	0.9961

Test 16

Table C. 31: Raw batch leach data for test 16

t (hr)	Sample Type	% Uranium extraction (batch test)	Oxidant addition (batch test)	Acid addition (batch test)
0	NA			
2	Subsample	74.9	0.000	25.02
4	Subsample	83.0	0.299	27.84
6	Subsample	83.4	0.424	29.46
6	Subsample	87.8	0.522	28.43
7	Residue	84.7	0.563	29.46
9	Subsample	86.1	0.639	31.07
11	Subsample	86.4	0.707	32.28
13	Residue	87.5	0.740	32.28

Table C. 32: Empirical model constants for test 16

Constant	% Uranium extraction	Constant	Acid addition	Constant	Oxidant addition
a	89.9	c	28.14	f	0.543
b	0.388	d	0.3233	g	2.370
		e	0.4016	h	0.022
Model fit: R^2	0.9978	Model fit: R2	0.9985	Model fit: R2	0.9989

Test 17

Table C. 33: Raw batch leach data for test 17

t (hr)	Sample Type	% Uranium extraction (batch test)	Oxidant addition (batch test)	Acid addition (batch test)
0	NA			
2	Subsample	72.2	0.287	21.91
4	Subsample	77.4	0.305	24.32
6	Subsample	80.1	0.463	26.33
6	Subsample	80.6	0.483	26.33
7	Residue	80.1	0.463	26.33
9	Subsample	81.9	0.541	30.80
11	Subsample	81.5	0.593	32.01
13	Residue	84.3	0.682	32.01

Table C. 34: Empirical model constants for test 17

Constant	% Uranium extraction	Constant	Acid addition	Constant	Oxidant addition
a	86.1	c	21.63	f	0.266
b	0.43	d	0.1627	g	0.548
		e	0.8974	h	0.032
Model fit: R2	0.9989	Model fit: R2	0.9933	Model fit: R2	0.9799

Test 18

Table C. 35: Raw batch leach data for test 18

t (hr)	Sample Type	% Uranium extraction (batch test)	Acid addition (batch test)	Oxidant addition (batch test)
0	NA			
2	Subsample	70.9	25.65	0.286
4	Subsample	80.0	27.58	0.381
6	Subsample	83.0	29.14	0.452
6	Subsample	83.8	27.62	0.444
7	Residue	82.7	29.14	0.478
9	Subsample	85.1	29.98	0.543
11	Subsample	82.7	31.23	0.595
13	Residue	87.5	31.23	0.646

Table C. 36: Empirical model constants for test 18

Constant	% Uranium extraction	Constant	Acid addition	Constant	Oxidant addition
a	90.4	c	27.17	f	0.345
b	0.57	d	0.1810	g	0.928
		e	0.3659	h	0.025
Model fit: R2	0.9975	Model fit: R2	0.9979	Model fit: R2	0.9998

Test 19

Table C. 37: Raw batch leach data for test 19

t (hr)	Sample Type	% Uranium extraction (batch test)	Oxidant addition (batch test)	Acid addition (batch test)
0	NA			
2	Subsample	68.1	0.269	24.91
4	Subsample	80.5	0.365	26.89
6	Subsample	79.9	0.445	28.47
6	Subsample	82.1	0.430	28.37
7	Residue	84.9	0.474	28.47
9	Subsample	85.2	0.525	30.87
11	Subsample	85.1	0.579	31.86
13	Residue	86.6	0.641	31.86

Table C. 38: Empirical model constants for test 19

Constant	% Uranium extraction	Constant	Acid addition	Constant	Oxidant addition
a	91.2	c	26.22	f	0.342
b	0.62	d	0.2007	g	1.123
		e	0.5083	h	0.025
Model fit: R2	0.9978	Model fit: R2	0.9983	Model fit: R2	0.9994

Appendix D: Leach test controls

Table D.1: Leach controls for pulp density tests

Pulp density	70%	75%
ORP control (Ag/AgCl)	450 ± 11 mV	451 ± 9 mV
pH control	1.6 ± 0.1	1.6 ± 0.1

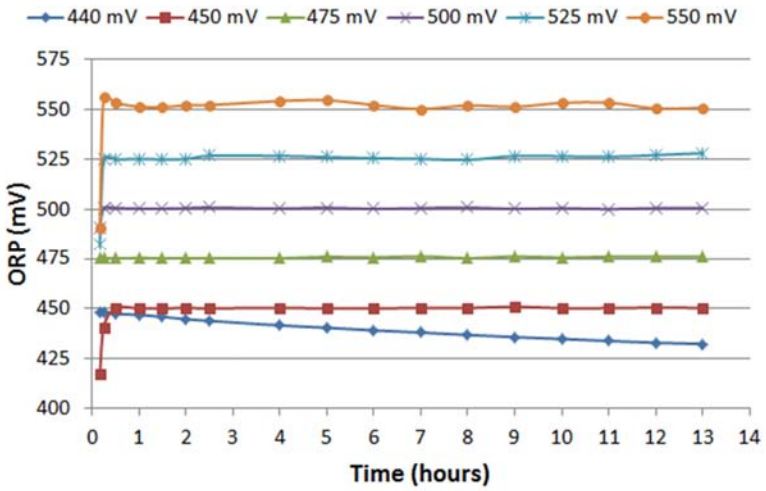

Figure D.1: ORP profiles for batch leach tests conducted at Fe = 4 g/l (ROM ore)

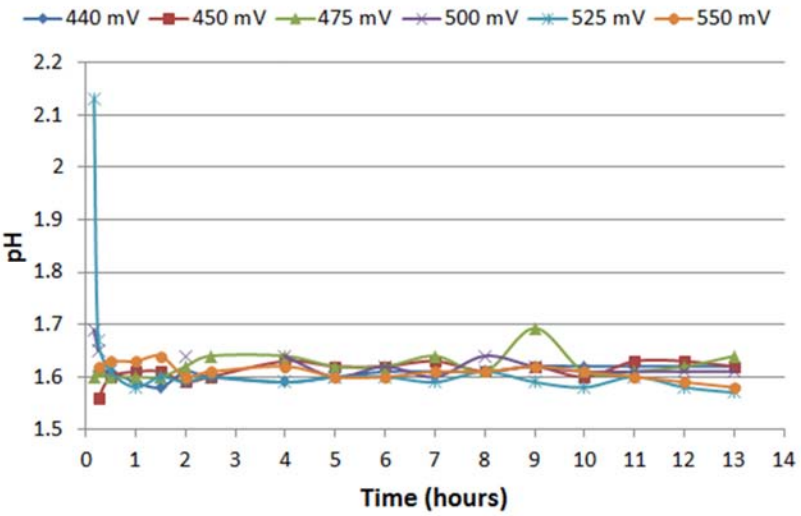

Figure D.2: pH profiles for batch leach tests conducted at Fe = 4 g/l (ROM ore)

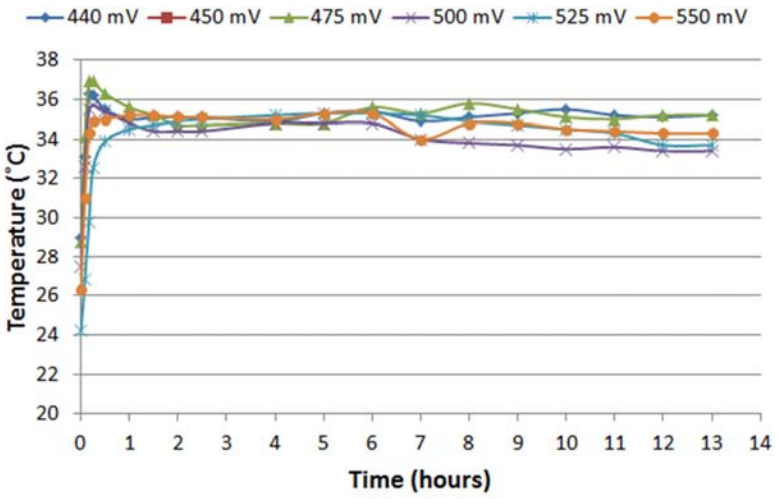

Figure D.3: Temperature profiles for batch leach tests conducted at Fe = 4 g/l (ROM ore)

Table D.2: Leach controls (4 g/L Fe, ore A)

ORP (Ag/AgCl, 3M KCl)	Test (hours)	ORP control after 15 min (mV)	pH control	Total Fe control (g/L)	Temperature control (°C)
440	7	444 ± 4	1.6 ± 0.0	3.8 ± 0.2	35.3 ± 0.7
	13	440 ± 6	1.6 ± 0.0	4.1 ± 0.1	35.3 ± 0.4
450	7	457 ± 4	1.6 ± 0.0	3.9 ± 0.2	34.9 ± 0.2
	13	450 ± 2	1.6 ± 0.0	4.0 ± 0.2	35.4 ± 0.7
475	7	476 ± 1	1.7 ± 0.2	3.8 ± 0.1	36.6 ± 1.6
	13	476 ± 0	1.6 ± 0.0	4.0 ± 0.1	35.4 ± 0.7
500	7	501 ± 1	1.7 ± 0.1	3.8 ± 0.0	34.6 ± 0.9
	13	501 ± 0	1.6 ± 0.0	4.2 ± 0.1	34.4 ± 0.7
525	7	526 ± 1	1.7 ± 0.2	3.8 ± 0.2	34.3 ± 1.7
	13	526 ± 1	1.6 ± 0.1	4.0 ± 0.1	34.2 ± 1.4
550	7	554 ± 2	1.7 ± 0.2	3.9 ± 0.2	34.4 ± 1.4
	13	552 ± 2	1.6 ± 0.0	4.2 ± 0.0	34.8 ± 0.3

Table D.3: Controls for batch leach tests conducted at Fe = 3 g/L (ore A)

ORP (Ag/AgCl, 3M KCl)	Test (hours)	ORP control after 15 min (mV)	pH control	Total Fe control (g/L)	Temperature control (°C)
450	7	458 ± 8	1.6 ± 0.0	2.9 ± 0.2	34.6 ± 0.8
	13	455 ± 7	1.6 ± 0.0	3.1 ± 0.1	35.2 ± 0.9
500	7	501 ± 1	1.6 ± 0.0	2.7 ± 0.2	34.7 ± 1.2
	13	501 ± 1	1.6 ± 0.0	3.1 ± 0.2	34.8 ± 0.6
550	7	557 ± 6	1.7 ± 0.1	2.9 ± 0.1	35.2 ± 0.9
	13	555 ± 3	1.6 ± 0.0	3.2 ± 0.2	35.7 ± 0.8

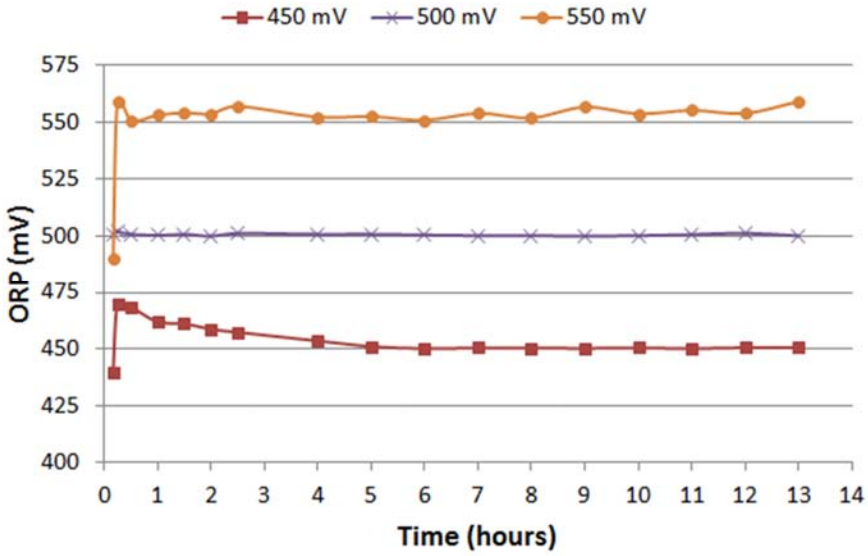

Figure D.4: ORP profiles for batch leach tests conducted at Fe = 3 g/l (ROM ore)

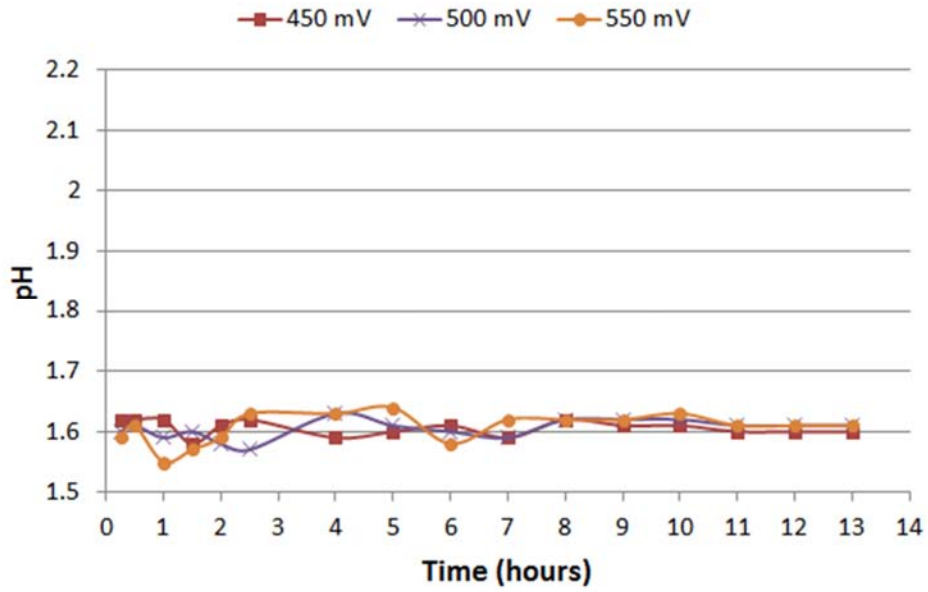

Figure D.5: pH profiles for batch leach tests conducted at Fe = 3 g/l (ROM ore)

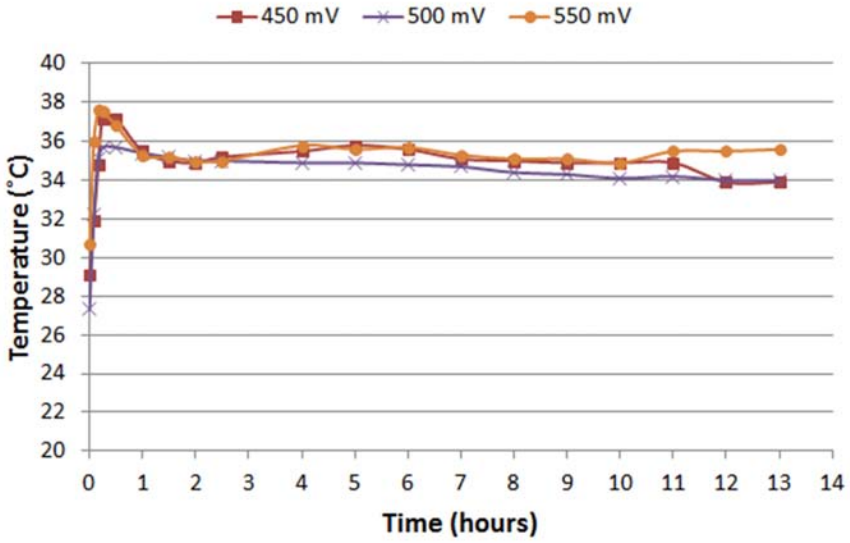

Figure D.6: Temperature profiles for batch leach tests conducted at Fe = 3 g/l (ROM ore)

Table D.4: Leach controls (4 g/L Fe, ore B)

ORP (Ag/AgCl, 3M KCl)	Test (hours)	ORP control after 15 min (mV)	pH control	Total Fe control (g/L)	Temperature control (°C)
450	7	453 ± 3	1.6 ± 0.0	4.1 ± 0.1	34.9 ± 0.6
	13	451 ± 2	1.6 ± 0.0	4.6 ± 0.3	35.0 ± 0.4
475	7	476 ± 0	1.6 ± 0.0	4.1 ± 0.2	34.6 ± 0.9
	13	475 ± 1	1.6 ± 0.0	4.4 ± 0.1	35.4 ± 0.8
500	7	501 ± 1	1.6 ± 0.1	4.3 ± 0.2	35.5 ± 0.6
	13	501 ± 1	1.6 ± 0.1	4.4 ± 0.6	34.5 ± 0.9
550	7	553 ± 2	1.6 ± 0.1	3.9 ± 0.2	34.5 ± 1.0
	13	552 ± 2	1.6 ± 0.0	4.6 ± 0.1	35.1 ± 0.3

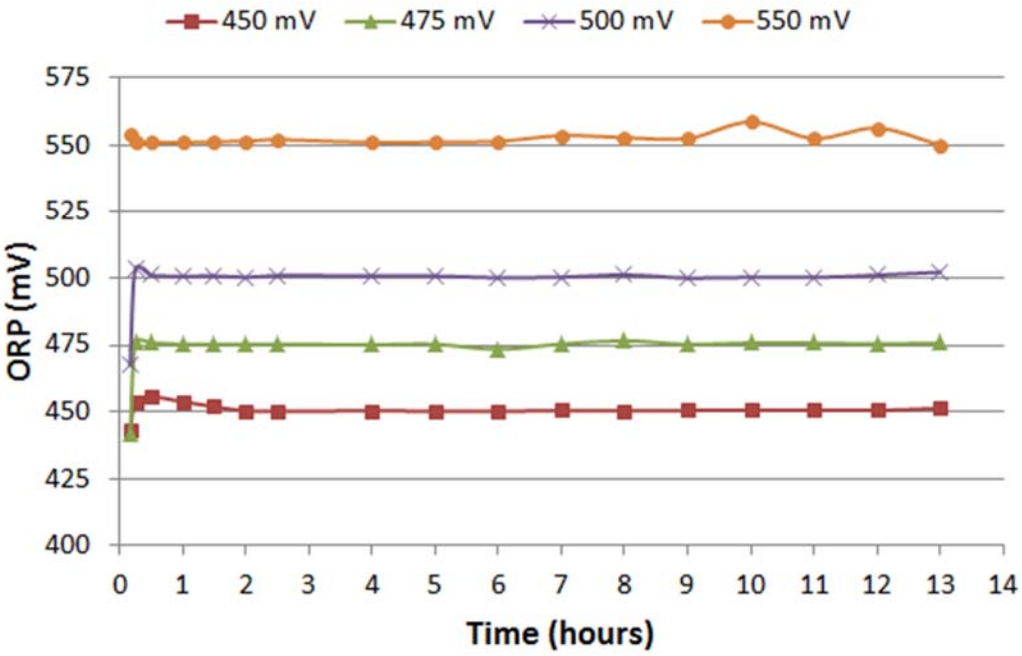

Figure D.7: ORP profiles for batch leach tests conducted at Fe = 4 g/l (CGS ore)

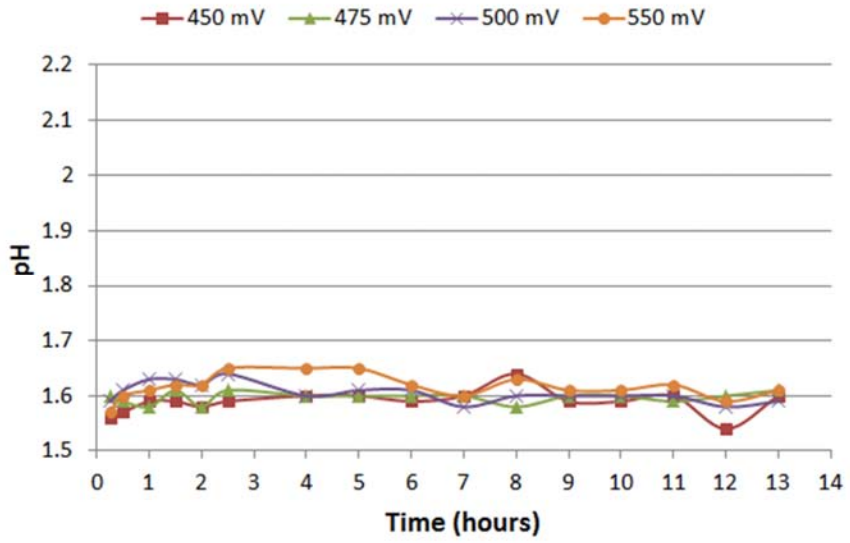

Figure D.8: pH profiles for batch leach tests conducted at Fe = 4 g/l (CGS ore)

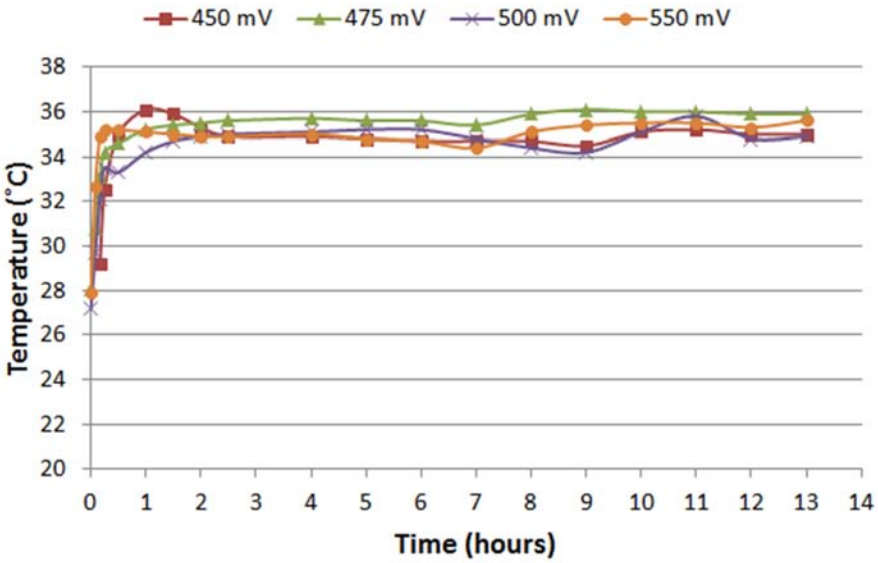

Figure D.9: Temperature profiles for batch leach tests conducted at Fe = 4 g/l (CGS ore)

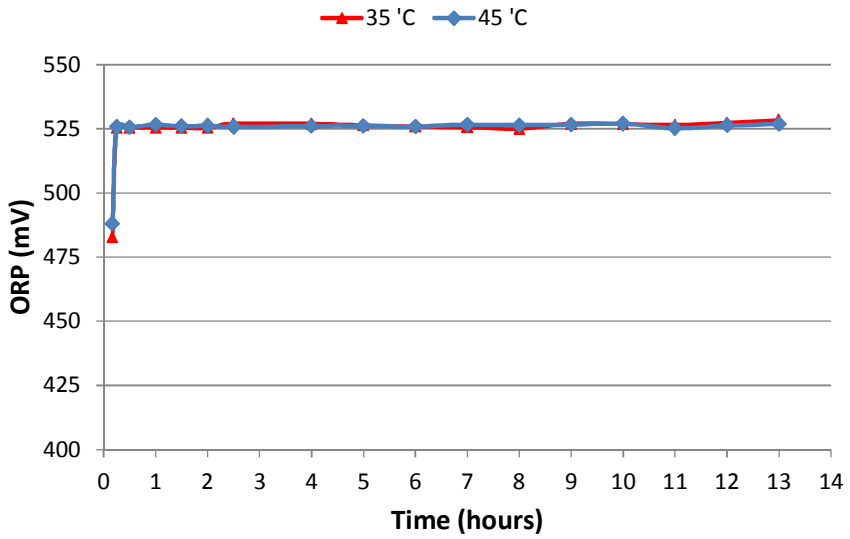

Figure D.10: ORP profiles for temperature tests conducted at Fe = 4 g/l (ROM ore)

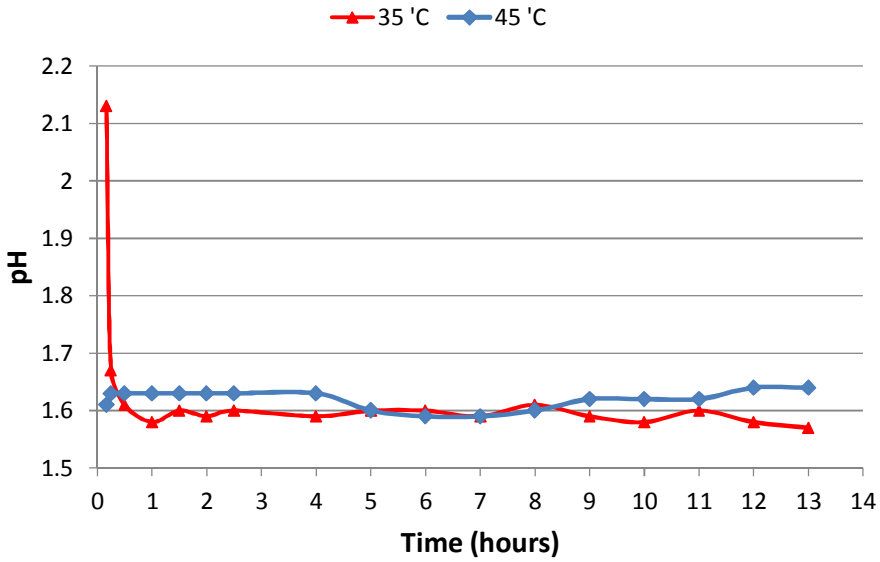

Figure D.11: pH profiles for temperature tests conducted at Fe = 4 g/l (ROM ore)

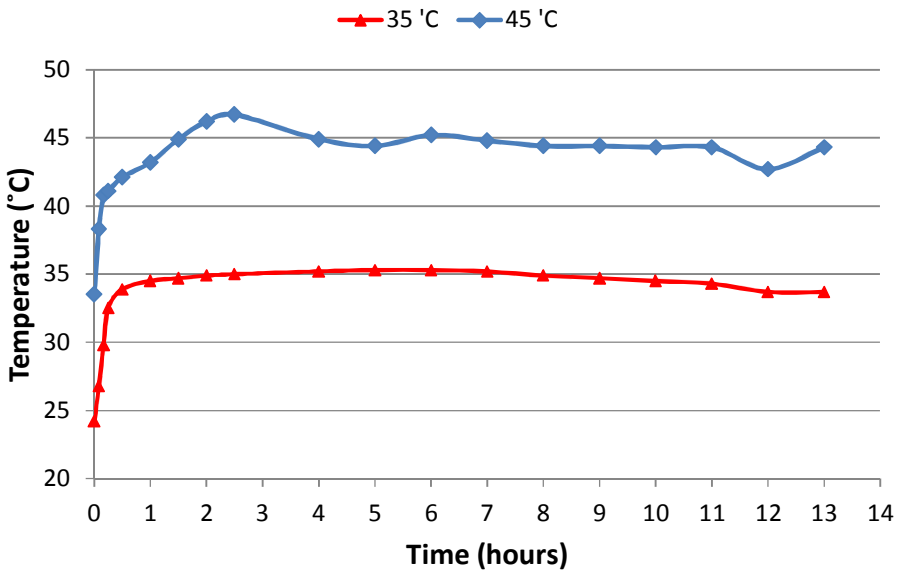

Figure D.12: Temperature profiles for temperature tests conducted at Fe = 4 g/l (ROM ore)

Appendix E: Results from oxidant chemical efficiency tests

To determine the oxidising chemical efficiency of $NaMnO_2$ and MnO_2, the following test was conducted. The results are presented in Table E.1.

1. Two starting solutions (2 x 0.5 L), both containing ~4 g/L ferrous and ~2 g/L ferric were made up, i.e. ferric sulphate and ferrous sulphate were added to the synthetic plant solution to achieve these target concentrations.
2. The solutions were poured into the agitated leach reactors and were continuously agitated. pH was controlled at pH 1.6 via the Tiamo pH PID controller.
3. The specified volume of $NaMnO_4$ and mass of MnO_2 (Table E.1) were added to the starting solutions ($NaMnO_4$ to solution A and MnO_2 to solution B).
4. Both reaction vessels were agitated for a period of 2 hours.

Table E.1: Results from oxidant chemical efficiency test

Volume of $NaMnO_4$ solution added		0.005	L
Concentration of $NaMnO_4$ solution		107	g/L
Mass of Pyrolusite added		1	g
Concentration of MnO_2 in Pyrolusite solution		72	wt%
	A $NaMnO_4$	**B MnO_2**	
Initial Ferrous	4.01	4.01	g/L
Final Ferrous	2.09	2.32	g/L
Ferrous oxidised	1.92	1.69	g/L
Ferrous oxidised	0.96	0.85	g
Moles of ferrous oxidised	0.02	0.02	mol
Mass of oxidant consumed	0.54	0.72	g
Moles of oxidant used	0.004	0.008	mol
Oxidant per mol of ferrous	0.22	0.55	mol/mol Fe^{2+}
mol electron	1.10	1.09	mol/mol Fe^{2+}

Appendix F: Error analysis

Table F. 1: In-situ sampling method error analysis

	U (ppm) Assay 1	U (ppm) Assay 2	U (ppm) Assay 3	U (ppm) Assay 4	U (ppm) Assay 5	U (ppm) Mean	% U extraction[26]
Sample S1	28.5	28.1	29.0	28.3	27.9	28.4	91.0
Sample S2	27.3	26.9	25.3	27.2	26.7	26.7	91.6
Sample S3	21.7	22.4	22.1	21.5	21.3	21.8	93.1
Sample S4	25.6	26.1	25.3	25.8	26.6	25.9	91.8
Sample S5	24.3	25.3	24.9	25.3	25.1	25.0	92.1
Sample S6	20.9	21.9	21.9	20.7	21.6	21.4	93.2
Mean							92.2
Standard deviation[27] (2SD)							1.74
Variance							0.76

Table F. 2: Residue sampling method error analysis

	U (ppm) Assay 1	U (ppm) Assay 2	U (ppm) Assay 3	U (ppm) Assay 4	U (ppm) Assay 5	U (ppm) Mean	% U extraction[28]
Sample R1	25.1	23.7	25.7	23.5	23.6	24.3	92.5
Sample R2	23.8	22.6	21.1	23.8	22.1	22.7	93.0
Sample R3	26.3	26.4	26.3	24.8	24.6	25.7	92.0
Sample R4	24.3	25.4	23.6	25.0	23.7	24.4	92.4
Sample R5	22.2	22.4	22.2	24.3	24.2	23.1	92.8
Sample R6	24.8	24.9	24.7	23.5	24.3	24.4	92.4
Mean							92.5
Standard deviation (2SD)							0.67
Variance							0.11

Table F. 3: Analytical error

	U (ppm) Assay 1	U (ppm) Assay 2	U (ppm) Assay 3	U (ppm) Assay 4	U (ppm) Assay 5	U (ppm) Mean	U (ppm) 2SD	%U extraction 2SD
Sample S1	28.5	28.1	29.0	28.3	27.9	28.4	0.42	0.27
Sample S2	27.3	26.9	25.3	27.2	26.7	26.7	0.81	0.51
Sample S3	21.7	22.4	22.1	21.5	21.3	21.8	0.45	0.28
Sample S4	25.6	26.1	25.3	25.8	26.6	25.9	0.50	0.31
Sample S5	24.3	25.3	24.9	25.3	25.1	25.0	0.41	0.26
Sample S6	20.9	21.9	21.9	20.7	21.6	21.4	0.57	0.36
Sample R1	25.1	23.7	25.7	23.5	23.6	24.3	1.01	0.63
Sample R2	23.8	22.6	21.1	23.8	22.1	22.7	1.16	0.72
Sample R3	26.3	26.4	26.3	24.8	24.6	25.7	0.90	0.56
Sample R4	24.3	25.4	23.6	25.0	23.7	24.4	0.79	0.49
Sample R5	22.2	22.4	22.2	24.3	24.2	23.1	1.09	0.68
Sample R6	24.8	24.9	24.7	23.5	24.3	24.4	0.57	0.36
Mean								0.45
Standard error in average of 5 assays (Mean/√5)								0.20

[26] Head grade = 317 ppm (U concentration)
[27] 95 % confidence interval (2 x Standard deviation, 2SD)
[28] Head grade = 322 ppm (U concentration)

Appendix G: Sample homogenization and splitting procedure

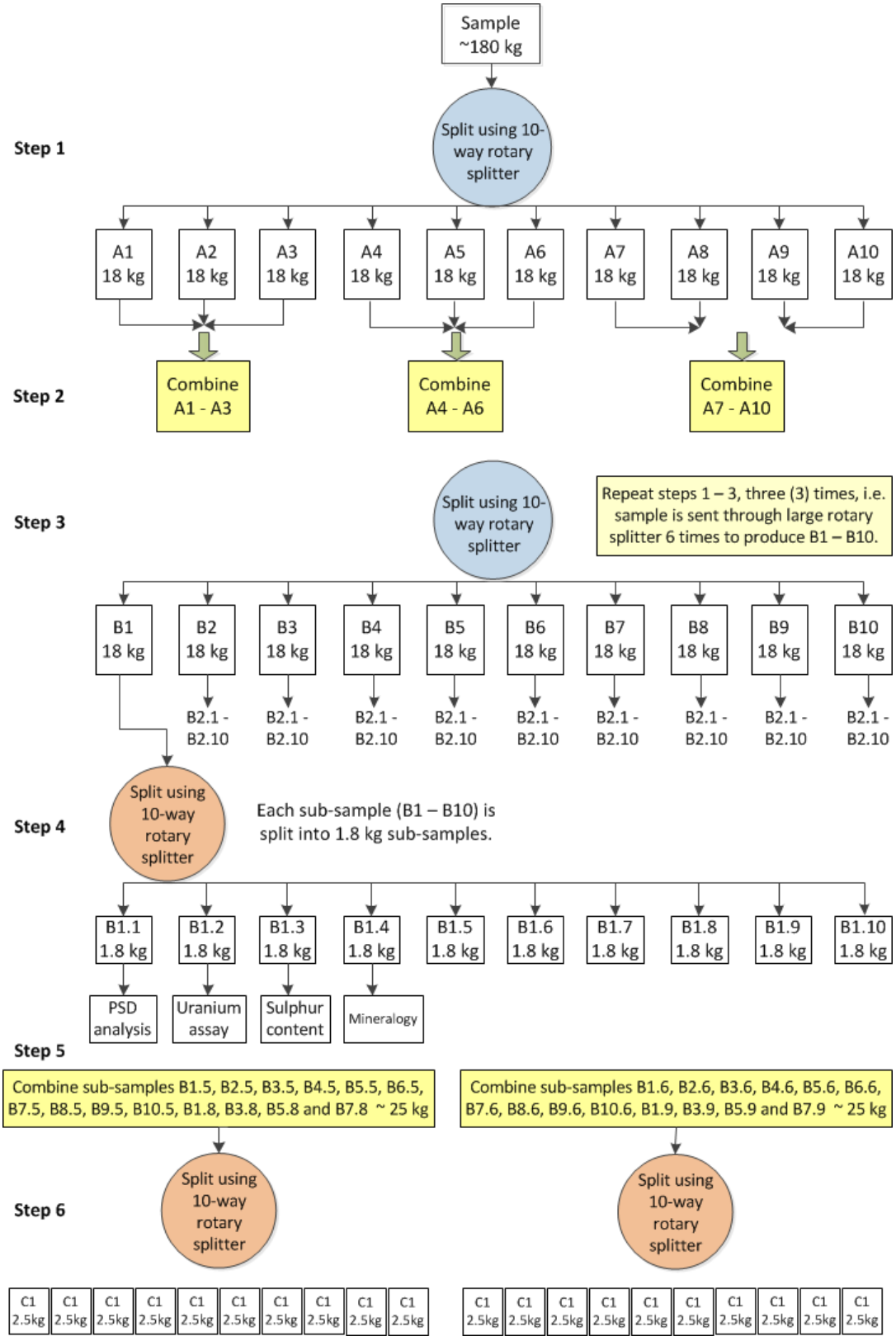

Figure G. 1: Sample homogenization and splitting procedure